Alma Mater Studiorum – Università di Bologna

DOTTORATO DI RICERCA IN

Scienze Mediche Generali e dei Servizi - Progetto n°4:
Ultrasonologia in Medicina Umana e Veterinaria

Ciclo XXV

Settori scientifico-disciplinari di afferenza:

Clinica Medica Veterinaria (VET/08)

ANATOMIC STUDY OF THE FELINE BRONCHIAL AND VASCULAR STRUCTURES WITH A 64 DETECTOR-ROW COMPUTED TOMOGRAPHY

Presentata da: **PANOPOULOS dott. IOANNIS**

Coordinatore Dottorato **Relatore**

BOLONDI prof. LUIGI **CIPONE prof. MARIO**

Esame finale anno 2013

INDEX

INTRODUCTION

Multidetector-row computed tomography (MDCT) is an evolutionary step in advanced imaging techniques based on the superior scanner's technology and on dedicated medical workstations with highly advanced softwares. Scanning speed is the basic parameter that allowed to obtain high quality images in wider scanning ranges. Volume data became the base for applications such as Computed Tomography Angiogram, which provides a non-invasive assessment of vascular disease. New methods and protocols can evaluate in 3D models the skeletal, vascular, bronchial and other organs with reliable images. These advanced technologies are more widely available than even before in small animal practice. MDCT has become a commonly used method for Computed Tomography Angiography (CTA) studies of the thorax. MDCT has significantly increased speed of scanning, spatial resolution, temporal resolution and allows high-resolution imaging compared with the conventional single-detector row CT, providing a dramatic impact on vascular studies. Up to date few reports of the normal tomographic features of the feline thorax are published. Feline bronchial and vascular structures till to date have not been well studied either from anatomists either from radiologists while pulmonary disease is common in feline patients. MDCT can provide high image quality with sub-millimeter images and by using advanced software applications we can achieve high quality imaging of both bronchial and vascular structures till dimension of 0.5mm in 2D images and 3D models.

Our purpose is to introduce a feline Computed Tomography Pulmonary Angiography (CTPA) protocol , to study by an isotropic study in 2D and 3D reconstruction images the anatomic structures of the normal feline thorax and to measure the dimensions of the bronchial and vascular components of the normal feline thorax. Our results with be discussed and compared with those of the till to date references.

1.1 Multidetector-row Computed Tomography (MDCT)

Technical review

Computed tomography is a tomographic technique in which an x-ray source rotates around the body and an x-ray beam passes through the animal from various directions. The x-ray attenuation along the animal's body is calculated with a mathematical algorithm and images are finally converted into shades of grayscale.

Till today five generations of computed tomography scanners exist. The first two generations (rotate/translate) of CT scanner geometries were used in the late 70s and were substituted by third (rotate/rotate) and fourth-generation (rotate/stationary) scanners. The fifth generation scanners (stationary/stationary, scanning electron beam) were developed for cardiac tomographic imaging. With the slip-ring technology the gantry was able to rotate without rewind after each rotation. The X- ray tube is rotating around the animal while the detector array collects the image data. This helical computed tomography technology could produce volume data images transporting the animal through the gantry in the longitudinal plane. Volume data became the very basis for applications such as CTA, which has revolutionized non-invasive assessment of vascular disease (Borsetto, 2011). The ability to acquire volume data also paved the way for the development of 3D image-processing techniques, that have become vital components of medical imaging. Isotropic volume data element («voxel») is the similar to a 3D pixel in which all dimensions in all three spatial axes are equal. The

main advantages of MDCT is the shorter acquisition time, wider scanning range, improved temporal and spatial resolution. Images could be reconstructed later in images of thinner slices. With single-slice spiral CT, the ideal of isotropic resolution can only be achieved for very limited scan ranges (Kalender, 1995). Strategies to achieve more substantial volume coverage with improved longitudinal resolution have included the simultaneous acquisition of more than one slice at a time and a reduction of the gantry rotation time. In early 90s a 2-slice CT scanner was introduced, the first step towards multi-slice acquisition in general radiology (Liang, 1996). CT manufacturers introduced multidetector CT (MDCT) systems in late 90s. MDCT extends the number of detectors to several rows. With this technology wider scanning ranges could evaluated in a certain scanning time that is influenced by a factor equal to the number of detector sections (Flohr, 2005). The increased longitudinal (Z-axis) resolution allowed users to perform real isotropic 3D imaging. Clinical advantage of these possibilities is the examination of wider anatomic areas in a single breath hold (Horton, 2002; Kalra, 2004). Vessel analysis, vascular diagnosis, high-resolution CT of the lung, virtual CT endoscopy and cardiac imaging with the addition of ECG gating capability nowadays with MDCT are examinations of routine. A 16-slice CT could acquire substantial anatomic volumes with isotropic sub-millimeter spatial resolution (Flohr, 2002a and 2002b). Whole-body angiographic studies with sub-millimeter resolution in a single breath-hold are also possible with 16-slice CT (Cademartiri, 2004; Napoli, 2004). Compared to invasive angiography, the same morphological information is obtained (Wintersperger, 2002a and 2002b). Whereas most of the scanners increase the number of acquired slices by increasing the number of the detector rows, some of the new scanners use additional refined z- sampling techniques with a periodic motion of the focal spot in the z-direction (z-

flying focal spot) which can further enhance longitudinal resolution and image quality in clinical routine (Flohr, 2003). The last few years all major CT manufacturers introduced the next generation of multi-slice CT systems, with 32, 40, and 64 simultaneously acquired slices, which brought about a further leap in volume coverage speed. Systems with 128-, 256- and 320-detector rows are now available for cardiac imaging.

• Primary reconstructions

Data are produced by the rotating x-ray source and detectors are processed by Fourier transforms to generate transverse reconstructions. Computed tomography data are volumetric data due to continuous acquisition during table translation and these data are exclusively reconstructed in transverse sections. These primary reconstructions when stacked together represent the entire volume while observers have a limited ability to mentally integrate and interpret the many images making up each volume. Three dimension visualization of the volumetric data using dedicated image processing workstations allows different aspect for visual evaluation and analysis of these primarily acquired and reconstructed data.

The advantages of post processing volumetric data fall into four broad categories:

Alternative visualization can overlap the substantial limitations that could have the volumetric rendering techniques of structures that have primarily reconstructed images arbitrarily orientation relative to these structures. For example the vascular system is a network of tubes oriented with complex relationships. The flexibility afforded by volumetric visualization techniques make possible the evaluation of the examined structure despite subtle shifts in the animals position between serial examinations. These techniques allow

assessment of anatomy by using landmarks and axes that are intrinsically relevant to structures of interest rather to the orientation of the imaging table.

Efficient interpretation is similar to the interpretation of such volumetric data that arises from ultrasonography. A single sonographic image is a cross sectional reconstruction similar to a primary planar reconstruction from CTA. The sonographer watches the image display changing in real time as the transducer is swept over the surface of the animal and the same could perform also with the volumetric data acquired from a CT examination. In a volume the observer could interactively explore this volumetric data set both to perform primary interpretation and to record views that are clinically relevant.

Effective communication could provide a basis for communication to referring doctor of anatomic findings with complex spatial relationships by individual screen shots saved during real time exploration of volumetric data.

Volumetric quantitation is the ability to quantify the complex geometric relationships and features of the vasculature. This volumetric analysis is important in order to understand the anatomy and the extension of a vascular disease in order to evaluate the severity.

• Primary planar reconstructions

The “source data” provide the highest spatial resolution and the lowest likelihood of motion-related misregistration and off-axis artifacts. Artifacts related to beam hardening in CT are results from metallic implants or high concentration of intravenous contrast medium along the course of a vessel.

• Multiplanar reformatted reconstruction (MPR) is a two-dimensional technique that can simultaneously display multiple view of the same volume, in sagittal, dorsal, transverse or any oblique plane. This is the post-processing technique most familiar to radiologists and still the most useful and versatile. The quality of multiplanar reconstructions is directly related to the image slice thickness. One of the main advantages of reviewing images on a workstation is the flexibility to instantly create and review MPRs in any plane. Because blood vessels have a curved course, MPRs are rarely the best means of summarizing vascular anatomy. When examining blood vessels, planar images must be evaluated in a stacked cine mode rather in a tiled presentation (Rubin, 2009).

•Algorithm Image reconstruction with 16-slice and higher MDCT scanners is much more complicated than with single-slice or even 4-slice scanners. In axial scanning with single-slice scanners, all of the views needed to reconstruct an image are acquired in the image plane, since the table does not move while the image is being acquired. With the introduction of helical or spiral scanning the table moves continuously during data collection and the views needed to reconstruct the axial image are not all in the same plane. To overcome this problem, views in the image plane are interpolated from measurements on either side of the image plane. The advent of 4-slice scanners required minor modifications to the existing helical reconstruction algorithms. The introduction of scanners with more than 4 simultaneous slices created further complications. Newer algorithms that accounted for the fact that the imaging ROI actually projected onto multiple detector rows in different planes were needed. Trying to reconstruct axial images without taking these various view angles (cone beam) into account produced significant artifacts. In order to maintain image quality, various cone beam

reconstruction algorithms were developed. The reconstruction algorithm chosen can have a significant effect on image quality and artifacts (Fuchs, 2000; Kohler, 2001 and 2002).

• *Reconstruction Filters* Once the basic reconstruction algorithm is chosen, a choice of filter kernel to be applied to the raw data must also be made. There are multiple filter options varying between the extremes of very smoothing to very sharpening filters. These filters can have a tremendous effect on how the final images look. The raw data can be reconstructed with as many different filter kernels as necessary to provide the desired information.

• *Slice Thickness* Thin (submillimeter) images are wonderful for generating volume reconstructions but are less than ideal for primary image review. These data sets are large and cumbersome to review even on the best PACS systems. The goal is to maintain the advantage of high-resolution imaging but to create image files that are manageable and easily reviewed. Since the acquired data sets are highly sampled volumes, it is quite feasible to construct images that are considerably thicker than the slices used during scanning. Image thickness may be greater than—but can never be less than—the slice thickness at which the data were acquired.

• *Overlapping Reconstructions* Conventional CT wisdom dictates that to achieve high-quality multiplanar and 3D reformations the images should be reconstructed with an overlap of approximately 50%. With current generation 16 or higher detector scanners, overlapping reconstructions are often unnecessary. When scans are generated with isotropic voxels, improvement in reconstruction quality from overlapping reconstructions is often quite minimal.

• *Curved Planar Reconstruction* Curved planar reconstruction is a very powerful technique for evaluating wall irregularities along the longitudinal course of blood vessels. Curved planar reconstructions allow the user to designate a centerline path around which the image will be reconstructed (Nino-Murcia, 2001; Raman, 2002; Desser, 2004). It can also be very useful for evaluating the relationship of filling defects such as thrombi or intimal flaps to the vessel wall and the origins of vessel branches.

• *Maximum Intensity Projection* Maximum intensity projection (MIP) has been the most widely used technique for visualization of blood vessels for both CT and MR angiography . It has been widely studied and evaluated and remains a very important tool. Maximum intensity projection images are created using a computer algorithm that evaluates each voxel along a line from the viewer's eye through the image and selects the voxel with the maximum intensity as the value of the corresponding display pixel. The resulting image is displayed as a collapsed or two-dimensional representation of the maximal intensity voxels that were present in the selected data set. The MIP images can be generated from the entire data set or only a portion of it. Current MR angiography techniques provide excellent background suppression which allows MIP images to be easily created from the entire data set. Unfortunately, with CT angiography there is significant nonvascular background which makes MIP imaging of the entire data set frequently limited. When other high-density structures such as bone, enhancing organs, or calcifications are present and overlying the blood vessels, these structures will be averaged in with the vessels and obscure them. There are two major methods for overcoming averaging effects. The first way is to segment the data set prior to display with the MIP algorithm.

The second method is to create the MIP image from only a portion of the data set (Napel, 1992; Schreiner, 1996; Prokop, 1997; Raman, 2003).

• *Minimum Intensity Projection* Minimum Intensity Projection (MinIP) images are the counterpart of MIP images: instead of projecting the maximum CT number into the viewing plane, they display the minimum CT number (Ravenel, 2003). MinIP is commonly used to create images of central airways. They have also been suggested for imaging pancreatic and bile ducts (Kim, 2005).

• *Volume Rendering* (VR) In recent years volume rendering has become the single most useful and versatile 3D imaging technique. It has applications in every type of examination performed with CT. With current workstations VR is quick, versatile, and extremely powerful. A great advantage of VR over other viewing techniques is that the entire volume of the data set is rendered without discarding any information. The resulting images therefore contain more information and are potentially much more clinically useful. This allows volume rendered images to display multiple tissues and show their relationships to one another. Volume-rendering techniques sum the contributions of each voxel along a line from the viewer's eye through the data set. This is done repeatedly for every pixel in the displayed image. The image is generated by assigning each voxel in the image an opacity value based on its Hounsfield units that will determine its contribution, along with other voxels in the same projection ray, to the final image. Unlike a MIP image that takes only the highest density value for a given ray, with VR no information is lost or discarded, and every voxel contributes to the final image. The intensity of each pixel can be determined for a tissue and applied to an arbitrary heat scale where it is assigned a color, brightness, and degree of opacity based on that scale. Most workstations contain multiple presets

with predetermined values for heat scale, opacity, brightness, lighting, and window/level function. These presets are used to emphasize different tissue types for different examinations. The image can be rotated and viewed from any angle. Parts of the data set can be edited out (segmentation) or windowed out so they are transparent. In addition, a viewer can define slabs to view only a portion of the data set at a time or define cut-planes to interactively slice into the data set from any angle. These techniques are useful both for vascular imaging and general body imaging (Udupa, 1999).

• *Surface Rendering* Surface rendering (SR), also known as surface-shaded display, maintain a role in biomechanical applications where luminal surface extraction facilitates modeling of complex blood flow phenomena. SR have been supplanted clinically by VR for purposes of visualization and diagnostic analysis. Surface Rendering overcome many of the limitations of MIP by delineating vessel ostia and allowing clear separation of overlapping blood vessels, their greatest limitation is the requirement for application of a single threshold value (Rubin, 2009).

• *Endoluminal Imaging* This technique allows a user to look inside the lumen of a structure as if it were hollow and the user were inside of it. It can be applied to air-containing structures such as the colon, stomach, or trachea, or structures with high density inside such as enhanced blood vessels or a contrast-filled bladder. Once inside, a user can “fly through” the structure, giving the appearance of a virtual colonoscopy or virtual bronchoscopy (Beaulieu, 1999;Vos, 2003).

• *Segmentation Techniques* Segmentation refers to the process of selectively removing or isolating information from the data set with the purpose of better demonstrating certain areas of anatomy or pathology. Segmentation

can be a relatively simple process, but also a time-consuming procedure to manually sculpting out an entire vascular tree. Current 3D workstation manufacturers have developed many powerful tools to make the segmentation process simpler and more automated. Manual, automatic, and semiautomatic image processing tools have been incorporated in many 3D workstations for the purposes of refining and enhancing 3D volume-rendered, surface-rendered, or MIP images. When properly performed, segmentation is an extremely helpful process that improves diagnosis and generates images that are more clinically useful (Van Bemmel, 2004).

Applications in Veterinary Medicine

MDCT provide the possibility of advanced imaging modalities in veterinary medicine. Clinical applications benefit from MDCT technology in several ways. Shorter scan time, extended scan range and improved longitudinal resolution are the most important benefits. Most protocols can be improved from a combination of these advantages.

MDCT is increasingly available in veterinary practice (Bertolini, 2010b). The following applications are described in small animals:

• MDCT Angiography (CTA)

CTA is reported in dogs with congenital extrahepatic portosystemic shunts using a 16-MDCT scanner and various post-processing techniques (Bertolini, 2006a). A 40- MDCT scanner has been used in a comparative study of transplenic CT portography and CTA to examine image quality, opacification of the portal venous system and the liver in normal dogs (Echandi, 2007). Recently, CTA with 16-MDCT combined with 3D post-processing techniques has been described for the detailed depiction of acquired portal collaterals in dogs and cats (Bertolini, 2010a). Oesophageal varices were first described in a dog with an arteriovenous communication between the aorta and the azygous vein using 16-MDCT (Bertolini, 2007). Other recent studies have examined pulmonary angiography protocols using intra-venous injections of contrast medium (Makara, 2011; Habing, 2011). Two reports up to date are describing protocols and anatomic evaluation of normal pulmonary and coronary vessels in dogs using a 64 MDCT (Drees, 2011a and 2011b).

• MDCT of the body

Quantification of adrenal gland volume and attenuation has been described in normal dogs and dogs with pituitary-dependent hyperadrenocorticism using MDCT (Bertolini, 2006b and 2008). Whole-body MDCT has been reported for canine multiple myeloma and diagnosis and clinical staging of myeloma-related disorders (Bertolini, 2007b). Data generated from a MDCT scanner have been used to simulate virtual endoscopy of the esophagus and stomach in dogs (Yamada, 2007a). One study has compared virtual CT endoscopy with conventional endoscopy and conventional 2D CT-imaging in brachycephalic dogs and cats for the assessment of upper and lower airways disease (Oechtering, 2005). Brachycephalic feline noses have been evaluated using CT and 3D models for the influence of head conformation on the course of the lacrimal drainage system (Schlueter, 2009). Virtual CT otoscopy of the middle ear and ossicles in dogs have been reported (Eom, 2008). Upper respiratory system of the dog can be examined with MDCT for the detection of primary laryngeal or tracheal airway obstruction (Stadler, 2011). Volumetric MDCT high-resolution imaging of the lungs in anaesthetized patients with induced transient apnea during the scan allowed for the first description of pulmonary interstitial emphysema in dog (Bertolini, 2009c). MDCT is useful for detection of liver malignancies, characterization of liver lesions suggested by other imaging tests, staging of malignancies, and evaluation of parenchymal perfusion (Bertolini, 2009a; Borsetto, 2011b).

• In vivo anatomy

MDCT has been suggested as an educational support system, to explain anatomy using living animals instead of specimens (Yamada, 2007b). In one study, 16-MDCT was used to assess normal abdominal vascular anatomy in more than 1400 dogs (Bertolini, 2009b). MDCT CTA in combination with silicon endocasts has been used to identify pulmonary veins with echocardiography (Brewer, 2011). University of Montreal introduced a new method improving the teaching in abdominal ultrasound of small animals using 3D models of computed tomography in combination of animation of the movement of the echographic transducer (http://www.medvet.umontreal.ca).

• Applications in Pulmonary Diseases

Computed tomography is more sensitive than radiography for the examination of the feline thorax and could be valuable while a patient with a suspected pulmonary disease has normal thoracic radiographs (Miller, 2007). The determination of the location and extend of lung diseases such as asthma, neoplasia and pneumonia in cats nowadays is based on CT examination (Henao-Guerrero, 2012). Newest technology and advanced methods improved the scanning modalities of the evaluation of tissues, organs and systems such as feline thorax. A new modality of CT scanning technique of the feline patient without sedation using the VetMouseTrap™ , mostly in patients with respiratory distress, is reported (Oliveira, 2011). Up to date there are few reports for the anatomic evaluation of the feline bronchial and vascular structures. Computed tomography could provide more information of the bronchial, vascular structures, intrathoracic and extrathoracic structures.

In human medicine MDCT of the chest is used for the characterization of pulmonary infiltrates unclear/suspected in chest X-ray, evaluation of metapneumonic or parapneumonic complications (abscess, empyema, mediastinitis), unfavorable course of pneumonia in pediatric patients, early diagnosis of atypical pneumonia in immunocompromised patients, evaluation of accompanying manifestation in lung tuberculosis and biopsy of lung infiltrates under CT-guidance (Horger, 2006).

Multislice CT has overcome past limitations of helical computed tomography . Scan length and spatial resolution can be simultaneously optimized with multislice CT, contrast medium can be saved, evaluation of

large anatomic areas and vessels smaller than 1 mm become possible. Tomographic examination of the thorax can evaluate the trachea, heart and great vessels, mediastinum, lungs and bronchi, pleura and thoracic boundaries. The diagnostic imaging examination of the lung parenchyma can detect malformations (bronchial collapse), trauma, infection (bronchitis, bronchiectasis, bronchial foreign body, lung infection and inflammation, granulomatous lung diseases and abscess formation), lung fibrosis, lung lobe torsion, pulmonary edema, neoplasia (primary pulmonary and bronchial and infiltrative tumors, metastastic neoplasia) and pulmonary vascular embolic events and infarction (Schwarz, 2011). Image processing techniques, and, in particular, volume rendering have made image presentation faster and easier. Multislice CTA exceeds MRA in spatial resolution and is now able to display even small vascular side branches (Hurst, 1999). CTA main indications will be aortic diseases, suspected pulmonary embolism but also renal artery stenosis, preoperative workup of abdominal or cerebral vessels, and acute vascular diseases. Multislice CTA will become a strong competitor of other minimally invasive vascular imaging techniques. The diagnosis or exclusion of acute PE is the most common and important application of CT pulmonary angiography. The possibility of fast scan acquisition and the high spatial resolution of modern CT techniques make this procedure ideally suited for the greatest majority of congenital and acquired, acute and chronic disorders of the pulmonary arteries in human medicine (Kuettner, 2006, Kopp, 2006). The high-resolution multi-slice computed tomography angiography (HRMS-CTA) is a new imaging method characterized by a precise isotropic imaging of any bronchial-cardiovascular system structure. In human and veterinary medicine MDCT provides the radiologist with unparalleled capabilities for detailed analysis of normal anatomy and pathology. However, as with any new technology or advances

in imaging there are potential pitfalls and limitations and despite major progress in the scanning of organs through the well-defined phase of enhancement, soft-tissue contrast resolution can remain critical in some many circumstances.

1.2 Computed Tomography Pulmonary Angiography in Small animal

CTPA is the most accurate method for the evaluation of pulmonary arteries and is well known as the gold standard for detection of pulmonary emboli in human medicine. Limited bibliography references in veterinary medicine in combination with different scanning and contrast-medium administration protocols are the main causes of a non well defined subject in our science. A study of comparison of CTA and MRA in canines, concluding that CTA is more sensitive than MRA for the detection of PE (Hurst, 1999). The effect of saline chase injected in two different rates in a canine experimental model for pulmonary CTA , concluded that saline chase prolongs the duration of plateau and delays peak enhancement of the pulmonary artery and aorta (Lee, 2007). The success of CTA in small animal imaging depends from many critical factors, including the iodine dose, iodine concentration, volume, correct time of data acquisition relative to the contrast medium injection, and selection of proper scanning parameters (Bertolini, 2010). An automated bolus tracking program and a single contrast medium injection rate results in rapid and consistent imaging of the canine pulmonary vasculature (Habing, 2010). Till 2011 no references for the use of 64 detector scanner in veterinary medicine were reported. The evaluation of the coronary arteries and pulmonary arteries in normal dogs with 64 multidetector row CT provided many details about the anatomy of these vessels (Drees, 2011). The effect of contrast medium injection duration on pulmonary artery peak enhancement and time to peak enhancement, concluded that the injection duration is a key feature in a CTA injection protocol (Makara, 2011). A 16 slice CT scanner and silicon endocasts were

used in order to identify pulmonary veins with echocardiography (Brewer, 2012).

1.3 Anatomical references

Pulmonary disease is a common disease of the feline patient. The last decade advanced imaging modalities have studied these diseases. Computed Tomography could provide detailed data of the feline thorax. Despite these last modalities normal feline anatomy of the thorax has been poorly documented either from radiologists and anatomists. Many authors describe the gross anatomy of the bronchial tree without precise description of the smaller branches and they don't introduce an official nomenclature. Few references have been published to nominate small branches of the bronchial tree (Ishaq, 1980, Caccamo, 2006) . Till to date does not exist a worldwide recognized model for the description of bronchial, arterial and vein main branches and their segmental.

Dimensions of the bronchial, arterial and vein structures have not yet been reported with equal methods and procedures. Bronchial tree of various species, among them also the feline with description about the diameter of each structure is reported (Horsfield, 1986, Schlesinger, 1981). Up to date all the references are a comparison of many species and there is not one study that is dedicated to feline anatomy. An anatomic-topographic and morfometric study of the feline bronchial system and its circulatory system more detailed is recently presented (Coccolini, 2012). In this last study of 13 cats, a precise nomenclature of the bronchial branches and their satellite arteries and veins has been documented. Feline principal bronchus, lobar and segmental bronchial branches tend to have a straight and attached relation with their satellite arteries till the level of segmental and more fine branches. Veins don't have this attached relation and usually after the bifurcation or in

the segmental branches tend to have a wider relation with the bronchial satellite structures. Arteries are divised : at the right cranial lobe have a dorsal-lateral aspect to the bronchus, right medial lobe have a lateral aspect, accessory lobe a ventral aspect, right caudal lobe satellite artery of the main branch has a ventral-lateral aspect and the arteries of the branches have a lateral aspect. Arteries of the left cranial lobe tend to have a dorsal-lateral aspect for the cranial branch and lateral aspect for the caudal one. In the left caudal lobe arteries have the same aspect as in the right caudal one. Veins tend to have a medial position respectively to the bronchus with exception of the accessory lobe in which they have a dorsal aspect. The morphometric study of the feline bronchial structures has evidenced the major dimension respectively to the satellite vascular structures. Arteries have wider diameter than veins fact that did not correspond to the previous studies. Considering morphometric studies (McLaughlin, 1959, Schlesinger, 1981) the feline bronchial architecture is a mixed type, accessory lobe has a dichotomic type while all the other lobes have a moderate monopedial type.

While CT was introduced in veterinary medicine a first report for the anatomy of the feline thorax and abdomen comparing the results of computed tomography and cadaver anatomy was published in late 90's (Sammi, 1998). High-resolution CT was used in order to introduce bronchial lumen to pulmonary artery ratio in anesthetized ventilated cats with normal lungs (Reid, 2012).

EXPERIMENTAL STUDY

2.1 Material and Methods

• Enrolment

House cats that were examined at “Alphavet” private veterinary clinic in Athens were considered for enrolment in this study. Enrolment consisted of 20 cats (12 males and 8 females, age range:1-6 years old) and included cats that have been brought to the clinic for a check-up routine. All patients had to undergo the following procedures within 5 days of each other, to meet the inclusion criteria:

1. Clinical evaluation
2. Complete hemato-biochemical work-up
3. Urine and fecal analysis
4. Multidetector-row computed tomography of the entire thorax and anterior abdomen
5. Owners of all cats included in the study provided informed consent.

Our criteria of inclusion were initially a normal clinical examination. Full history of every the cat including nutrition, vaccination, living conditions and antiparasitic treatment was performed. Only cats that had normal clinical condition, full vaccinated, absence of past respiratory pathology, full antiparasitic treatment, normal hematobiochemical exams, normal urine and fecal analysis and finally normal CT examination of the thorax were included in the study.

The presence of intrathoracic abnormalities and in particular pulmonary lesions and mild pneumothorax were our criteria of exclusion. Six of the twenty cats of the study were excluded. Five of them showed older pulmonary pathology with solitary or multiple pulmonary nodules and one of them had mild spontaneous pneumothorax.

• Multidetector-row Computed Tomography scanner technology

The study was performed with a 64-row computed tomography (MDCT) system Aquilion 64 (Toshiba Medical Systems, Europe). Acquilion 64 is a Rotate/Rotate 3rd generation scanner. The system is capable of both spiral/helical and multislice scanning. This technology could provide slice thicknesses in helical mode of 0,5 mm, 1mm, 2mm, 3mm, 5mm, 7mm, and 10mm. The available beam energies are 80kVp, 100kVp, 120kVp and 135kVp. The system has a solid state detectors 64 in number of 0,5mm. XYZ modulation (Sure Exposure) software is the dose reduction option. Acquilion 64 has an excellent slice thickness, spatial resolution and temporal resolution. The Aquilion offers the SureExposure 3-D dose-modulation technique, which automatically adjusts the exposure parameters based on the patient's measured x-ray composition, operating on the principle of keeping the noise level constant. In addition, pediatric protocols are automatically triggered by the patient's date of birth.

The system uses two bow-tie filters to shape the x-ray beam before it is incident on the patient. The bow-tie filter is automatically selected to match the field of view. These filters help optimize the dose to the clinical requirements. During image acquisition, the Surescan feature displays a subnet of the images to the operator at 12 fps, so the user has feedback and can stop the exam if necessary.

Toshiba relies on Vital Images' Vitrea workstation for most applications and develops applications in close partnership with Vital Images. The Vitrea offers a comprehensive range of clinical 3-D applications. These include full cardiac analysis, brain perfusion, vessel analysis, computer-aided lung

nodule detection (using the R2 CAD algorithm, which has FDA premarket approval), and virtual colonography.

Cats were positioned in sternal recumbency on the CT table, head first and with the limbs extended (fig.1.1). The direction of the scanning was cranio-caudal from the thoracic inlet till the caudal margins of the left kidney. An unenhanced scan performed in helical mode using pediatric protocol with 0,5 mm slice thickness, 0,5 rotation time, 120 kVp and 50 mA. Placing the ROI at the descending aorta at 115 HU sensitivity and with a bolus triggering technique in inspiration apnea, for a scanning time of 6 seconds in all cats we had a constant inspiration apnea using peak inspiration pressure (PIP) maintained at 20 cm H_2O, we acquired volume data. A standard delay scanning of 80 sec and 240 sec following contrast medium injection was performed in the same scanning range.

fig.1.1: Positioning of the cat in sternal recumbency and head first

• Anesthetic protocol

Food and water was withheld from cats four hours before the MDCT procedures.

For premedication 25μg/Kg of dexmedetomidine (Dexdomitor, Orion corporation, Orionintie, Finland) and 0,1 mg/Kg of butorphanol (Dolorex, Intervet Inc, Merck animal health, US) were injected intramuscularly (im). While the cat was in sternal recumbency an intravenous catheter (20G) with a 3-way stopcock was placed in the right cephalic vein. 1-2mg/Kg of Propofol (Propofol-lipuro 1 %, B.Braun Melsungen Ag, Germany) were injected intravenously (iv) to effect. Prior to intubation, 0,2 ml of lidocaine was topically applied to the larynx to prevent laryngospasm. After induction to anesthesia the trachea was intubated. Anesthesia was maintained with isoflurane (IsoFLo, Abbott, Berkshire UK) in oxygen through a bain breathing system, with an oxygen flow-rate of 2 L/min. The vaporizer dial was set to deliver 1.5% isoflurane. The anesthetic machine used was a Drager Titus with a Bourdon gauge. Throughout the procedure heart rate (HR), respiratory rate (RR), arterial haemoglobin oxygen saturation (SpO2), inspired carbon dioxide concentration (FiCO2), partial pressure of PE′CO2, and end-tidal isoflurane (ETiso) concentration (Datex Ohmeda), were constantly monitored. At the end of the procedure atipamezole (Antisedan, Orion corporation, Orionintie, Finland) was injected im.

• Contrast Medium administration strategy

Iobitridol (Xenetix 300mg/ml, Guerbet, Cedex, France) is an iodinated contrast agent, nonionic water soluble tri-iodinated that we used in this study.

A saline flush iv of 3 ml/Kg with a rate of injection 2 ml/sec performed twice , once before the injection of contrast medium and one immediately afterwards. Contrast medium of 150mg iobitridol/ml was injected throught a dual-barrel injector, system with heating cuff, extravasation detection device and communication interface between the scanner and the injector. CM was injected with a constant rate of 2ml/sec and maximum pressure of 300 lb/in^2. Temperature of CM was always at 37 C.

A fast acquisition injection strategy was followed with a bolus triggering software in order to perform CTPA. As above mentioned ROI was placed at the descending aorta with a sensitivity of 115 HU. While CM was injected, a series of low dose non incremental images were obtained and the attenuation within the ROI was monitored while inspiration apnea was performed during scanning. The CT acquisition initiated when the desired enhancement was reached.

• On-line and Off-line analysis

Laser pointers of the gantry allowed the perfect position of the cat and to obtain in each scanogram a scanning range from the head till the pelvis (fig.1.2, 1.3). During the first direct scan we evaluated gross pathology, scanning range, motion artifacts and detecting the descending aorta. During the CTPA scanning we could evaluate the successful contrast enhancement (fig.1.4). Delay scanning was always performed in order to evaluate wash out of the contrast medium. All volume data and reconstructed images with an original resolution of a 512X512 matrix size were automatically transferred to a freestanding workstation for post-processing. For this purpose a Vitrea workstation (Vital images, version 4.1.14.0) was used in order to obtain volume rendering images using advanced software (fig.1.5, 1.6, 1.7, 1.8). The bronchial lumen and the vessels were evaluated at the scanning timing during arterial enhancement and inspiration apnea. A qualitative study was performed to better understand the anatomy and to visualize the correlation between bronchial lumen and vessels. In the same study the segmental arterial branches were identified and counted. The qualitative study includes the measurement of the diameter of the bronchial and vascular structures. A MIP protocol (fig. 1.9, 1.10, 1.11) was used to evaluate and understand the anatomy of the bronchial lumen and vascular correlation. This fundamental first path improved the knowledge of the anatomy in order to evaluate precisely the bronchial lumen and the vessels of the thorax. A 27inch iMac, using a medical dicom viewer Osirix (Osirix Imaging Software, version 3.3.2, 32 bit, Osirix Foundation, Los Angeles, California) was used in order to measure the diameter of the vascular and bronchial structures of the thorax at the CTPA scanning time. Every cat was

evaluated in a MPR protocol in order to place measurements in sagittal, axial and coronal plane (fig.1.12). Each structure was measured four times for each diameter(two dimensions in axial plane, one in sagittal and one in coronal) optimizing the axis at the center of the tubular structure. Every structure was evaluated with the same method in all the cats of this study. An inner to inner edge protocol was used for all the measurements. The vascular structures were evaluated based on the bronchial ramification. To follow the course of vessels during real-time evaluation, every arbitrary plane is interactively chosen in a fourth oblique view. While we evaluating the bronchial lumen or the vessels we had to manually optimize different standard filters for bronchial lumen and vessels in order to minimize blooming artifact and measurements errors.

All the volume data were reconstructed in volume rendered images in order to obtain a morphometric overview of the bronchial and vascular structures of the thorax. Multiplanar reformatted reconstruction (MPR), surface rendering, maximum intensity projection, volume rendering and endoluminal segmentation were the basic image rendering techniques that we used in order to evaluate the whole thorax and its structures before we proceed in measurements. The better understanding of each anatomy improved our knowledge and protocol of measurement. A medical dicom viewer could produce a multiplanar reconstruction in which we could adjust the window level individually to optimize the structure that we measure. With this method we could obtain four measurements for every structure in the same time that we had optical visualization of the three planes

fig.1.2: Scanogram in coronal plane

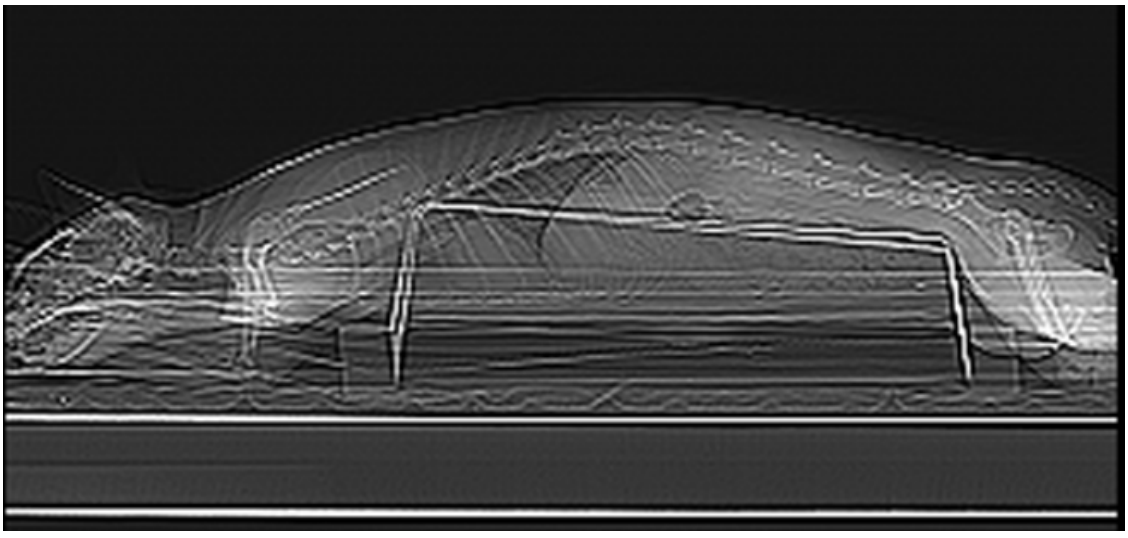

fig.1.3: Scanogram in sagittal plane

fig.1.4: On line analysis during the procedure: primary evaluation of the feline thorax during scanning

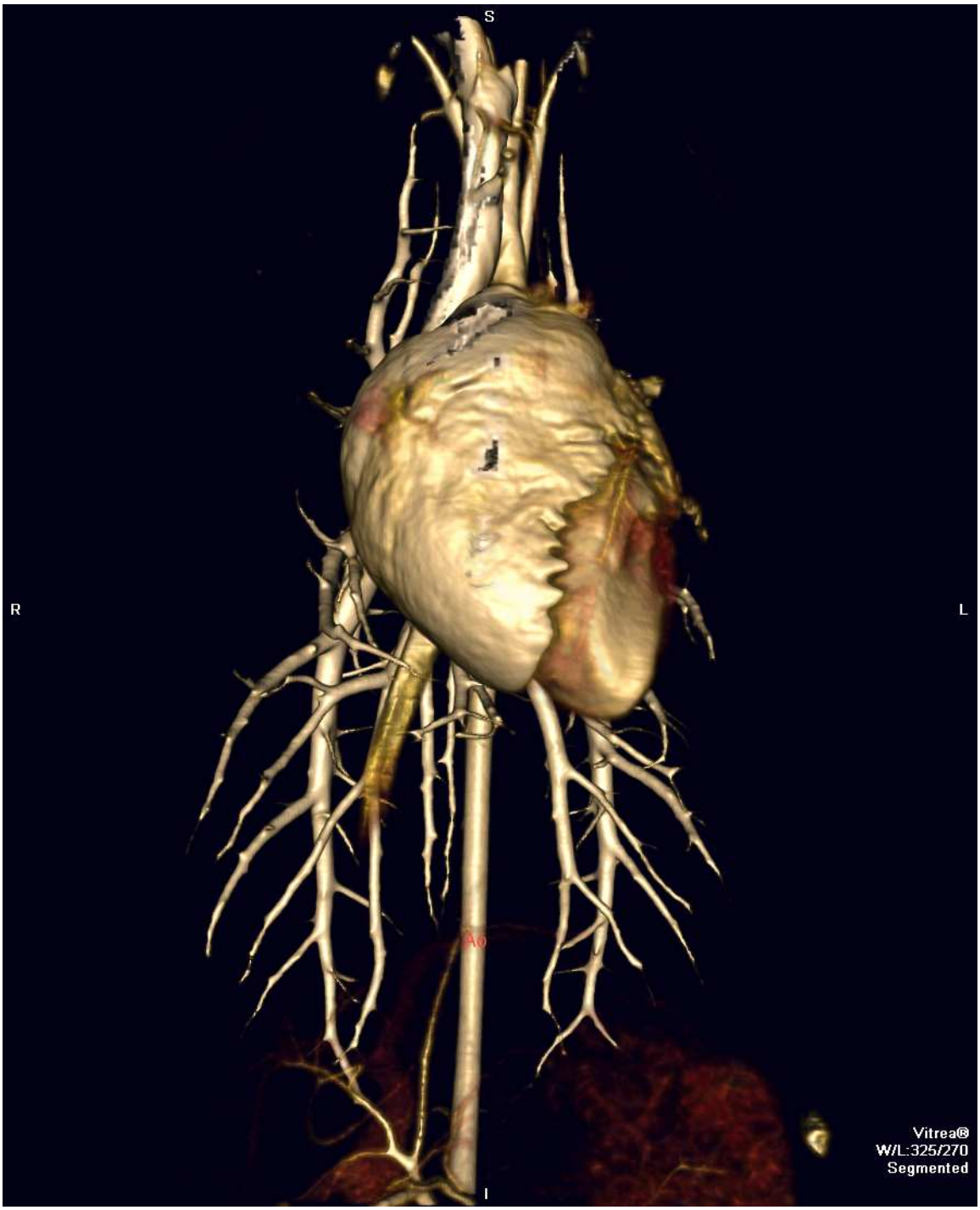

fig.1.5: 3D volume rendering: ventral view of the pulmonary vasculature. (Ao:Aorta)

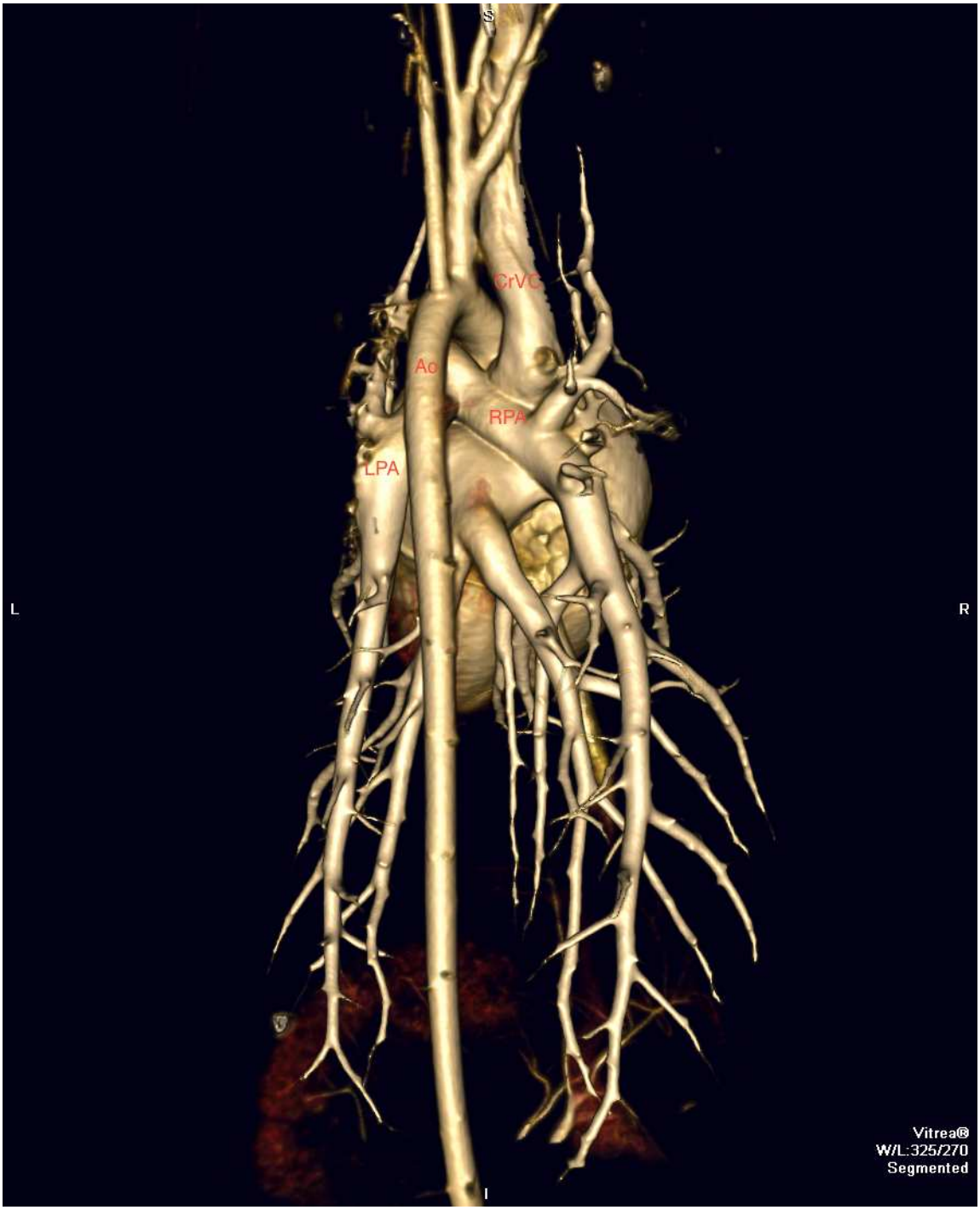

fig.1.6 : 3D volume rendering dorsal view of the pulmonary vasculature (Ao:Aorta, CrVC: cranial vena cava, RPA: right pulmonary artery, LPA: left pulmonary artery)

fig.1.7 : 3D volume rendering left lateral view of the pulmonary vasculature (Ao:Aorta, LPA: left pulmonary artery)

fig.1.8 : 3D volume rendering right lateral view of the pulmonary vasculature (Ao:Aorta, RPA: right pulmonary artery, CVC: caudal vena cava)

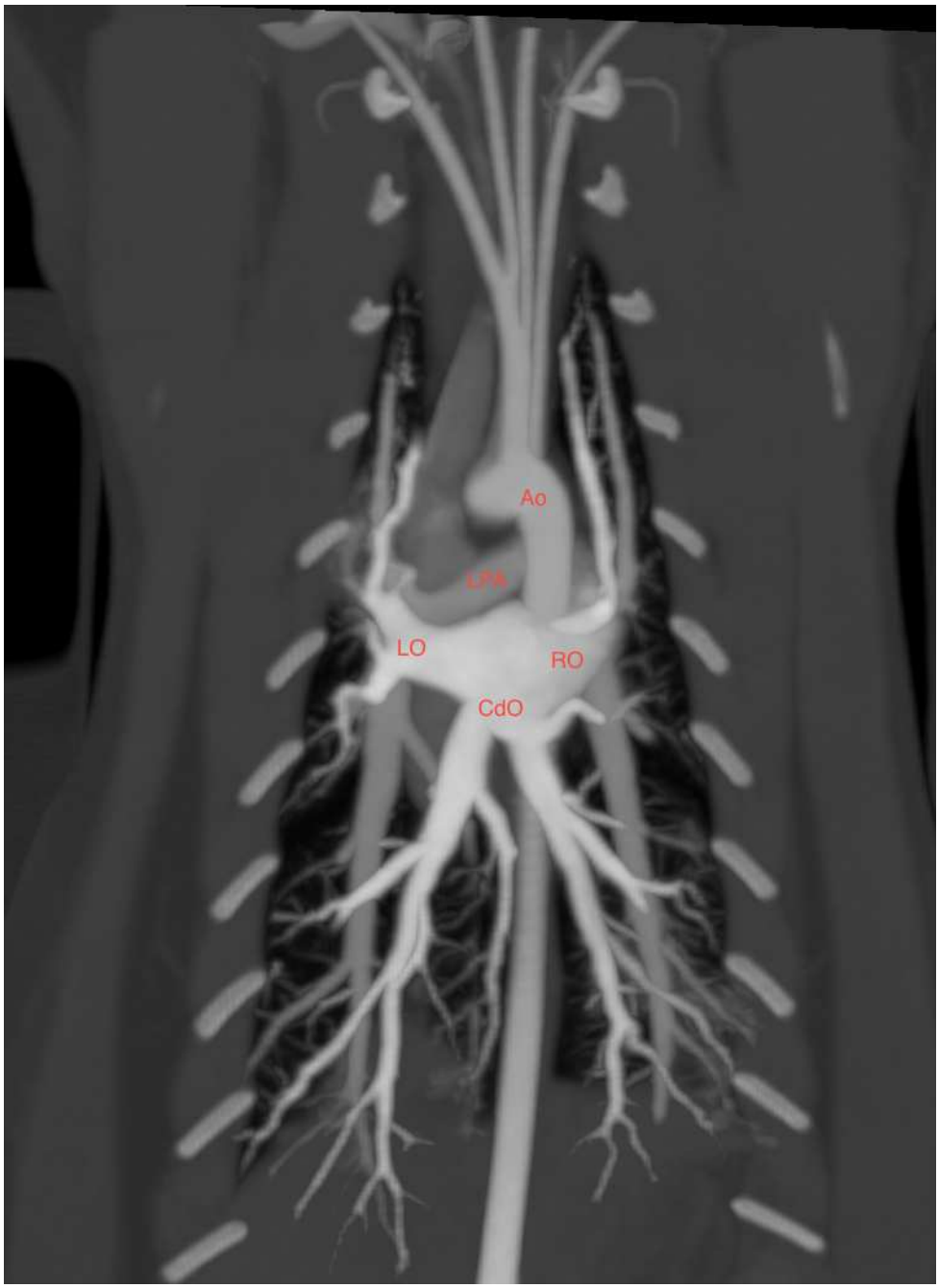

fig.1.9: MIP reconstruction of the pulmonary vasculature in coronal plane (Ao:aorta, LPA: left pulmonary artery, LO: left ostia, CdO: caudal ostia, RO:right ostia).

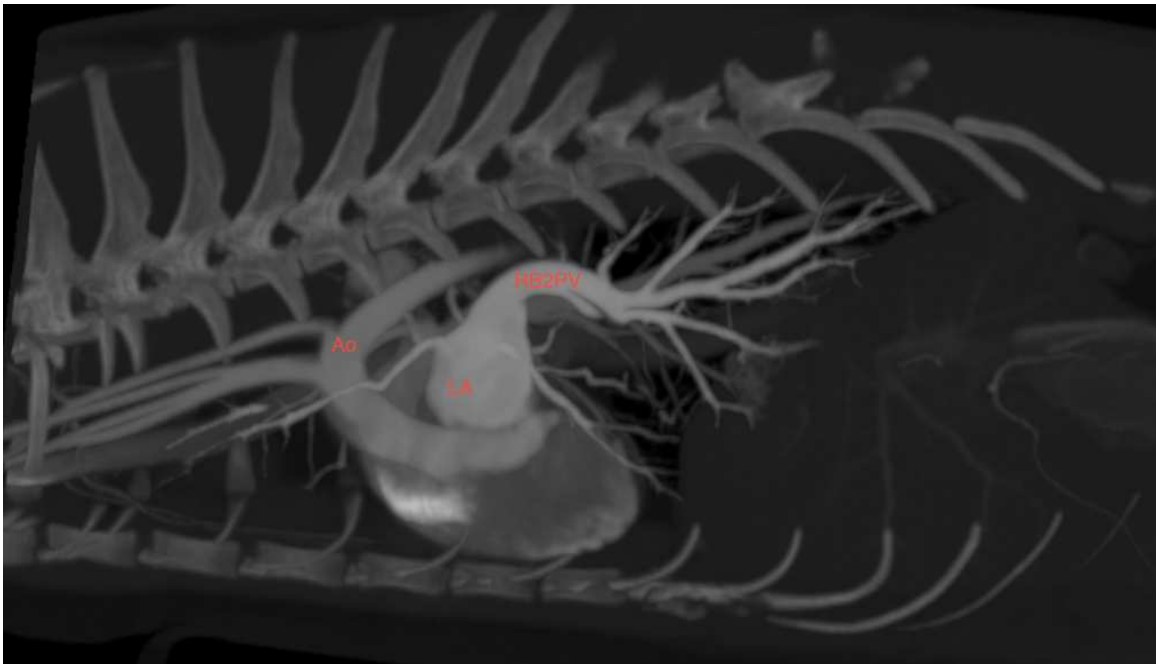

fig.1.10 : MIP reconstruction of the pulmonary vessels in sagittal plane (Ao:aorta, LA:left atrium, RB2PV: left caudal pulmonary vein).

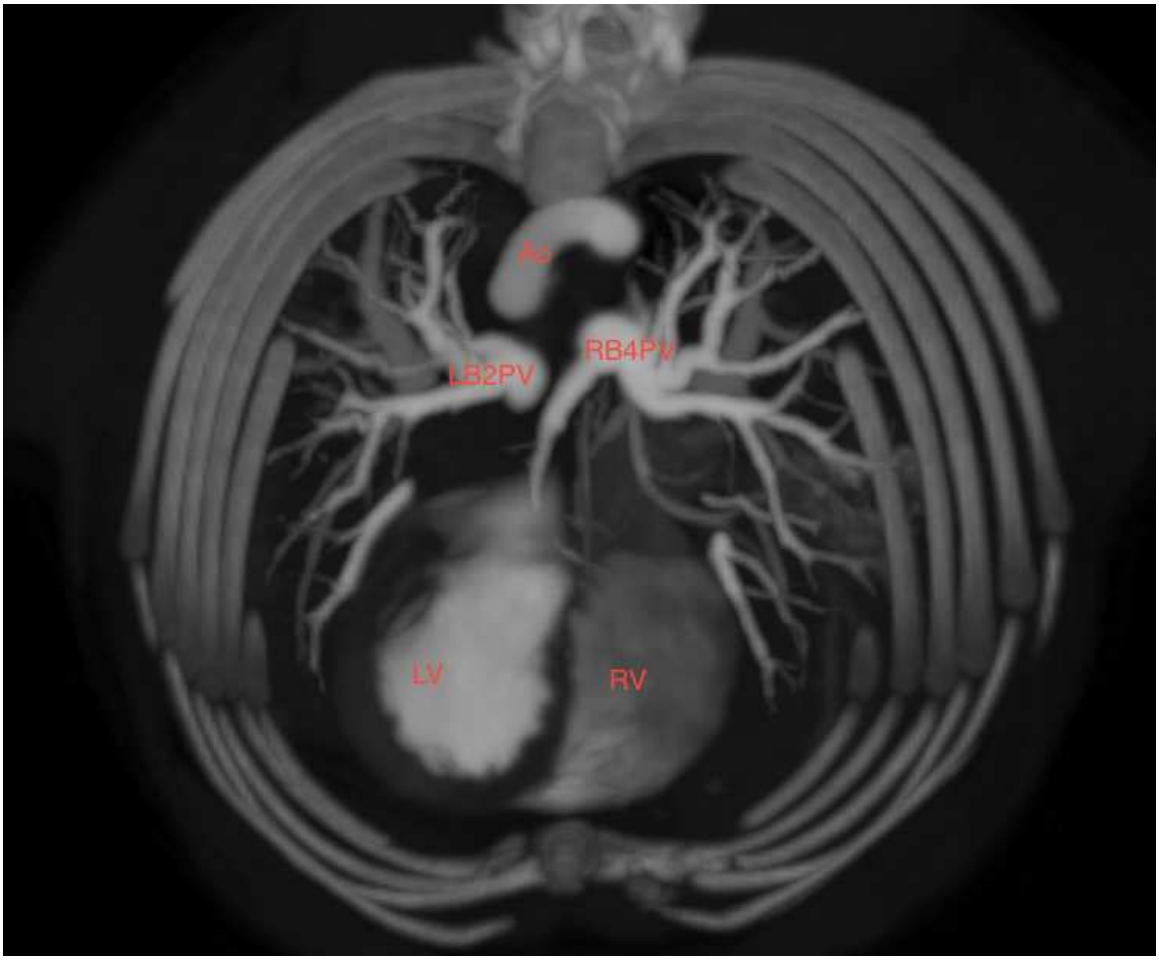

fig.1.11 : MIP reconstruction of the pulmonary vessels in axial plane (Ao:aorta, LB2PV:left caudal pulmonary vein, RB4PV:right caudal pulmonary vein, LV: left ventricle, RV:right ventricle).

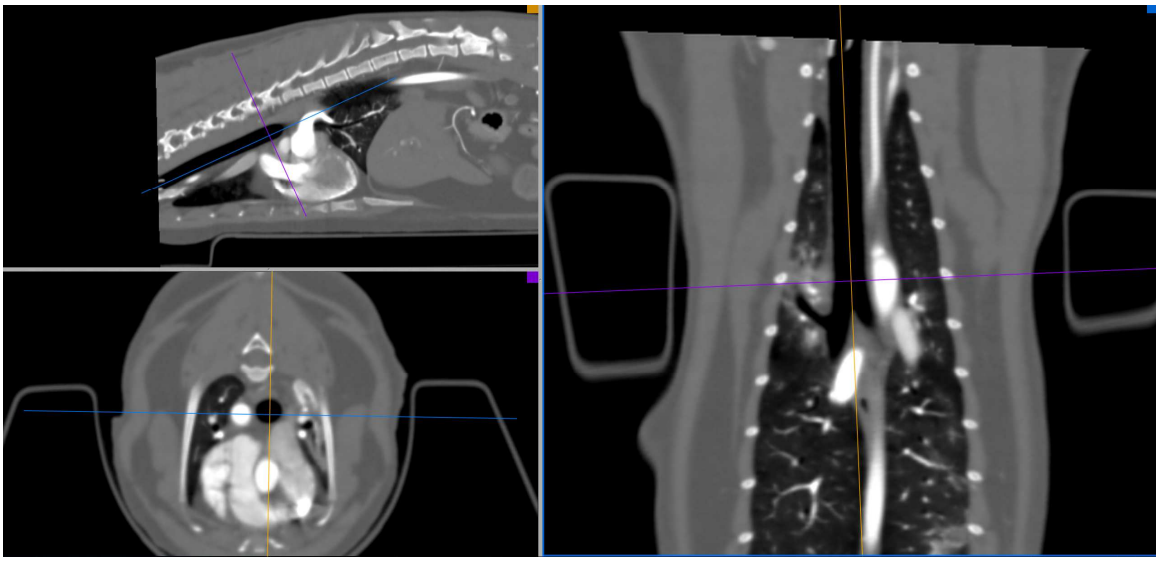

fig.1.12 : A three plane view focusing on the trachea before the bifurcation in order to measure the tracheal diameter

• Statistical analysis

In order to select the values that we need to compare we made seven categories for the structures that we measured. We separate the left from the right lung and the trachea. This division was made every time for the bronchial lumen, arteries and veins. The seven categories that we produced are trachea, right lung, left lung, pulmonary arteries of the right lung, pulmonary arteries of the left lung, pulmonary veins of the right lung and pulmonary veins of the left lung.

A linear generalized estimating equations analysis using a Pearson test we correlated in one test dimensions with age and a second one dimensions with weight. All analyses were performed with statistical software. Values of $P < 0.05$ were considered significant.

2.2 RESULTS

Pulmonary angiography was performed successfully in all the included cats of the study. Six of the twenty cats were excluded due to detection of pulmonary nodules and in one case of mild spontaneous pneumothorax. A 64 MDCT scanner is capable to produce excellent images of the feline thorax in a 7 seconds inspiratory breath hold. The possibility of using pediatric presets and slice thickness of 0.5 mm produced high quality images not only in axial plane but also reconstructions in MPR, MIP and 3D volume rendering . This advanced technology of MDCT could provide a high quality images and reconstructions using low-dose scanning and indeed 120kVp, 50 mA, 500 milliseconds rotation time and a matrix of 512X512 were sufficient for the study of the feline thorax. Bolus triggering technique by placing ROI at descending aorta (sensitivity of 115 HU) and by injection of contrast medium (150mg/ ml) via a dual barrel power injector (inj rate: 2ml/sec, max. pressure: 300 lb/in^2) showed an homogeneous enhancement of the pulmonary vasculature in all the examined cats. None intolerance reaction was recorded in this study due to contrast medium. A four hours food and water withheld from cats did not revealed any gastrointestinal problems during or after the examination. The anesthetic protocol did not produce any abnormalities during sedation, scanning or after the examination. An oxygen flow rate of 2 L/min and by setting the vaporizer dial to deliver 1.5% isoflurane kept all the cats of the study without breathing abnormalities during the procedure. The bain breathing system that was connected with a Bourdon gauge gave us the possibility of introducing an inspiration apnea of 8 seconds with a constant pressure of 20 cm H2O. No records of severe cardiovascular depression and overdistended lungs were noticed.

BRONCHIAL LUMEN

Immediately after the tracheal bifurcation origins the right principal bronchus with a mean diameter of 6.05 mm. Right cranial lobe detaches and after that origins the medial lobe. Principal lobe continues as right caudal lobe which detaches also the accessory lobe. The right cranial lobe detaches a dorsal-lateral and a ventral branch. The dorsal-lateral one bifurcates in a dorsal and in a ventral branch. The right cranial lobe has a cranial direction with multiple dorsal and ventral segmental branches . The right middle lobe origins directly from the right principal bronchus after the right cranial lobe. The middle lobe bronchus runs ventral-caudal close to the heart and bifurcates unequally in a ventral-cranial and in a ventral-caudal branch. Segmental branches arise cranially and caudally with progressive minor dimensions. Accessory lobe origins from the right caudal bronchus and bifurcates in a ventral-medial and in a caudal branch. Both branches divide multiple dorsal and ventral segmental branches. The direct continuation of the right principal bronchus provides the right caudal lobe. The right caudal lobe divides a ventral branch, a ventral-caudal branch and finally continues directly as a caudal branch. The ventral branch bifurcates in a ventral-cranial and in a ventral-caudal branch. The caudal branch provides finally two minor branches one caudal-dorsal and one caudal-ventral. Seven dorsal segmental branches are observed from the right caudal lobe. A ventral segmental branch origins from the ventral-caudal branch and runs ventral and medial. Immediately after the tracheal bifurcation origins also the left principal bronchus with a mean diameter of 5 mm. The LPB provides the cranial and caudal left lung lobes. The left cranial lobe origins after the tracheal bifurcation and provides immediately one cranial-ventral branch and one caudal-ventral. Segmental branches arise dorsally and ventrally from

both cranial and caudal branches. Direct continuation of the left principal bronchus, after detaching the left cranial lobe, is the left caudal bronchus. During its path detaches one ventral branch, one ventral-caudal branch and continues straight as caudal branch. Dorsal and ventral segmental branches arise from the left caudal lobe. In cat No3 motion artifact made impossible to evaluate the lobar branches of both left and right caudal lobes. The ventral cranial lobar branch of the middle lobe in Cat No 5 had dimensions similar to the voxels and did not let us to evaluate it, fact that was noticed also for its satellite vein. A monopedial model of the accessory lobe is seen Cat No8 (fig 2.1).

fig.2.1 a. Accessory pulmonary artery is separating in a dichotomic aspect in RB3D1 and RB3V1 pulmonary artery in 13 of 14 examined cats, b. cat No 8 shows a monopedial aspect of the accessory pulmonary artery (RPA:right pulmonary artery, RtCdPV:right caudal pulmonary vein, RB3: right accessory pulmonary artery, blue arrow: accessory pulmonary vein, orange arrow: accessory pulmonary artery).

PULMONARY ARTERIES

Right cranial lobe has two main arteries one for the ventral (main branch) and one for the dorsal-lateral one. These two arteries origin in different position directly from the right pulmonary artery. The right cranial lobe artery shows a cranial direction detaching segmental branches dorsally and ventrally. The artery of the right cranial lobe has an initial ventral-medial aspect to the cranial lobe and at the level of the fourth rib takes a dorsal-lateral position. The first arterial dorsal segmental branch of the RB1 shows a medial aspect to the bronchus while all the other branches have a lateral one. The first ventral arterial segmental branch demonstrates a lateral-ventral direction while all next ones have a ventral direction. At 6 mm from the detachment of the satellite artery of the RB1 origins directly from the right pulmonary artery the satellite artery of the dorsal-lateral branch, which has an immediate bifurcation that follows the dorsal and ventral branches with both vessels to have a caudal-medial aspect to the bronchial branches. The right middle lobe lobar artery runs ventral and lateral to the bronchus till bifurcates unequally to a ventral cranial and a ventral caudal. Multiple segmental branches arise with progressive minor dimensions running ventrally and have a lateral aspect except the first one that shows a dorsal one. Accessory lobar artery runs ventral to the bronchus and medial till bifurcates in two branches, one ventral-medial and one caudal. Both branches continue with a bifurcation in one dorsal and ventral minor branches. Segmental arteries are visible and positioned dorsally to the bronchial. Caudal lobar artery runs ventral-lateral to the bronchus providing segmental branches that follow the bronchial diramation. In particular the first two dorsal branches origin cranially to the bronchi while the rest origin caudally. The artery of the ventral branch runs cranial to the bronchial

branch while the other ventral branches have a lateral position. Segmental branches arise from the ventral, ventral-caudal and caudal branch. Directly from the left pulmonary artery origin, two of the four main arteries that we can distinguish for the left cranial lobe, the cranial ventral and the caudal ventral lobar arteries. Two arteries that are part of the cranial part origin from the cranial lobar artery that run over the bronchus, laterally and then ventral. The left caudal pulmonary lobar artery runs attached and dorsal-lateral to the bronchus while detaches dorsal segmental branches, one ventral branch, one ventral-caudal and continues as caudal branch. Segmental branches arise from the ventral, ventral-caudal and caudal branch. A sudden cut-off of the RB1V1 pulmonary artery and vein is seen in Cat No3 , Cat No 4 and Cat No 9 (fig.2.2). A detectable filing defect in the caudal left caudal and right caudal pulmonary artery is seen in Cat No5 (fig.2.3). In the same cat the right cranial pulmonary artery has minor length than the others.

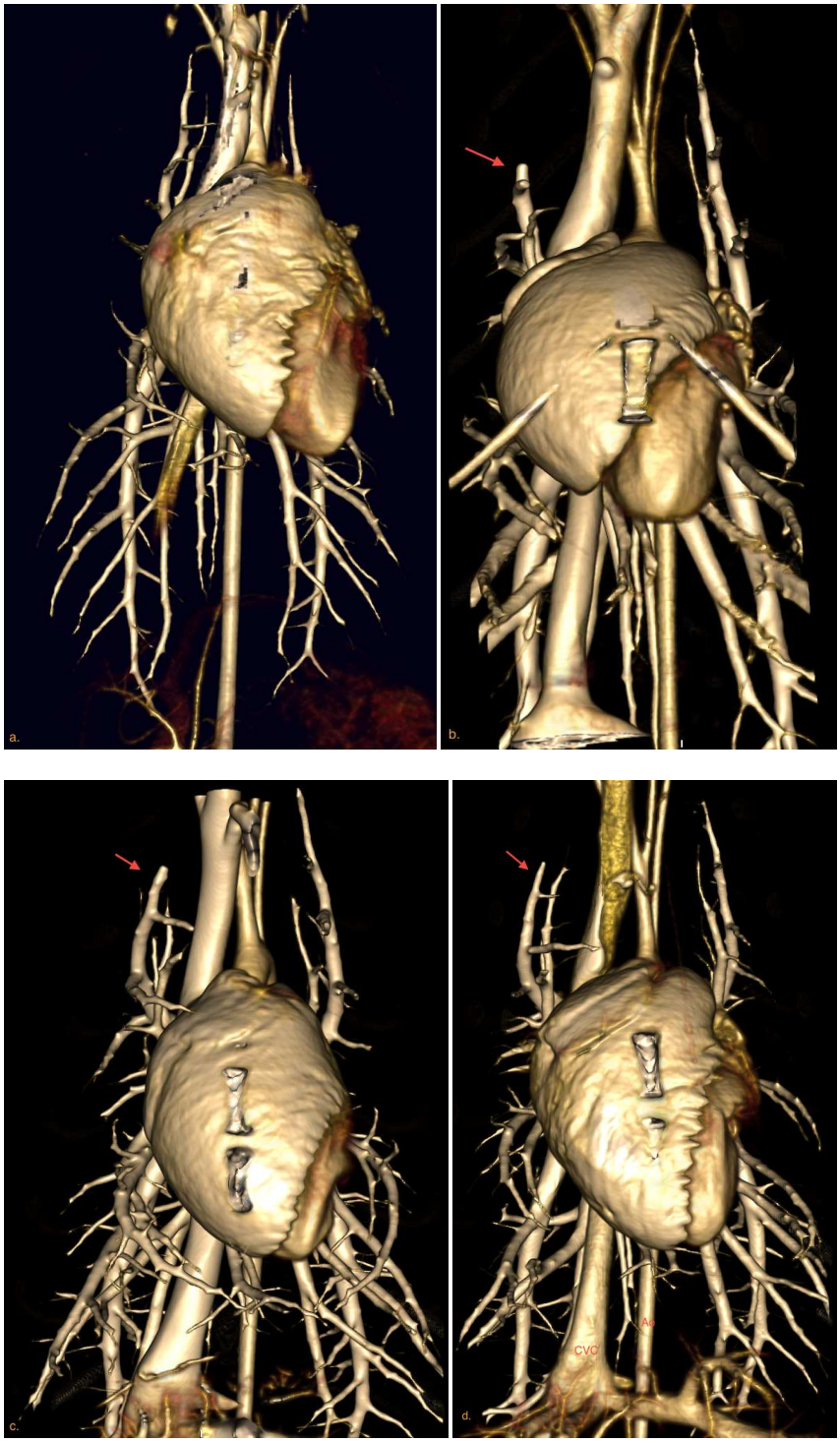

fig.2.2:a. RB1V1 pulmonary artery has almost the same length with the LB1D1 pulmonary artery, in figures b, c and d, a sudden cut off of the RB1V1 pulmonary artery and vein is present

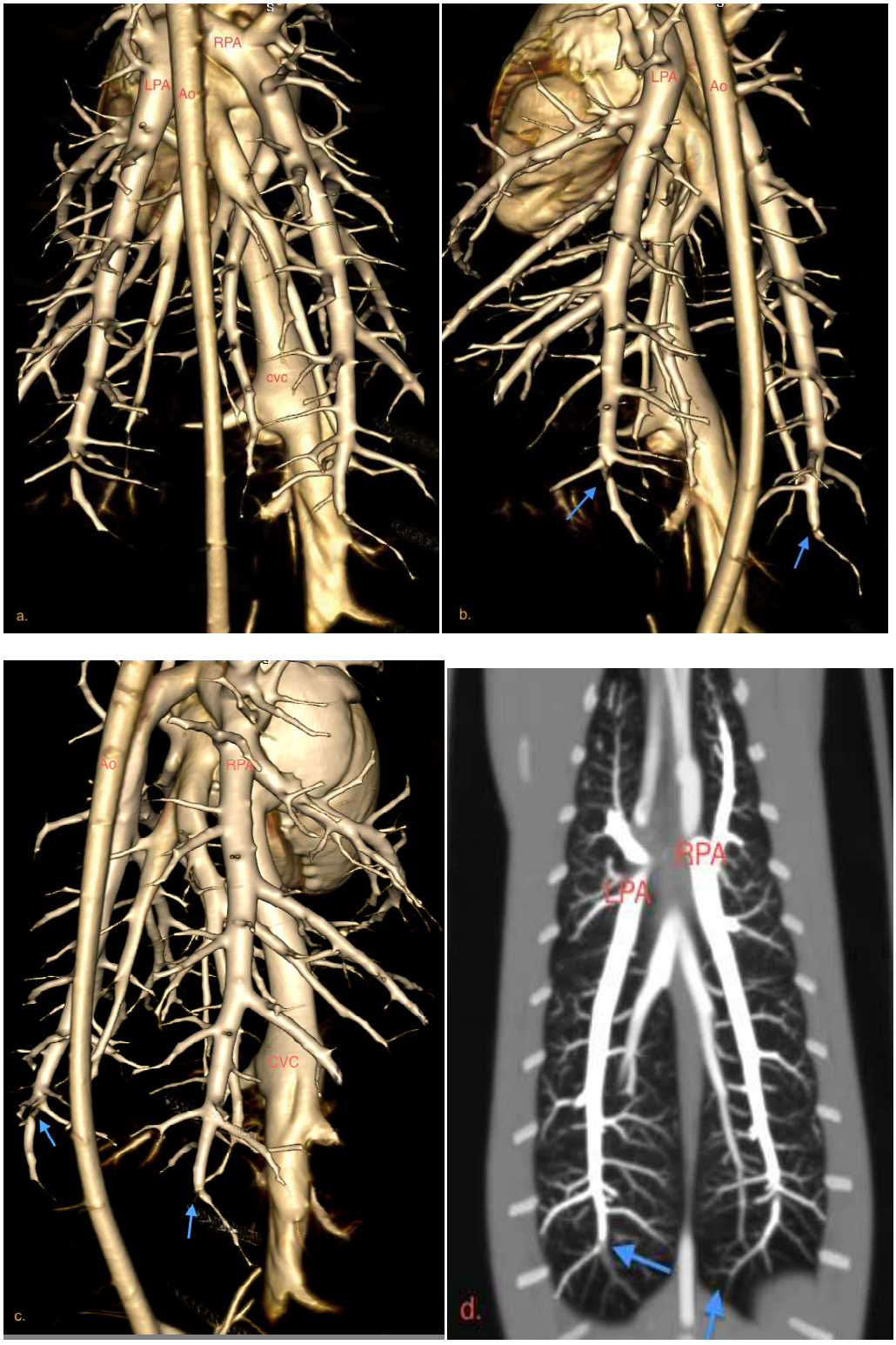

fig.2.3: Filling defect (blue arrows) at the caudal portion of the left caudal and right caudal pulmonary artery is seen in the 3D volume rendering as a shortening of the vascular diameter (a) or a cut-off of the vessel (b,c). MIP projection in coronal plane demonstrate the filling defect in the peripheral pulmonary arteries (d). (Ao:aorta, CVC:caudal vena cava, RPA:right pulmonary artery, LPA:left pulmonary artery)

PULMONARY VEINS

Right cranial lobe vein anastomose with the right middle lobe pulmonary vein and consist the right ostia. The right cranial lobe pulmonary vein has two branches that follows the ventral and dorsal-lateral bronchus, which veins anastomose before attaching the right middle lobe pulmonary artery. The ventral bronchus has an attached and with medial aspect vein, which vein receives multiple dorsal and lateral segmental branches. The right cranial pulmonary vein branch of the dorsal-lateral bronchus, that is located cranial-ventral and not attached to the bronchus, bifurcates in a cranial and in a ventral branch. The cranial one initiates cranial-ventral to the bronchus and continues dorsal-medial. Middle lobe lobar vein runs medially and attached to the bronchus for half of its length where takes place cranially till consist with the cranial lobe pulmonary vein the right ostia. Segmental branches follow medial-ventral the bronchial one. Similar to the arterial, ventral-cranial and ventral-caudal branches veins are positioned medially and ventral. Accessory lobar vein runs dorsal to the bronchus and jets into the right caudal lobar vein. This vein shows the similar division with the bronchial branches and the veins of the segmental branches are positioned distally to the bronchial. The caudal ostia drains the right caudal lobar vein, the accessory lobar vein and the left caudal lobar vein. Right caudal lobar vein drains two branches one dorsal and one ventral. The right caudal lobar vein drains the two main branches(one dorsal and one ventral). The left cranial ostia consisted of the left cranial and caudal branches of the left cranial lobe pulmonary vein. Both branches run medially not attached and parallel to the bronchus till attaching the left cranial ostia. Segmental branches that arise from both cranial and caudal branches have a separate path to the bronchial or arterial one. The caudal pulmonary lobar vein drains

the left caudal lobe with its branches the ventral, the ventral caudal and the caudal. The caudal pulmonary vein is attached medially and lateral to the bronchus while the ventral and the ventral-caudal one are positioned in distance and caudal-medial to the bronchus. The ventral cranial pulmonary vein of the middle lobe in Cat No 5 had dimensions similar to the voxels and did not let us to evaluate it, fact that was noticed also for the bronchial lumen at the same anatomic area. In eight of the fourteen cats the absence of the caudal-ventral pulmonary vein of the right caudal lobe was noticed and this portion was drained by segmental branches of the ventral lobar pulmonary vein of the right caudal lobe (fig.2.4). The cranial left ostia consisted of the left cranial and caudal branches of the left cranial lobe pulmonary vein. In 13/14 cats the cranial and caudal portion anastomose before they attach to the left atrium but Cat No 11 showed a different aspect. The cranial and caudal portion of the left cranial pulmonary vein in Cat No11 attach separately to the left atrium (fig 2.5). A sudden cut-off of the RB1V1 pulmonary artery and vein is seen in Cat No3 , Cat No 4 and Cat No 9 (fig.2.2).

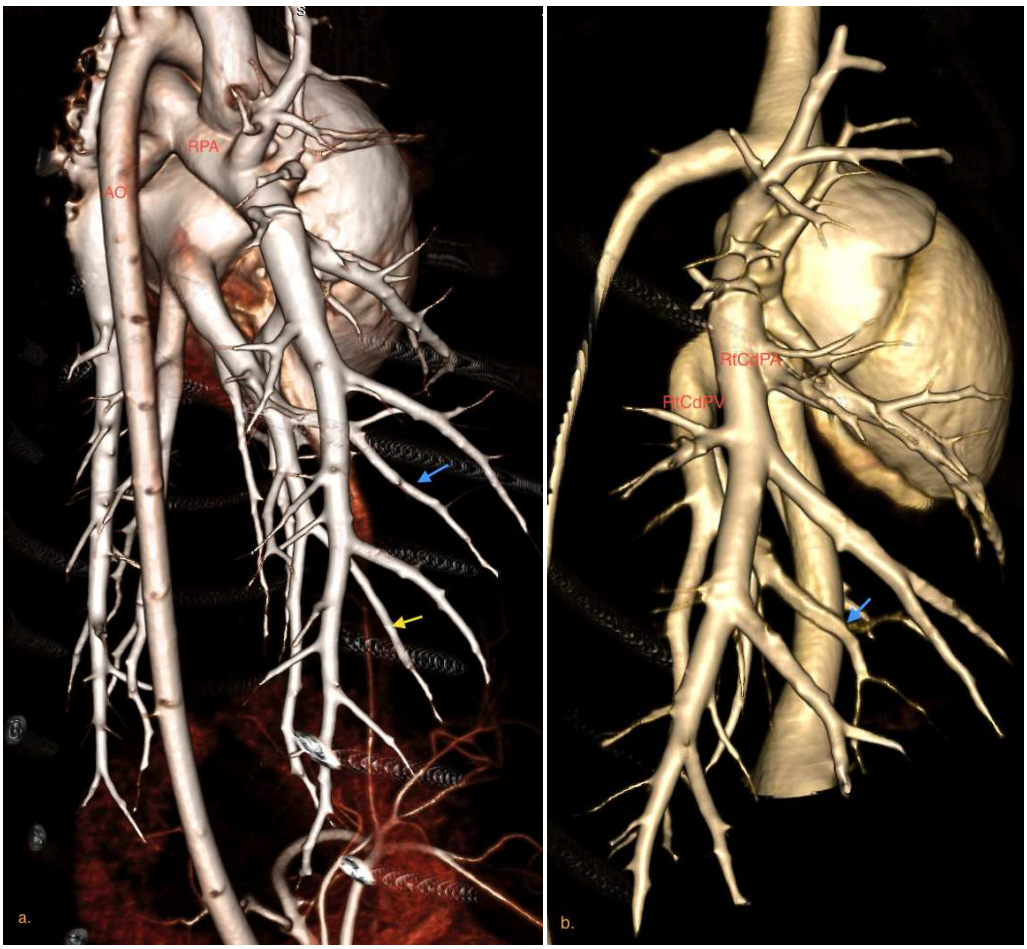

fig.2.4: a. in cat No 1 the right caudal pulmonary vein has both the ventral (blue arrow) and ventral-caudal pulmonary vein of the right caudal pulmonary vein (yellow arrow), b. cat No 3 the ventral-caudal pulmonary vein does not exist and the area is drained from the ventral and caudal pulmonary vein of the right caudal lobe

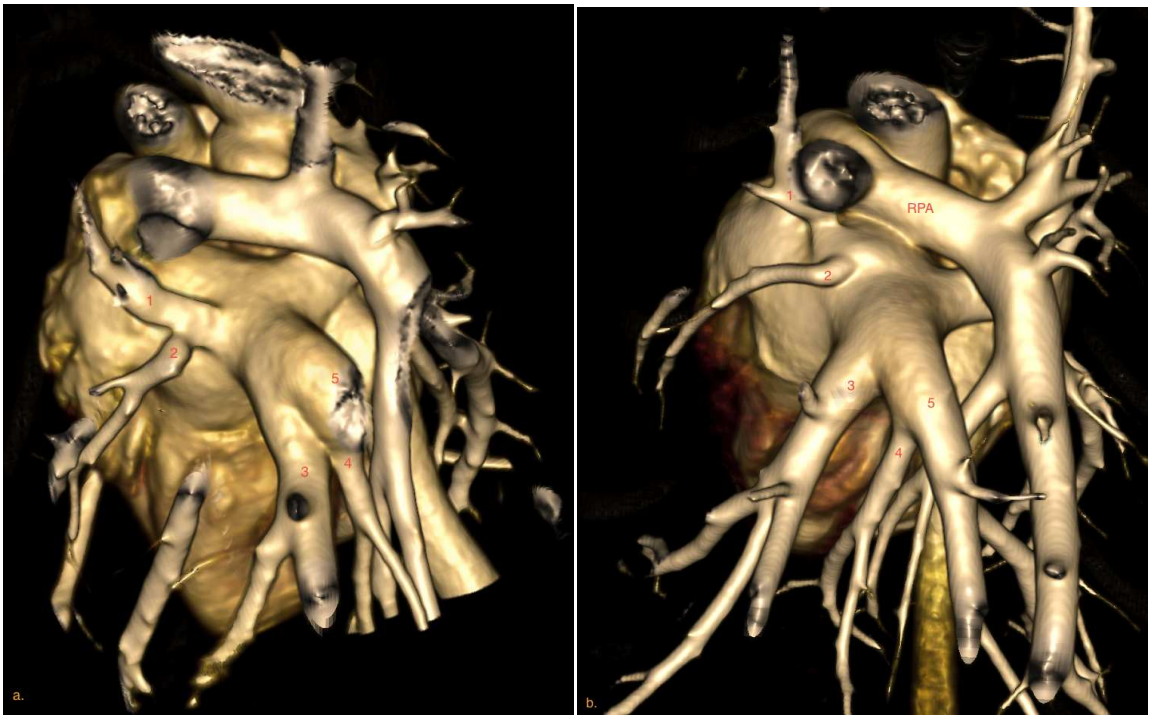

fig.2.5: two different aspects of the left ostia : a. in cat No 3 the LB1D1 pulmonary vein and the LB1V1 anastomose before attaching the left atrium left , b. cat No 11 has a different aspect while the LB1D1 pulmonary vein and the LB1V1 attach the left atrium separately. (1:left cranial (cranial part) lobe pulmonary vein, 2: left cranial(caudal part) lobe pulmonary vein, 3: left caudal lobe pulmonary vein, 4: accessory lobe pulmonary vein, 5:right caudal pulmonary vein, RPA:right pulmonary artery).

In eleven of the fourteen cats was noticed the enhancement of the hepatic veins without having yet a portal flow (fig.2.6).

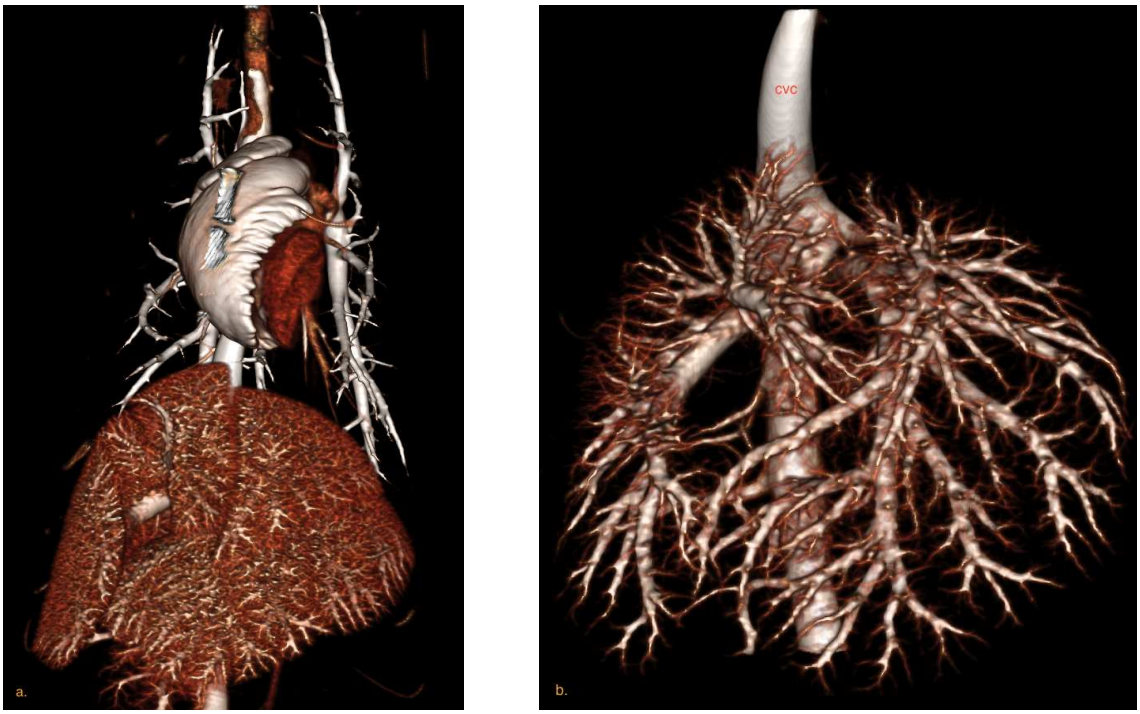

fig.2.6: a. 3D volume rendering of the CTPA in which is seen a well enhancing hepatic venous vasculature(a) .Ventral view of the hepatic veins (b), (CVC:caudal vena cava).

All the cats that were selected for this study are reported in the table 1.1.

CAT ID	AGE(months)	SEX(m/f)	WEIGHT(Kg)
Cat No 1	22	m	4
Cat No 2	18	m	4
Cat No 3	14	f	4.2
Cat No 4	12	m	2.8
Cat No 5	12	m	2.7
Cat No 6	20	f	3.8
Cat No 7	17	f	4.2
Cat No 8	30	m	5.2
Cat No 9	14	m	4.6
Cat No 10	20	f	5.2
Cat No 11	23	m	5.2
Cat No 12	26	f	3.3
Cat No 13	60	m	5.6
Cat No 14	12	m	5.2

Table 1.1 Data of all the included cats of the study: age, sex and weight

Abbreviations) of the thoracic structures were based on the till to date anatomic and endoscopic studies (table 1.2, 1.3, 1.4, 1.5. A medical dicom viewer was used to measure in millimeters, in each examined cat, the diameter of the bronchial lumen, pulmonary arteries and vein which are reported in the tables 1.6-1.19.

Abbreviations	Bronchial
RPB	right principal bronchus
RB1	right cranial lobe
RB1D1	dorsal-lateral branch of the right cranial lobe
RB1V1	ventral branch of the right cranial lobe
RB2	middle lobe
RB2R1	cranial branch of the middle lobe
RB2C1	caudal branch of the middle lobe
RB3	accessory lobe
RB3V1	ventral-medial branch of the accessory lobe
RB3D1	caudal branch of the accessory lobe
RB4	right caudal lobe
RB4V1	ventral branch of the right caudal lobe
RB4V2	caudal-ventral branch of the right caudal lobe
RB4V3	caudalbranch of the right caudal lobe
LPB	left principal bronchus
LB1	left cranial lobe
LB1D1	cranial-ventral branch of the left cranial lobe
LB1V1	caudal-ventral branch of the left cranial lobe
LB2	left caudal lobe
LB2V1	ventral branch o fthe left caudal lobe
LB2V2	caudal-ventral branch of the left caudal lobe
LB2V3	caudal branch of the left caudal lobe

Table1.2 Abbreviations of the bronchial lumen for the right and left lung

Abbreviations	Arterial
RPA	right pulmonary artery
RB1	RPA
RB1D1	dorsal-lateral branch of the right cranial lobe
RB1V1	ventral branch of the right cranial lobe
RB2	middle lobe
RB2R1	cranial branch of the middle lobe
RB2C1	caudal branch of the middle lobe
RB3	accessory lobe
RB3V1	ventral-medial branch of the accessory lobe
RB3D1	caudal branch of the accessory lobe
RB4	right caudal lobe
RB4V1	ventral branch of the right caudal lobe
RB4V2	caudal-ventral branch of the right caudal lobe
RB4V3	caudalbranch of the right caudal lobe
LPA	left pulmonary artery
LB1	LPA
LB1D1	cranial-ventral branch of the left cranial lobe
LB1V1	caudal-ventral branch of the left cranial lobe
LB2	left caudal lobe
LB2V1	ventral branch o fthe left caudal lobe
LB2V2	caudal-ventral branch of the left caudal lobe
LB2V3	caudal branch of the left caudal lobe

Table1.3 Abbreviations of the pulmonary arteries for the right and left lung

Abbreviations	Venous
RB1	right cranial lobe pulmonary vein
RB1D1	dorsal-lateral branch of the right cranial lobe
RB1V1	ventral branch of the right cranial lobe
RB2	right middle lobe pulmonary vein
RB2R1	cranial branch of the middlel lobe
RB2C1	caudal branch of the middle lobe
RB3	accessory lobe pulmonary vein
RB3V1	ventral-medial branch of the accessory lobe
RB3D1	caudal branch of the accessory lobe
RB4	right caudal lobe pulmonary vein
RB4V1	ventral branch of the right caudal lobe
RB4V2	caudal-ventral branch of the right caudal lobe
RB4V3	caudal branch of the right caudal lobe
LB1	left cranial lobe pulmonary vein
LB1D1	left cranial portion of the left cranial lobe pulmonary vein
LB1V1	left caudal portion of the left cranial lobe pulmonary vein
LB2	left caudal lobe pulmonary vein
LB2V1	ventral branch o fthe left caudal lobe
LB2V2	caudal-ventral branch of the left caudal lobe
LB2V3	caudal branch of the left caudal lobe

Table1.4 Abbreviations of the pulmonary veins for the right and left lung

Abbreviations	
de	Does not exist
nv	Non evaluated

Table 1.5 Abbreviations for structures that wasn't present or non evaluated

CAT No 1

	DIAMETER 1	DIAMETER 2	DIAMETER 3	DIAMETER 4	MEAN	SD
TRACHEA	7.46	8.11	7.52	8.03	7.78	0.34
RPB	6.01	7.09	6.36	6.94	6.6	0.50
RB1	3.51	5.11	3.43	4.85	4.23	0.88
RB1 pulmonary artery	4.66	4.91	4.61	3.96	4.54	0.41
RB2 pulmonary vein	4.35	3.21	3.19	4.34	3.77	0.66
RB1D1	1.84	1.76	1.73	1.89	1.81	0.07
RB1D1 pulmonary artery	1.57	1.57	1.24	1.46	1.46	0.16
RB1D1 pulmonary vein	1.28	1.54	1.46	1.35	1.41	0.12
RB1V1	3.62	3.07	2.68	3.57	3.24	0.45
RB1V1 pulmonary artery	3.22	3.24	3.24	3.13	3.21	0.05
RB1V1 pulmonary vein	2.55	2.64	2.27	2.32	2.45	0.18
RB2	2.81	2.81	2.62	3.15	2.85	0.22
RB2 pulmonary artery	2.27	2.29	2.25	2.37	2.30	0.05
RB2 pulmonary vein	1.38	1.55	1.28	1.43	1.41	0.11
RB2R1	1.6	1.47	1.39	1.05	1.38	0.23
RB2R1 pulmonary artery	1.03	1.2	1	1.14	1.09	0.09
RB2R1 pulmonary vein	0.77	0.75	0.89	0.87	0.82	0.07
RB2C2	2.06	2.02	1.96	1.82	1.97	0.11
RB2C2 pulmonary artery	1.43	1.44	1.46	1.55	1.47	0.05
RB2C2 pulmonary vein	1.08	1.01	1.46	0.99	1.14	0.22
RB3	3.03	2.94	2.57	2.53	2.77	0.25
RB3 pulmonary artery	2.67	2.71	2.47	2.47	2.58	0.13
RB3 pulmonary vein	2.29	2	2.3	1.99	2.15	0.17
RB3V1	2.23	2.22	1.86	2.3	2.15	0.20
RB3V1 pulmonary artery	2.01	2.16	2.11	2.09	2.09	0.06
RB3V1 pulmonary vein	1.87	1.79	2.08	2.06	1.95	0.14
RB3D1	1.29	1.59	1.85	1.65	1.60	0.23
RB3D1 pulmonary artery	2.44	2.12	2.13	1.99	2.17	0.19
RB3D1 pulmonary vein	1.5	1.44	1.59	1.36	1.47	0.10
RB4	5.07	4.85	4.94	4.85	4.93	0.10
RB4 pulmonary artery	5.12	5.1	4.97	4.94	5.03	0.09
RB4 pulmonary vein	4.12	3.8	4.03	3.76	3.93	0.18
RB4V1	2.81	2.29	2.3	2.98	2.60	0.35

	DIAMETER 1	DIAMETER 2	DIAMETER 3	DIAMETER 4	Mean	SD
RB4V1 pulmonary artery	2.34	2.78	2.59	2.55	2.57	0.18
RB4V1 pulmonary vein	2.19	2.35	2.24	2.1	2.22	0.10
RB4V2	2.11	1.99	1.97	2.11	2.05	0.08
RB4V2 pulmonary artery	2.12	2.28	2.05	2.15	2.15	0.10
RB4V2 pulmonary vein	1.52	1.71	1.57	1.65	1.61	0.08
RB4V3	3.3	3.23	3.85	3.52	3.48	0.28
RB4V3 pulmonary artery	3.31	3.39	3.05	3.29	3.26	0.15
RB4V3 pulmonary vein	2.49	2.48	2.21	2.37	2.39	0.13
LPB	6.39	5.81	6.51	5.71	6.11	0.40
LB1	3.39	4.99	4.78	3.47	4.16	0.85
LB1 pulmonary artery	5.49	4.91	5.95	5.1	5.36	0.46
LB1 pulmonary vein	4.76	2.03	4.2	2.17	3.29	1.39
LB1D1	2.19	2.25	2.06	1.98	2.12	0.12
LB1D1 pulmonary artery	2.96	2.86	2.85	2.83	2.88	0.06
LB1D1 pulmonary vein	2.25	2.32	2.31	2.32	2.30	0.03
LB1V1	2.17	2.24	2.03	2.23	2.17	0.10
LB1V1 pulmonary artery	2.32	2.47	2.19	2.49	2.37	0.14
LB1V1 pulmonary vein	1.77	1.85	1.87	1.71	1.80	0.07
LB2	4.27	3.98	4.7	3.91	4.22	0.36
LB2 pulmonary artery	6.28	5.16	6.65	5.01	5.78	0.81
LB2 pulmonary vein	3.57	4.02	3.96	3.53	3.77	0.26
LB2V1	2.03	1.87	1.66	2.23	1.95	0.24
LB2V1 pulmonary artery	2.01	1.89	1.76	2.02	1.92	0.12
LB2V1 pulmonary vein	1.82	1.69	1.52	1.78	1.70	0.13
LB2V2	2.58	2.12	2.29	2.54	2.38	0.22
LB2V2 pulmonary artery	1.94	2.06	1.94	1.87	1.95	0.08
LB2V2 pulmonary vein	1.6	1.65	1.64	1.55	1.61	0.05
LB2V3	3.78	4.21	3.96	3.53	3.87	0.29
LB2V3 pulmonary artery	3.85	3.67	3.71	3.57	3.70	0.12
LB2V3 pulmonary vein	2.77	2.82	2.83	2.72	2.79	0.05

Table 1.6 Measurements of Cat No1 with mean values and standard deviation

CAT No 2

	DIAMETER 1	DIAMETER 2	DIAMETER 3	DIAMETER 4	Mean	SD
TRACHEA	6.76	6.05	6.49	6.18	6.37	0.32
RPB	6.18	5.69	5.56	5.49	5.73	0.31
RB1	3.74	3.13	3.41	3.15	3.36	0.29
RB1 pulmonary artery	4.81	3.92	4.86	3.82	4.35	0.56
RB1 pulmonary vein	3.27	3.92	3.48	3.3	3.49	0.30
RB1D1	0.89	0.93	0.86	0.85	0.88	0.04
RB1D1 pulmonary artery	2.16	1.95	1.78	2.04	1.98	0.16
RB1D1 pulmonary vein	1.23	1.01	1.05	1.14	1.11	0.10
RB1V1	2.74	2.89	2.64	2.84	2.78	0.11
RB1V1 pulmonary artery	3.17	3.73	3.08	3.43	3.35	0.29
RB1V1 pulmonary vein	1.86	1.82	1.86	1.92	1.87	0.04
RB2	2.22	2.17	2.32	2.17	2.22	0.07
RB2 pulmonary artery	3.45	3.03	3.02	3.31	3.20	0.21
RB2 pulmonary vein	2.68	2.55	2.7	2.58	2.63	0.07
RB2R1	1.1	1.2	1.1	1.4	1.20	0.14
RB2R1 pulmonary artery	1.67	1.39	1.34	1.67	1.52	0.18
RB2R1 pulmonary vein	1.41	1.46	1.48	1.35	1.43	0.06
RB2C1	1.33	1.25	1.17	1.07	1.21	0.11
RB2C1 pulmonary artery	2.53	2.45	2.39	2.5	2.47	0.06
RB2C1 pulmonary vein	2.64	2.71	2.63	2.94	2.73	0.14
RB3	2.09	1.37	1.89	1.58	1.73	0.32
RB3 pulmonary artery	2.59	2.72	2.5	2.67	2.62	0.10
RB3 pulmonary vein	1.33	1.36	1.39	1.31	1.35	0.03
RBEV1	0.82	0.76	0.96	0.89	0.86	0.09
RB3V1 pulmonary artery	2.28	1.97	2.25	1.96	2.12	0.17
RB3V1 pulmonary vein	0.76	0.62	0.75	0.58	0.68	0.09
RB3D1	1.01	0.91	1.34	0.92	1.05	0.20
RB3D1 pulmonary artery	2.27	2.13	2.13	2.17	2.18	0.07
RB3D1 pulmonary vein	0.93	0.98	0.91	0.92	0.94	0.03
RB4	3.76	3.71	3.77	3.7	3.74	0.04
RB4 pulmonary artery	4.29	4.38	4.4	4.17	4.31	0.10
RB4 pulmonary vein	1.95	2.84	2.77	2.02	2.40	0.48
RB4V1	1.16	1.15	1.12	1.35	1.20	0.10

	DIAMETER 1	DIAMETER 2	DIAMETER 3	DIAMETER 4	Mean	SD
RB4V1 pulmonary artery	1.71	1.44	1.4	1.77	1.58	0.19
RB4V1 pulmonary vein	1.21	1.28	1.25	1.22	1.24	0.03
RB4V2	1.23	1.18	1.38	1.57	1.34	0.18
RB4V2 pulmonary artery	2.16	2.09	2.07	2.1	2.11	0.04
RB4V2 pulmonary vein	1.3	1.3	1.31	1.27	1.30	0.02
RB4V3	1.92	1.89	1.82	1.89	1.88	0.04
RB4V3 pulmonary artery	2.9	3.25	3.22	2.84	3.05	0.21
RB4V3 pulmonary vein	1.13	1.11	1.07	1.11	1.11	0.03
LPB	5.28	4.56	4.38	5.27	4.87	0.47
LB1	2.82	4.05	3.79	2.89	3.39	0.62
LB1 pulmonary artery	6.19	5.98	5.95	6.13	6.06	0.12
LB1 pulmonary vein	4.29	2.82	4.56	2.82	3.62	0.93
LB1D1	2.55	2.45	2.35	2.65	2.50	0.13
LB1D1 pulmonary artery	4.07	3.58	3.65	4.11	3.85	0.28
LB1D1 pulmonary vein	1.73	2.31	1.7	2.29	2.01	0.34
LB1V1	1.26	1.15	1.12	1.16	1.17	0.06
LB1V1 pulmonary artery	2.82	3.31	2.77	3.25	3.04	0.28
LB1V1 pulmonary vein	2.1	1.74	1.76	2.06	1.92	0.19
LB2	3.42	4.01	3.95	3.59	3.74	0.28
LB2 pulmonary artery	4.81	4.85	4.86	4.67	4.80	0.09
LB2 pulmonary vein	4.98	3.86	3.7	4.82	4.34	0.65
LB2V1	1.55	2	1.62	2.28	1.86	0.34
LB2V1 pulmonary artery	2.37	2.28	2.26	2.35	2.32	0.05
LB2V1 pulmonary vein	1.99	2.25	2.23	1.97	2.11	0.15
LB2V2	nv				######	####
LB2V2 pulmonary artery	1.66	1.71	1.74	1.71	1.71	0.03
LB2V2 pulmonary vein	0.95	0.89	0.93	0.97	0.94	0.03
LB2V3	1.23	1.29	1.16	1.41	1.27	0.11
LB2V3 pulmonary artery	2.61	2.9	2.61	2.95	2.77	0.18
LB2V3 pulmonary vein	1.21	1.33	1.22	1.34	1.28	0.07

Table 1.7 Measurements of Cat No2 with mean values and standard deviation

CAT No 3

	DIAMETER 1	DIAMETER 2	DIAMETER 3	DIAMETER 4	Mean	SD
TRACHEA	6.33	5.65	5.57	6.22	5.94	0.39
RPB	5.03	4.7	4.58	5	4.83	0.22
RB1	4.29	2.61	2.69	4.34	3.48	0.96
RB1 pulmonary artery	5.37	2.87	5.35	2.85	4.11	1.44
RB1 pulmonary vein	4.86	2.14	4.9	2.12	3.51	1.59
RB1D1	1.08	1.3	0.98	1.28	1.16	0.16
RB1D1 pulmonary artery	2.08	1.86	1.89	2.14	1.99	0.14
RB1D1 pulmonary vein	2.23	2.02	2.25	2.04	2.14	0.12
RB1V1	2.26	3.33	2.18	3.22	2.75	0.61
RB1V1 pulmonary artery	2.98	2.69	2.72	3	2.85	0.17
RB1V1 pulmonary vein	1.82	2.09	1.84	2.09	1.96	0.15
RB2	2.11	1.75	2.09	1.69	1.91	0.22
RB2 pulmonary artery	2.68	2.35	2.69	2.34	2.52	0.20
RB2 pulmonary vein	2.58	2.27	2.59	2.3	2.44	0.17
RB2R1	0.93	0.8	0.87	0.75	0.84	0.08
RB2R1 pulmonary artery	1.59	1.78	1.61	1.85	1.71	0.13
RB2R1 pulmonary vein	1.09	0.82	0.79	0.95	0.91	0.14
RB2C1	0.81	0.86	0.81	0.77	0.81	0.04
RB2C1 pulmonary artery	2.47	2.75	2.48	2.75	2.61	0.16
RB2C1 pulmonary vein	1.22	1.52	1.21	1.53	1.37	0.18
RB3	1.71	1.97	2.03	1.8	1.88	0.15
RB3 pulmonary artery	3.14	3.01	3.15	2.98	3.07	0.09
RB3 pulmonary vein	2.52	2.72	2.54	2.73	2.63	0.11
RB3V1	1.17	1.33	1.14	1.3	1.24	0.09
RB3V1 pulmonary artery	2.2	2.38	2.39	2.17	2.29	0.12
RB3V1 pulmonary vein	2.21	2.13	2.11	2.19	2.16	0.05
RB3D1	1.59	1.17	1.51	1.19	1.37	0.22
RB3D1 pulmonary artery	2.52	2.33	2.36	2.54	2.44	0.11
RB3D1 pulmonary vein	1.75	1.75	1.74	1.76	1.75	0.01
RB4	4.02	3.8	3.73	3.92	3.87	0.13
RB4 pulmonary artery	5.4	5.25	5.29	5.36	5.33	0.07
RB4 pulmonary vein	5.07	4.33	4.31	5.05	4.69	0.43
RB4V1	nv	0	0	0	0.00	0.00

	DIAMETER 1	DIAMETER 2	DIAMETER 3	DIAMETER 4	Mean	SD
RB4V1 pulmonary artery	3.06	3.18	3.08	3.17	3.12	0.06
RB4V1 pulmonary vein	3.26	2.99	3.02	3.28	3.14	0.15
RB4V2	nv	0	0	0	0.00	0.00
RB4V2 pulmonary artery	2.47	3.04	2.47	3.06	2.76	0.33
RB4V2 pulmonary vein	de	0	0	0	0.00	0.00
RB4V3	nv	0	0	0	0.00	0.00
RB4V3 pulmonary artery	3.72	3.75	3.74	3.7	3.73	0.02
RB4V3 pulmonary vein	2.88	2.75	2.71	2.83	2.79	0.08
LPB	4.28	3.63	4.2	3.55	3.92	0.38
LB1	2.37	2.14	2.11	2.33	2.24	0.13
LB1 pulmonary artery	4.87	5.16	5.13	4.91	5.02	0.15
LB1 pulmonary vein	4.08	1.5	1.47	4.19	2.81	1.53
LB1D1	1.66	1.27	1.36	1.69	1.50	0.21
LB1D1 pulmonary artery	3.01	3.05	3.02	3.05	3.03	0.02
LB1D1 pulmonary vein	3.24	2.26	2.24	3.28	2.76	0.58
LB1V1	1.49	1.16	1.49	1.16	1.33	0.19
LB1V1 pulmonary artery	2.67	2.96	2.94	2.65	2.81	0.17
LB1V1 pulmonary vein	2.7	2.52	2.72	2.54	2.62	0.10
LB2	4.27	4.12	4.1	4.31	4.20	0.11
LB2 pulmonary artery	5.14	6.03	5.14	5.99	5.58	0.50
LB2 pulmonary vein	4.73	4.69	4.73	4.75	4.73	0.03
LB2V1	nv	0	0	0	0.00	0.00
LB2V1 pulmonary artery	2.88	2.84	2.87	2.83	2.86	0.02
LB2V1 pulmonary vein	3	2.84	2.81	2.91	2.89	0.08
LB2V2	nv	0	0	0	0.00	0.00
LB2V2 pulmonary artery	2.89	1.98	1.89	2.79	2.39	0.53
LB2V2 pulmonary vein	2.94	1.5	2.99	1.51	2.24	0.84
LB2V3	nv	0	0	0	0.00	0.00
LB2V3 pulmonary artery	3.63	3.95	3.89	3.58	3.76	0.18
LB2V3 pulmonary vein	2.46	2.42	2.36	2.49	2.43	0.06

Table 1.8 Measurements of Cat No3 with mean values and standard deviation

CAT No 4

	DIAMETER 1	DIAMETER 2	DIAMETER 3	DIAMETER 4	Mean	SD
TRACHEA	6.4	6.99	6.91	6.4	6.68	0.32
RPB	5.11	6.12	6.05	5.13	5.60	0.56
RB1	4.41	3.63	3.68	4.4	4.03	0.43
RB1 pulmonary artery	5.47	5.75	5.44	5.71	5.59	0.16
RB1 pulmonary vein	4.54	2.16	2.02	4.49	3.30	1.40
RB1D1	1.86	2.09	1.88	2.04	1.97	0.11
RB1D1 pulmonary artery	1.77	1.65	1.8	1.69	1.73	0.07
RB1D1 pulmonary vein	2.32	2.27	2.32	2.29	2.30	0.02
RB1V1	3.82	3.01	2.98	3.79	3.40	0.47
RB1V1 pulmonary artery	3.53	3.2	3.55	3.17	3.36	0.21
RB1V1 pulmonary vein	2.31	2.72	2.3	2.76	2.52	0.25
RB2	2.32	1.5	2.26	1.53	1.90	0.45
RB2 pulmonary artery	3.29	3.08	3.27	3.03	3.17	0.13
RB2 pulmonary vein	1.92	2.27	2.25	1.91	2.09	0.20
RB2R1	0.79	0.55	0.73	0.56	0.66	0.12
RB2R1 pulmonary artery	1.09	0.91	1.07	0.9	0.99	0.10
RB2R1 pulmonary vein	1.41	1.21	1.41	1.21	1.31	0.12
RB2C1	1.57	1.37	1.54	1.33	1.45	0.12
RB2C1 pulmonary artery	2.15	2.19	2.2	2.2	2.19	0.02
RB1C1 pulmonary vein	1.02	0.87	1.02	0.87	0.95	0.09
RB3	1.74	1.95	1.69	2.1	1.87	0.19
RB3 pulmonary artery	3.02	2.82	2.82	3.03	2.92	0.12
RB3 pulmonary vein	2.7	2.56	2.78	2.59	2.66	0.10
RB3V1	1.12	1.87	1.98	1.23	1.55	0.44
RB3V1 pulmonary artery	1.95	1.6	1.63	1.95	1.78	0.19
RB3V1 pulmonary vein	1.89	1.88	1.86	1.88	1.88	0.01
RB3D1	0.76	0.74	0.84	0.88	0.81	0.07
RB3D1 pulmonary artery	1.31	1.37	1.33	1.35	1.34	0.03
RB3D1 pulmonary vein	1.53	1.64	1.54	1.66	1.59	0.07
RB4	3.25	2.81	3.31	2.92	3.07	0.25
RB4 pulmonary artery	4.73	4.48	4.77	4.59	4.64	0.13
RB4 pulmonary vein	3.38	3.43	3.34	3.44	3.40	0.05
RB4V1	1.75	1.88	1.77	1.91	1.83	0.08

	DIAMETER 1	DIAMETER 2	DIAMETER 3	DIAMETER 4	Mean	SD
RB4V1 pulmonary artery	2.63	2.84	2.79	2.59	2.71	0.12
RB4V1 pulmonary vein	2.4	2.49	2.4	2.5	2.45	0.05
RB4V2	1.54	1.67	1.68	1.47	1.59	0.10
RB4V2 pulmonary artery	2.12	2.39	2.11	2.33	2.24	0.14
RB4V2 pulmonary vein	de				######	####
RB4V3	2.59	2.62	2.57	2.6	2.60	0.02
RB4V3 pulmonary artery	3.07	3.13	3.04	3.15	3.10	0.05
RB4V3 pulmonary vein	2.63	2.52	2.62	2.55	2.58	0.05
LPB	4.33	4.85	4.82	4.28	4.57	0.31
LB1	2.98	3.55	3.53	3.06	3.28	0.30
LB1 pulmonary artery	5.19	6	5.2	5.96	5.59	0.45
LB1 pulmonary vein	3.43	2.42	2.39	3.49	2.93	0.61
LB1D1	3.45	2.08	3.5	2.09	2.78	0.80
LB1D1 pulmonary artery	2.62	2.68	2.62	2.64	2.64	0.03
LB1D1 pulmonary vein	2.26	1.26	2.29	1.25	1.77	0.59
LB1V1	3.68	2.51	3.56	2.44	3.05	0.66
LB1V1 pulmonary artery	2.93	3.17	2.94	3.06	3.03	0.11
LB1V1 pulmonary vein	1.9	3.01	1.88	3.01	2.45	0.65
LB2	3.95	4.12	3.92	4.12	4.03	0.11
LB2 pulmonary artery	5.79	5.29	5.31	5.86	5.56	0.30
LB2 pulmonary vein	4.81	5.47	5.53	4.98	5.20	0.36
LB2V1	1.85	1.33	1.85	1.36	1.60	0.29
LB2V1 pulmonary artery	2.87	2.84	2.85	2.86	2.86	0.01
LB2V1 pulmonary vein	2.15	2.66	2.13	2.62	2.39	0.29
LB2V2	1.38	1.67	1.62	1.45	1.53	0.14
LB2V2 pulmonary artery	2.68	2.61	2.59	2.61	2.62	0.04
LB2V2 pulmonary vein	1.94	1.67	1.95	1.68	1.81	0.16
LB2V3	2.85	2.34	2.93	2.21	2.58	0.36
LB2V3 pulmonary artery	3.43	3.1	3.07	3.38	3.25	0.19
LB2V3 pulmonary vein	2.04	2.34	2.35	2.04	2.19	0.18

Table 1.9 Measurements of Cat No4 with mean values and standard deviation

CAT No 5

	DIAMETER 1	DIAMETER 2	DIAMETER 3	DIAMETER 4	Mean	SD
TRACHEA	6.42	7.11	6.41	7.16	6.78	0.42
RPB	4.75	6.11	4.74	6.16	5.44	0.80
RB1	4.22	3.22	4.24	3.18	3.72	0.59
RB1 pulmonary artery	5.37	3.96	3.95	5.45	4.68	0.84
RB1 pulmonary vein	4.27	2.1	2.2	3.84	3.10	1.11
RB1D1	1.26	1.53	1.41	1.51	1.43	0.12
RB1D1 pulmonary artery	2.01	1.84	2.04	1.84	1.93	0.11
RB1D1 pulmonary vein	1.63	1.62	1.64	1.65	1.64	0.01
RB1V1	3.21	3.35	3.31	3.26	3.28	0.06
RB1V1 pulmonary artery	3.5	3.53	3.51	3.56	3.53	0.03
RB1V1 pulmonary vein	3.36	3.69	3.37	3.75	3.54	0.21
RB2	2.58	2.37	2.29	2.57	2.45	0.15
RB2 pulmonary artery	3.55	3.51	3.76	3.82	3.66	0.15
RB2 pulmonary vein	1.67	1.82	1.87	1.62	1.75	0.12
RB2R1	nv	0	0	0	0.00	0.00
RB2R1 pulmonary artery	1.3	1.42	1.43	1.3	1.36	0.07
RB2R1 pulmonary vein	nv	0	0	0	0.00	0.00
RB2C1	1.36	1.54	1.44	1.45	1.45	0.07
RB2C1 pulmonary artery	2.8	2.77	2.74	2.78	2.77	0.02
RB2C1 pulmonary vein	1.6	1.86	1.62	1.87	1.74	0.15
RB3	1.78	1.7	1.8	1.74	1.76	0.04
RB3 pulmonary artery	3.7	3.07	3.69	3.09	3.39	0.36
RB3 pulmonary vein	2.79	2.76	2.79	2.79	2.78	0.02
RB3V1	1.06	1.25	0.92	1.32	1.14	0.18
RB3V1 pulmonary artery	2.27	2.25	2.28	2.32	2.28	0.03
RB3V1 pulmonary vein	1.94	1.74	1.94	1.71	1.83	0.12
RB3D1	1.5	1.66	1.73	1.61	1.63	0.10
RB3D1 pulmonary artery	2.88	2.68	2.92	2.68	2.79	0.13
RB3D1 pulmonary vein	1.37	1.28	1.38	1.27	1.33	0.06
RB4	4.33	3.11	4.42	3.11	3.74	0.73
RB4 pulmonary artery	4.94	5.32	5.01	5.38	5.16	0.22
RB4 pulmonary vein	4.11	3.25	4.07	3.22	3.66	0.49
RB4V1	1.47	1.58	1.63	1.43	1.53	0.09

	DIAMETER 1	DIAMETER 2	DIAMETER 3	DIAMETER 4	Mean	SD
RB4V1 pulmonary artery	2.86	3.36	3.35	2.87	3.11	0.28
RB4V1 pulmonary vein	2.45	2.17	2.41	2.13	2.29	0.16
RB4V2	1.73	1.74	1.68	1.86	1.75	0.08
RB4V2 pulmonary artery	2.52	2.54	2.53	2.54	2.53	0.01
RB4V2 pulmonary vein	de	0	0	0	0.00	0.00
RB4V3	2.8	2.11	2.2	2.86	2.49	0.39
RB4V3 pulmonary artery	3.76	3.29	3.77	3.29	3.53	0.27
RB4V3 pulmonary vein	2.55	2.67	2.71	2.54	2.62	0.09
LPB	4.98	4.33	5.01	4.16	4.62	0.44
LB1	2.8	5	2.89	4.95	3.91	1.23
LB1 pulmonary artery	5.33	4.97	4.94	5.3	5.14	0.21
LB1 pulmonary vein	5.75	3.14	5.81	3.32	4.51	1.47
LB1D1	2.47	3.51	3.36	2.39	2.93	0.58
LB1D1 pulmonary artery	3.51	3.55	3.53	3.5	3.52	0.02
LB1D1 pulmonary vein	2.36	1.71	1.71	2.31	2.02	0.36
LB1V1	2.67	2.14	2.71	2.18	2.43	0.31
LB1V1 pulmonary artery	2.78	3.36	2.76	3.35	3.06	0.34
LB1V1 pulmonary vein	2.48	2.66	2.55	2.65	2.59	0.09
LB2	3.75	3.8	3.97	3.83	3.84	0.09
LB2 pulmonary artery	5.52	5.95	5.93	5.47	5.72	0.26
LB2 pulmonary vein	4.39	3.87	3.83	4.34	4.11	0.30
LB2V1	1.33	1.41	1.24	1.32	1.33	0.07
LB2V1 pulmonary artery	2.56	2.56	2.57	2.54	2.56	0.01
LB2V1 pulmonary vein	2.34	1.89	2.3	1.89	2.11	0.25
LB2V2	2.1	1.55	1.96	1.39	1.75	0.33
LB2V2 pulmonary artery	2.59	2.85	2.63	2.84	2.73	0.14
LB2V2 pulmonary vein	1.7	1.5	1.68	1.49	1.59	0.11
LB2V3	2.51	2.63	2.66	2.36	2.54	0.14
LB2V3 pulmonary artery	3.61	3.44	3.47	3.61	3.53	0.09
LB2V3 pulmonary vein	1.44	1.5	1.43	1.55	1.48	0.06

Table 1.10 Measurements of Cat No5 with mean values and standard deviation

CAT No 6

	DIAMETER 1	DIAMETER 2	DIAMETER 3	DIAMETER 4	Mean	SD
TRACHEA	6.12	6.5	6.09	6.49	6.30	0.23
RPB	4.58	5.22	4.55	5.11	4.87	0.35
RB1	3.4	3.84	3.87	3.39	3.63	0.27
RB1 pulmonary artery	4.41	5.63	5.62	4.39	5.01	0.71
RB1 pulmonary vein	4.38	3.14	3.12	4.35	3.75	0.71
RB1D1	1.58	1.88	1.64	1.64	1.69	0.13
RB1D1 pulmonary artery	1.96	2.43	1.96	2.47	2.21	0.28
RB1D1 pulmonary vein	2.17	2.85	2.14	2.85	2.50	0.40
RB1V1	2.93	2.77	2.7	3.1	2.88	0.18
RB1V1 pulmonary artery	3.65	3.75	3.72	3.62	3.69	0.06
RB1V1 pulmonary vein	3	3.27	3.3	3.02	3.15	0.16
RB2	2.31	1.44	2.35	1.55	1.91	0.48
RB2 pulmonary artery	2.63	3.53	2.65	3.28	3.02	0.45
RB2 pulmonary vein	2.94	2.82	2.91	2.81	2.87	0.06
RB2R1	1.25	1.16	1.5	1.28	1.30	0.14
RB2R1 pulmonary artery	1.49	1.33	1.33	1.47	1.41	0.09
RB2R1 pulmonary vein	0.92	0.8	0.92	0.8	0.86	0.07
RB2C1	1.27	1.41	1.4	1.37	1.36	0.06
RB2C1 pulmonary artery	2.2	2.42	2.21	2.43	2.32	0.13
RB2C1 pulmonary vein	1.77	1.72	1.67	1.77	1.73	0.05
RB3	2.06	1.73	1.88	2.11	1.95	0.17
RB3 pulmonary artery	3.22	2.26	2.24	3.25	2.74	0.57
RB3 pulmonary vein	2.29	2.72	2.65	2.34	2.50	0.22
RB3V1	2.04	1.42	2.2	1.39	1.76	0.42
RB3V1 pulmonary artery	2.13	2.08	2.07	2.07	2.09	0.03
RB3V1 pulmonary vein	1.62	1.59	1.56	1.6	1.59	0.03
RB3D1	1.59	1.79	1.59	1.74	1.68	0.10
RB3D1 pulmonary artery	1.83	1.83	1.79	1.85	1.83	0.03
RB3D1 pulmonary vein	1.56	1.56	1.52	1.53	1.54	0.02
RB4	3.56	3.15	3.54	3.24	3.37	0.21
RB4 pulmonary artery	4.25	4.38	4.26	4.4	4.32	0.08
RB4 pulmonary vein	3.79	4.19	4.14	3.78	3.98	0.22
RB4V1	2.27	1.8	2.11	1.91	2.02	0.21

	DIAMETER 1	DIAMETER 2	DIAMETER 3	DIAMETER 4	Mean	SD
RB4V1 pulmonary artery	2.71	2.89	2.75	2.84	2.80	0.08
RB4V1 pulmonary vein	2.38	2.8	2.4	2.79	2.59	0.23
RB4V2	1.76	1.47	1.72	1.42	1.59	0.17
RB4V2 pulmonary artery	1.71	1.86	1.73	1.88	1.80	0.09
RB4V2 pulmonary vein	1.93	1.92	1.72	1.72	1.82	0.12
RB4V3	2.86	3.08	2.95	2.7	2.90	0.16
RB4V3 pulmonary artery	3.1	3.14	3.08	3.15	3.12	0.03
RB4V3 pulmonary vein	2.2	2.25	2.21	2.24	2.23	0.02
LPB	4.92	4.75	4.75	5.01	4.86	0.13
LB1	2.35	4.12	4.15	2.4	3.26	1.02
LB1 pulmonary artery	5.12	5.48	5.11	5.5	5.30	0.22
LB1 pulmonary vein	4.29	1.7	1.5	4.65	3.04	1.67
LB1D1	2.71	1.74	1.73	2.69	2.22	0.56
LB1D1 pulmonary artery	3.15	2.98	2.96	3.1	3.05	0.09
LB1D1 pulmonary vein	2.43	2.63	2.45	2.61	2.53	0.10
LB1V1	2.07	1.73	1.67	1.95	1.86	0.19
LB1V1 pulmonary artery	3.3	2.86	3.24	2.8	3.05	0.26
LB1V1 pulmonary vein	2.88	2.99	2.88	3.03	2.95	0.08
LB2	3.41	3.95	3.89	3.44	3.67	0.29
LB2 pulmonary artery	4.44	4.6	4.57	4.58	4.55	0.07
LB2 pulmonary vein	5.03	4.45	4.41	5.06	4.74	0.36
LB2V1	1.97	2.13	1.79	2.19	2.02	0.18
LB2V1 pulmonary artery	2.29	2.42	2.42	2.32	2.36	0.07
LB2V1 pulmonary vein	2.93	2.49	2.91	2.49	2.71	0.25
LB2V2	2.06	2.2	2.16	1.95	2.09	0.11
LB2V2 pulmonary artery	1.99	2.11	2.05	1.99	2.04	0.06
LB2V2 pulmonary vein	0.93	1.5	1.14	0.95	1.13	0.26
LB2V3	3.65	4.26	4.15	3.74	3.95	0.30
LB3V3 pulmonary artery	3.33	3.36	3.36	3.34	3.35	0.02
LB3V3 pulmonary vein	2.99	2.62	2.97	2.63	2.80	0.21

Table 1.11 Measurements of Cat No6 with mean values and standard deviation

CAT No 7

	DIAMETER 1	DIAMETER 2	DIAMETER 3	DIAMETER 4	Mean	SD
TRACHEA	7.6	7.71	7.71	7.7	7.68	0.05
RPB	6.38	6.26	6.52	6.42	6.40	0.11
RB1	4.57	3.45	4.69	3.63	4.09	0.64
RB1 pulmonary artery	4.95	4	3.95	4.92	4.46	0.55
RB1 pulmonary vein	5.64	5.81	5.8	5.64	5.72	0.10
RB1D1	2.5	2.4	2.5	2.62	2.51	0.09
RB1D1 pulmonary artery	1.93	2.51	1.87	2.44	2.19	0.33
RB1D1 pulmonary vein	3.29	2.75	2.72	3.23	3.00	0.30
RB1V1	4.56	4.12	4.09	4.56	4.33	0.26
RB1V1 pulmonary artery	3.53	3.24	3.55	3.23	3.39	0.18
RB1V1 pulmonary vein	3.99	3.93	3.89	3.87	3.92	0.05
RB2	3.54	3.74	3.76	3.51	3.64	0.13
RB2 pulmonary artery	2.9	3.01	3.02	2.92	2.96	0.06
RB2 pulmonary vein	3.59	3.57	3.6	3.58	3.59	0.01
RB2R1	3.05	2.83	3.07	2.96	2.98	0.11
RB2R1 pulmonary artery	1.92	1.98	1.97	2.05	1.98	0.05
RB2R1 pulmonary vein	2.02	1.45	2.03	1.53	1.76	0.31
RB2C1	2.97	3.16	2.87	3	3.00	0.12
RB2C1 pulmonary artery	2.01	2.06	2.02	2.07	2.04	0.03
RB2C1 pulmonary vein	1.99	1.95	1.99	1.95	1.97	0.02
RB3	3.04	3.55	3.55	3.04	3.30	0.29
RB3 pulmonary artery	3.93	3.3	3.94	3.28	3.61	0.37
RB3 pulmonary vein	2.39	2.65	2.74	2.46	2.56	0.16
RB3V1	3.76	3.07	3.86	2.95	3.41	0.47
RB3V1 pulmonary artery	2.31	1.99	1.95	2.33	2.15	0.20
RB3V1 pulmonary vein	1.66	1.35	1.65	1.36	1.51	0.17
RB3D1	3.76	2.79	2.91	3.72	3.30	0.52
RB3D1 pulmonary artery	2.05	2.1	2.1	2.09	2.09	0.02
RB3D1 pulmonary vein	1.56	1.6	1.56	1.65	1.59	0.04
RB4	5.11	5	4.92	5.1	5.03	0.09
RB4 pulmonary artery	5.56	5.48	5.46	5.54	5.51	0.05
RB4 pulmonary vein	5.09	5.07	5.06	5.06	5.07	0.01
RB4V1	3.16	3.26	3.07	3.14	3.16	0.08

	DIAMETER 1	DIAMETER 2	DIAMETER 3	DIAMETER 4	Mean	SD
RB4V1 pulmonary artery	2.8	2.86	2.9	2.91	2.87	0.05
RB4V1 pulmonary vein	3.74	3.16	3.74	3.14	3.45	0.34
RB4V2	3.32	3.49	3.36	3.51	3.42	0.09
RB4V2 pulmonary artery	2.6	2.68	2.72	2.67	2.67	0.05
RB4V2 pulmonary vein	de	0	0	0	0.00	0.00
RB4V3	4.63	4.79	4.4	4.62	4.61	0.16
RB4V3 pulmonary artery	3.78	3.89	3.76	3.89	3.83	0.07
RB4V3 pulmonary vein	2.29	2.38	2.4	2.3	2.34	0.06
LPB	4.77	5.8	4.78	5.9	5.31	0.62
LB1	4.32	3.06	4.26	3.12	3.69	0.69
LB1 pulmonary artery	6.52	6.76	6.73	6.56	6.64	0.12
LB1 pulmonary vein	3.98	2.21	3.83	2.19	3.05	0.99
LB1D1	3.37	2.46	3.36	2.47	2.92	0.52
LB1D1 pulmonary artery	3.14	3.09	3.16	3.13	3.13	0.03
LB1D1 pulmonary vein	4.02	2.18	2.17	3.99	3.09	1.06
LB1V1	2.47	2.3	2.52	2.33	2.41	0.11
LB1V1 pulmonary artery	2.63	3.03	2.64	3.08	2.85	0.24
LB1V1 pulmonary vein	2.86	2.19	2.19	2.89	2.53	0.40
LB2	4.69	5.04	4.71	5.06	4.88	0.20
LB2 pulmonary artery	5.17	5.35	5.29	5.21	5.26	0.08
LB2 pulmonary vein	4.07	4.13	4.06	4.17	4.11	0.05
LB2V1	3.72	2.87	2.71	3.6	3.23	0.51
LB2V1 pulmonary artery	2.56	2.69	2.7	2.6	2.64	0.07
LB2V1 pulmonary vein	2.17	2.85	2.84	2.16	2.51	0.39
LB2V2	2.69	3.4	3.45	2.91	3.11	0.37
LB2V2 pulmonary artery	2.31	2.29	2.26	2.32	2.30	0.03
LB2V2 pulmonary vein	2.23	2.47	2.26	2.51	2.37	0.14
LB2V3	4.69	4.24	4.76	4.35	4.51	0.25
LB2V3 pulmonary artery	4.11	3.96	4.04	3.97	4.02	0.07
LB2V3 pulmonary vein	2.2	2.05	2.04	2.19	2.12	0.09

Table 1.12 Measurements of Cat No7 with mean values and standard deviation

CAT No 8

	DIAMETER 1	DIAMETER 2	DIAMETER 3	DIAMETER 4	Mean	SD
TRACHEA	8.18	7.11	7.07	8.14	7.63	0.62
RPB	7.19	6.07	6.14	7.34	6.69	0.67
RB1	4.79	3.08	3.21	4.75	3.96	0.94
RB1 pulmonary artery	5.16	3.57	5.17	3.54	4.36	0.93
RB1 pulmonary vein	3.12	6.66	6.66	3.2	4.91	2.02
RB1D1	2.19	2.6	2.16	2.62	2.39	0.25
RB1D1 pulmonary artery	2.43	2.41	2.45	2.46	2.44	0.02
RB1D1 pulmonary vein	2.17	2.24	2.14	2.23	2.20	0.05
RB1V1	3.5	2.63	3.58	2.65	3.09	0.52
RB1V1 pulmonary artery	3.39	3.51	3.57	3.35	3.46	0.10
RB1V1 pulmonary vein	2.58	2.59	2.59	2.61	2.59	0.01
RB2	1.97	2.38	2.36	1.97	2.17	0.23
RB2 pulmonary artery	2.4	2.12	2.16	2.43	2.28	0.16
RB2 pulmonary vein	2.22	2.24	2.26	2.28	2.25	0.03
RB2R1	1.24	1.17	1.08	1.47	1.24	0.17
RB2R1 pulmonary artery	1.03	1.01	1.02	1.05	1.03	0.02
RB2R1 pulmonary vein	1.06	1.02	1.07	0.99	1.04	0.04
RB2C1	2.21	1.76	1.73	2.38	2.02	0.33
RB2C1 pulmonary artery	2.08	2.12	1.89	1.89	2.00	0.12
RB2C1 pulmonary vein	1.39	1.63	1.66	1.41	1.52	0.14
RB3	2.72	2.49	2.35	2.68	2.56	0.17
RB3 pulmonary artery	2.31	1.92	1.91	2.32	2.12	0.23
RB3 pulmonary vein	2.22	2.28	2.27	2.2	2.24	0.04
RB3V1	1.06	0.99	1.38	1.41	1.21	0.22
RB3V1 pulmonary artery	1.53	1.5	1.42	1.49	1.49	0.05
RB3V1 pulmonary vein	1.55	1.71	1.67	1.58	1.63	0.08
RB3D1	1.55	1.26	1.38	1.17	1.34	0.16
RB3D1 pulmonary artery	1.73	1.74	1.67	1.67	1.70	0.04
RB3D1 pulmonary vein	0.9	0.88	0.9	0.9	0.90	0.01
RB4	4.42	4.42	4.41	4.39	4.41	0.01
RB4 pulmonary artery	3.95	3.67	3.66	3.92	3.80	0.16
RB4 pulmonary vein	3.74	3.89	3.89	3.77	3.82	0.08
RB4V1	2.07	1.79	1.8	1.99	1.91	0.14

	DIAMETER 1	DIAMETER 2	DIAMETER 3	DIAMETER 4	Mean	SD
RB4V1 pulmonary artery	1.69	1.69	1.69	1.73	1.70	0.02
RB4V1 pulmonary vein	1.72	2.29	1.72	2.33	2.02	0.34
RB4V2	1.36	1.89	1.78	1.2	1.56	0.33
RB4V2 pulmonary artery	1.55	1.57	1.7	1.75	1.64	0.10
RB4V2 pulmonary vein	de	0	0	0	0.00	0.00
RB4V3	4.37	4.05	3.94	4.33	4.17	0.21
RB4V3 pulmonary artery	3.12	3.08	3.12	3.07	3.10	0.03
RB4V3 pulmonary vein	3.19	2.97	2.96	3.14	3.07	0.12
LPB	5.46	6.44	5.5	6.39	5.95	0.54
LB1	5.41	3.27	5.44	3.27	4.35	1.24
LB1 pulmonary artery	4.68	5.04	5.04	4.69	4.86	0.21
LB1 pulmonary vein	3.44	3.6	3.56	3.3	3.48	0.14
LB1D1	2.22	3.63	3.57	2.31	2.93	0.77
LB1D1 pulmonary artery	3.79	3.05	3.82	3.04	3.43	0.44
LB1D1 pulmonary vein	3.44	3.6	3.56	3.3	3.48	0.14
LB1V1	2.67	2.56	2.53	2.45	2.55	0.09
LB1V1 pulmonary artery	2.71	3.27	3.25	2.72	2.99	0.31
LB1V1 pulmonary vein	3.23	2.19	3.18	2.24	2.71	0.57
LB2	4.29	4.05	4.02	4.28	4.16	0.14
LB2 pulmonary artery	4.07	3.96	4.06	3.95	4.01	0.06
LB2 pulmonary artery	3.99	4.75	3.98	4.68	4.35	0.42
LB2V1	1.57	1.88	1.57	1.89	1.73	0.18
LB2V1 pulmonary artery	2.03	1.97	2.02	2.06	2.02	0.04
LB2V1 pulmonary vein	2.04	1.64	2.04	1.64	1.84	0.23
LB2V2	2.61	2.2	2.02	2.52	2.34	0.28
LB2V2 pulmonary artery	1.3	1.13	1.16	1.32	1.23	0.10
LB2V2 pulmonary vein	1.01	1.08	1.01	1.09	1.05	0.04
LB2V3	3.86	3.91	4.1	3.82	3.92	0.12
LB2V3 pulmonary artery	3.34	3.16	3.21	3.18	3.22	0.08
LB2V3 pulmonary vein	2.33	2.79	2.33	2.76	2.55	0.26

Table 1.13 Measurements of Cat No8 with mean values and standard deviation

CAT No 9

	DIAMETER 1	DIAMETER 2	DIAMETER 3	DIAMETER 4	Mean	SD
TRACHEA	7.77	8.26	8.25	7.84	8.03	0.26
RPB	5.52	7.44	7.43	5.69	6.52	1.06
RB1	3.72	3.31	3.85	3.38	3.57	0.26
RB1 pulmonary artery	6.31	4.63	4.66	6.27	5.47	0.95
RB1 pulmonary vein	4.98	4.04	4.06	4.96	4.51	0.53
RB1D1	1.56	1.69	1.68	1.72	1.66	0.07
RB1D1 pulmonary artery	2.31	2.34	2.3	2.33	2.32	0.02
RB1D1 pulmonary vein	2.3	2.92	2.34	2.93	2.62	0.35
RB1V1	3.38	2.97	3.42	3.06	3.21	0.23
RB1V1 pulmonary artery	3.84	3.73	3.85	3.76	3.80	0.06
RB1V1 pulmonary vein	3.2	3.37	3.25	3.34	3.29	0.08
RB2	2.3	2.64	2.24	2.56	2.44	0.19
RB2 pulmonary artery	1.93	1.51	1.92	1.48	1.71	0.25
RB2 pulmonary vein	2.25	1.86	2.25	1.82	2.05	0.24
RB2R1	0.93	0.83	1.03	0.81	0.90	0.10
RB2R1 pulmonary artery	1.13	1.25	1.13	1.3	1.20	0.09
RB2R1 pulmonary vein	1.24	1.22	1.22	1.29	1.24	0.03
RB2C1	1.08	1.38	1.35	1.08	1.22	0.16
RB2C1 pulmonary artery	2.41	2.47	2.47	2.46	2.45	0.03
RB2C1 pulmonary vein	1.6	1.69	1.72	1.64	1.66	0.05
RB3	2.64	2.72	2.64	2.76	2.69	0.06
RB3 pulmonary artery	2.83	2.23	2.82	2.2	2.52	0.35
RB3 pulmonary vein	3.15	2.95	2.95	3.18	3.06	0.12
RB3V1	1.9	1.28	1.24	1.97	1.60	0.39
RB3V1 pulmonary artery	1.34	1.41	1.42	1.35	1.38	0.04
RB3V1 pulmonary vein	2.46	2.32	2.45	2.31	2.39	0.08
RB3D1	1.12	1.03	1.09	0.98	1.06	0.06
RB3D1 pulmonary artery	1.12	1.2	1.19	1.14	1.16	0.04
RB3D1 pulmonary vein	1.74	1.68	1.78	1.68	1.72	0.05
RB4	4.83	4.63	4.93	4.5	4.72	0.19
RB4 pulmonary artery	4.88	4.68	4.7	4.91	4.79	0.12
RB4 pulmonary vein	5.12	5.53	5.52	5.18	5.34	0.22
RB4V1	1.57	2.28	1.55	2.22	1.91	0.40

	DIAMETER 1	DIAMETER 2	DIAMETER 3	DIAMETER 4	Mean	SD
RB4V1 pulmonary artery	2.39	2.56	2.37	2.63	2.49	0.13
RB4V1 pulmonary vein	3.04	2.85	2.8	3.05	2.94	0.13
RB4V2	1.4	1.92	1.84	1.48	1.66	0.26
RB4V2 pulmonary artery	2.04	2.13	2.05	2.16	2.10	0.06
RB4V2 pulmonary vein	de	0	0	0	0.00	0.00
RB4V3	2.83	2.8	2.88	2.94	2.86	0.06
RB4V3 pulmonary artery	2.94	2.97	2.95	2.92	2.95	0.02
RB4V3 pulmonary vein	3.61	3.37	3.38	3.61	3.49	0.14
LPB	5.41	5.3	5.44	5.27	5.36	0.08
LB1	2.8	3.12	3.09	2.85	2.97	0.16
LB1 pulmonary artery	6.1	6.06	6.22	6.04	6.11	0.08
LB1 pulmonary vein	4.17	1.98	4.16	1.95	3.07	1.27
LB1D1	1.88	2.01	1.9	1.94	1.93	0.06
LB1D1 pulmonary artery	2.97	2.55	2.92	2.61	2.76	0.21
LB1D1 pulmonary vein	3.02	3.31	3.03	3.31	3.17	0.16
LB1V1	2.06	2.01	1.98	2.11	2.04	0.06
LB1V1 pulmonary artery	2.06	2.76	2.04	2.76	2.41	0.41
LB1V1 pulmonary vein	2.96	2.63	2.95	2.6	2.79	0.20
LB2	4.03	3.34	3.96	3.34	3.67	0.38
LB2 pulmonary artery	4.16	4.86	4.81	4.17	4.50	0.39
LB2 pulmonary vein	5.58	4.34	5.59	4.32	4.96	0.72
LB2V1	1.89	1.67	1.78	1.86	1.80	0.10
LB2V1 pulmonary artery	2.14	1.9	1.94	2.2	2.05	0.15
LB2V1 pulmonary vein	2.74	2.5	2.53	2.73	2.63	0.13
LB2V2	1.57	2.15	1.71	2.35	1.95	0.37
LB2V2 pulmonary artery	2.66	2.22	2.23	2.7	2.45	0.26
LB2V2 pulmonary vein	2.77	2.45	2.7	2.45	2.59	0.17
LB2V3	3.42	3.38	3.51	3.34	3.41	0.07
LB2V3 pulmonary artery	3.25	3.4	3.38	3.25	3.32	0.08
LB2V3 pulmonary vein	3.55	3.7	3.66	3.57	3.62	0.07

Table 1.14 Measurements of Cat No9 with mean values and standard deviation

CAT No 10

	DIAMETER 1	DIAMETER 2	DIAMETER 3	DIAMETER 4	Mean	SD
TRACHEA	7.09	6.97	6.89	7.06	7.00	0.09
RPB	5.94	5.75	5.97	5.61	5.82	0.17
RB1	3.41	3.02	3.41	3.05	3.22	0.22
RB1 pulmonary artery	4.69	4.32	4.28	4.69	4.50	0.23
RB1 pulmonary vein	3.12	4.66	2.61	3.91	3.58	0.90
RB1D1	0.61	0.6	0.67	0.67	0.64	0.04
RB1D1 pulmonary artery	2.08	2.15	2.15	2.14	2.13	0.03
RB1D1 pulmonary vein	1.88	1.5	1.49	1.84	1.68	0.21
RB1V1	2.79	2.9	2.87	2.77	2.83	0.06
RB1V1 pulmonary artery	2.85	2.77	2.85	2.77	2.81	0.05
RB1V1 pulmonary vein	2.44	2.35	2.36	2.28	2.36	0.07
RB2	1.83	2.02	1.87	2.2	1.98	0.17
RB2 pulmonary artery	4.2	3.26	4.16	3.19	3.70	0.55
RB2 pulmonary vein	2.05	2.45	2.03	2.41	2.24	0.23
RB2R1	0.68	0.64	0.55	0.52	0.60	0.07
RB2R1 pulmonary artery	1.45	1.8	1.75	1.44	1.61	0.19
RB2R1 pulmonary vein	0.94	0.98	0.93	0.97	0.96	0.02
RB2C1	1.13	1.35	1.55	1.18	1.30	0.19
RB2C1 pulmonary artery	2.03	2.07	2.04	2.09	2.06	0.03
RB2C1 pulmonary vein	1.88	1.74	1.76	1.88	1.82	0.08
RB3	1.99	1.58	1.7	1.94	1.80	0.19
RB3 pulmonary artery	2.71	3.32	3.33	2.72	3.02	0.35
RB3 pulmonary vein	1.7	1.77	1.76	1.7	1.73	0.04
RB3V1	0.91	0.88	1.18	0.95	0.98	0.14
RB3V1 pulmonary artery	1.74	1.69	1.68	1.72	1.71	0.03
RB3V1 pulmonary vein	1.21	1.2	1.19	1.19	1.20	0.01
RB3D1	0.74	0.82	0.75	0.94	0.81	0.09
RB3D1 pulmonary artery	2.22	2.47	2.44	2.2	2.33	0.14
RB3D1 pulmonary vein	0.77	0.89	0.85	0.79	0.83	0.06
RB4	3.64	3.91	3.9	3.7	3.79	0.14
RB4 pulmonary artery	4.17	4.35	4.29	4.17	4.25	0.09
RB4 pulmonary vein	3.23	2.88	3.25	2.86	3.06	0.21
RB4V1	0.71	0.62	0.72	0.7	0.69	0.05

	DIAMETER 1	DIAMETER 2	DIAMETER 3	DIAMETER 4	Mean	SD
RB4V1 pulmonary artery	2.47	2.6	2.49	2.61	2.54	0.07
RB4V1 pulmonary vein	1.8	1.94	1.84	1.98	1.89	0.08
RB4V2	0.85	0.73	1.01	0.82	0.85	0.12
RB4V2 pulmonary artery	2.11	2.17	2.1	2.15	2.13	0.03
RB4V2 pulmonary vein	1.27	1.33	1.27	1.33	1.30	0.03
RB4V3	2.44	2.52	2.41	2.59	2.49	0.08
RB4V3 pulmonary artery	2.99	3.05	3.01	3.02	3.02	0.02
RB4V3 pulmonary vein	1.39	1.35	1.36	1.36	1.37	0.02
LPB	4.28	4.82	4.25	4.88	4.56	0.34
LB1	3.14	1.87	3.17	1.85	2.51	0.75
LB1 pulmonary artery	5.28	5.48	5.29	5.48	5.38	0.11
LB1 pulmonary vein	3.4	1.48	3.48	1.5	2.47	1.13
LB1D1	1.89	1.95	1.78	1.84	1.87	0.07
LB1D1 pulmonary artery	3.57	3.32	3.6	3.31	3.45	0.16
LB1D1 pulmonary vein	1.61	1.53	1.63	1.51	1.57	0.06
LB1V1	1.24	1.14	1.22	1.17	1.19	0.05
LB1V1 pulmonary artery	3.23	3.04	3.2	3.06	3.13	0.10
LB1V1 pulmonary vein	2.42	2.44	2.41	2.47	2.44	0.03
LB2	3.76	3.02	3.78	2.91	3.37	0.47
LB2 pulmonary artery	4.96	5.75	4.98	5.72	5.35	0.44
LB2 pulmonary vein	4.28	3.52	4.23	3.48	3.88	0.44
LB2V1	1.18	1.01	1.14	1.04	1.09	0.08
LB2V1 pulmonary artery	2.57	2.62	2.63	2.57	2.60	0.03
LB2V1 pulmonary vein	1.78	2.06	2.07	1.78	1.92	0.16
LB2V2	1.16	1.03	0.82	1.17	1.05	0.16
LB2V2 pulmonary artery	2.34	2.27	2.33	2.28	2.31	0.04
LB2V2 pulmonary vein	1.25	1.24	1.29	1.25	1.26	0.02
LB2V3	1.99	1.86	1.95	1.88	1.92	0.06
LB2V3 pulmonary artery	3.04	3.07	3.08	3.13	3.08	0.04
LB2V3 pulmonary vein	1.64	1.82	1.85	1.68	1.75	0.10

Table 1.15 Measurements of Cat No10 with mean values and standard deviation

CAT No 11

	DIAMETER 1	DIAMETER 2	DIAMETER 3	DIAMETER 4	Mean	SD
TRACHEA	7.97	7.27	7.15	7.90	7.57	0.42
RPB	6.37	5.31	5.43	6.47	5.90	0.61
RB1	4.14	3.65	3.56	4.08	3.86	0.29
RB1 pulmonary artery	6.35	5.12	6.26	5.16	5.72	0.67
RB1 pulmonary vein	4.97	4.5	5	4.32	4.70	0.34
RB1D1	1.8	1.76	1.84	1.78	1.80	0.03
RB1D1 pulmonary artery	2.82	2.58	2.55	2.79	2.69	0.14
RB1D1 pulmonary vein	2.56	2.4	2.42	2.51	2.47	0.08
RB1V1	3.01	3.14	3.14	2.99	3.07	0.08
RB1V1 pulmonary artery	3.88	3.84	3.88	3.81	3.85	0.03
RB1V1 pulmonary vein	3.58	4.01	3.52	3.92	3.76	0.24
RB2	1.55	2.31	2.38	1.58	1.96	0.45
RB2 pulmonary artery	3.27	3.46	3.23	3.44	3.35	0.12
RB2 pulmonary vein	2.77	2.82	2.79	2.73	2.78	0.04
RB2R1	0.93	0.74	1	0.88	0.89	0.11
RB2R1 pulmonary artery	0.99	0.95	0.89	0.95	0.95	0.04
RB2R1 pulmonary vein	1.36	1.33	1.33	1.36	1.35	0.02
RB2C1	1.42	1.33	1.47	1.39	1.40	0.06
RB2C1 pulmonary artery	2.32	2.41	2.43	2.33	2.37	0.06
RB2C1 pulmonary vein	2	2.27	2.04	2.28	2.15	0.15
RB3	1.71	1.68	1.66	1.78	1.71	0.05
RB3 pulmonary artery	3.01	3.04	2.93	2.95	2.98	0.05
RB3 pulmonary vein	3.06	2.92	2.88	3.06	2.98	0.09
RB3V1	1.41	1.98	1.5	1.96	1.71	0.30
RB3V1 pulmonary artery	2.23	1.95	1.97	2.25	2.10	0.16
RB3V1 pulmonary vein	2.1	1.89	1.9	2.07	1.99	0.11
RB3D1	1.43	1.22	1.35	1.19	1.30	0.11
RB3D1 pulmonary artery	1.8	1.76	1.82	1.76	1.79	0.03
RB3D1 pulmonary vein	1.75	1.77	1.77	1.77	1.77	0.01
RB4	4.54	3.74	3.69	4.51	4.12	0.47
RB4 pulmonary artery	5.46	5.48	5.5	5.49	5.48	0.02
RB4 pulmonary vein	4.41	4.68	4.72	4.47	4.57	0.15
RB4V1	1.65	2.25	2.23	1.6	1.93	0.36

	DIAMETER 1	DIAMETER 2	DIAMETER 3	DIAMETER 4	Mean	SD
RB4V1 pulmonary artery	2.64	2.66	2.61	2.63	2.64	0.02
RB4V1 pulmonary vein	2.27	2.76	2.77	2.27	2.52	0.29
RB4V2	3.03	1.93	2.1	3.1	2.54	0.61
RB4V2 pulmonary artery	2.22	2.4	2.45	2.25	2.33	0.11
RB4V2 pulmonary vein	1.77	1.56	1.54	1.71	1.65	0.11
RB4V3	2.96	3.66	3.53	3.13	3.32	0.33
RB4V3 pulmonary artery	3.38	3.4	3.39	3.44	3.40	0.03
RB4V3 pulmonary vein	2.37	2.6	2.35	2.57	2.47	0.13
LPB	4.21	5.7	4.19	5.71	4.95	0.87
LB1	2.61	2.75	2.8	2.65	2.70	0.09
LB1 pulmonary artery	4.86	5.47	5.49	4.86	5.17	0.36
LB1 pulmonary vein	de	0	0	0	0.00	0.00
LB1D1	1.66	1.64	1.78	1.8	1.72	0.08
LB1D1 pulmonary artery	2.98	3.14	3.15	2.98	3.06	0.10
LB1D1 pulmonary vein	2.03	2.04	2	2.05	2.03	0.02
LB1V1	2.32	1.92	1.92	2.33	2.12	0.23
LB1V1 pulmonary artery	2.67	3.17	3.24	2.72	2.95	0.30
LB1V1 pulmonary vein	2.1	2.2	2.06	2.21	2.14	0.07
LB2	3.63	3.49	3.52	3.57	3.55	0.06
LB2 pulmonary artery	5.48	5.3	5.33	5.44	5.39	0.09
LB2 pulmonary vein	5.4	5.68	5.37	5.71	5.54	0.18
LB2V1	2.16	1.74	1.62	2.18	1.93	0.29
LB2V1 pulmonary artery	2.15	2.15	2.34	2.3	2.24	0.10
LB2V1 pulmonary vein	2.45	2.59	2.59	2.48	2.53	0.07
LB2V2	1.63	1.73	1.67	1.68	1.68	0.04
LB2V2 pulmonary artery	2.43	2.54	2.43	2.5	2.48	0.05
LB2V2 pulmonary vein	2	1.87	2.04	1.88	1.95	0.09
LB2V3	3.31	3.14	3.16	3.29	3.23	0.09
LB2V3 pulmonary artery	3.23	3.17	3.22	3.19	3.20	0.03
LB2V3 pulmonary vein	2.7	2.51	2.51	2.7	2.61	0.11

Table 1.16 Measurements of Cat No11 with mean values and standard deviation

CAT No 12

	DIAMETER 1	DIAMETER 2	DIAMETER3	DIAMETER 4	Mean	SD
TRACHEA	6.49	6.82	6.52	6.79	6.66	0.17
RPB	5.27	7.27	5.23	7.25	6.26	1.16
RB1	3.19	3.55	3.08	3.62	3.36	0.27
RB1 pulmonary artery	2.97	2.84	3.01	2.82	2.91	0.09
RB1 pulmonary vein	3.19	3.05	3.09	2.98	3.08	0.09
RB1D1	1.44	1.49	1.6	1.45	1.50	0.07
RB1D1 pulmonary artery	1.34	1.65	1.7	1.33	1.51	0.20
RB1D1 pulmonary vein	1.38	1.47	1.37	1.48	1.43	0.06
RB1V1	2.82	2.73	2.71	2.74	2.75	0.05
RB1V1 pulmonary artery	2.97	2.84	3.01	2.82	2.91	0.09
RB1V1 pulmonary vein	2.33	2.28	2.35	2.27	2.31	0.04
RB2	1.78	1.72	1.74	1.79	1.76	0.03
RB2 pulmonary artery	2.29	2.36	2.22	2.33	2.30	0.06
RB2 pulmonary vein	1.56	1.72	1.54	1.72	1.64	0.10
RB2R1	0.8	0.77	0.74	0.87	0.80	0.06
RB2R1 pulmonary artery	1.18	0.9	0.87	1.11	1.02	0.15
RB2R1 pulmonary vein	0.78	0.73	0.74	0.68	0.73	0.04
RB2C1	1.12	1.16	0.99	1.22	1.12	0.10
RB2C1 pulmonary artery	1.97	2.03	1.93	2	1.98	0.04
RB2C1 pulmonary vein	1.26	1.3	1.26	1.28	1.28	0.02
RB3	1.56	1.9	1.6	1.83	1.72	0.17
RB3 pulmonary artery	2.63	3.43	2.63	3.49	3.05	0.48
RB3 pulmonary vein	2.28	2.69	2.25	2.65	2.47	0.23
RB3V1	0.57	1.03	0.69	1.05	0.84	0.24
RB3V1 pulmonary artery	2	2.14	2.15	1.99	2.07	0.09
RB3V1 pulmonary vein	1.75	1.8	1.76	1.77	1.77	0.02
RB3D1	0.71	0.8	0.65	0.77	0.73	0.07
RB3D1 pulmonary artery	2	2.13	2.13	2.03	2.07	0.07
RB3D1 pulmonary vein	1.19	1.16	1.15	1.17	1.17	0.02
RB4	3.36	3.11	3.36	3.14	3.24	0.14
RB4 pulmonary artery	4.29	4.52	4.56	4.35	4.43	0.13
RB4 pulmonary vein	3.81	3.51	3.82	3.5	3.66	0.18
RB4V1	1.76	1.63	1.58	1.78	1.69	0.10

	DIAMETER 1	DIAMETER 2	DIAMETER 3	DIAMETER 4	Mean	SD
RB4V1 pulmonary artery	2.12	2.27	2.27	2.1	2.19	0.09
RB4V1 pulmonary vein	2.09	1.94	1.95	2.11	2.02	0.09
RB4V2	1.79	2	1.71	1.82	1.83	0.12
RB4V2 pulmonary artery	2.13	2.16	2.16	2.15	2.15	0.01
RB4V2 pulmonary vein	1.27	1.18	1.28	1.18	1.23	0.05
RB4V3	2.52	1.94	2.37	2.03	2.22	0.28
RB4V3 pulmonary artery	2.88	2.76	2.9	2.79	2.83	0.07
RB4V3 pulmonary vein	2.27	1.74	2.27	1.73	2.00	0.31
LPB	5.41	4.65	5.32	4.72	5.03	0.40
LB1	2.75	3.34	2.74	3.35	3.05	0.35
LB1 pulmonary artery	4.49	5.16	5.13	4.42	4.80	0.40
LB1 pulmonary vein	3.18	1.65	3.14	1.69	2.42	0.86
LB1D1	1.68	2.3	1.64	2.18	1.95	0.34
LB1D1 pulmonary artery	2.46	2.59	2.64	2.47	2.54	0.09
LB1D1 pulmonary vein	1.97	1.51	2.04	1.53	1.76	0.28
LB1V1	1.53	1.49	1.5	1.5	1.51	0.02
LB1V1 pulmonary artery	2.15	1.96	2.13	1.87	2.03	0.14
LB1V1 pulmonary vein	1.16	1.13	1.12	1.11	1.13	0.02
LB2	3.19	3.37	3.28	3.17	3.25	0.09
LB2 pulmonary artery	4.55	4.46	4.47	4.49	4.49	0.04
LB2 pulmonary vein	4.19	3.9	4.16	3.87	4.03	0.17
LB2V1	1.2	1.25	1.27	1.23	1.24	0.03
LB2V1 pulmonary artery	2.19	2.17	2.08	2.15	2.15	0.05
LB2V1 pulmonary vein	1.74	1.84	1.75	1.95	1.82	0.10
LB2V2	1.36	1.26	1.21	1.47	1.33	0.12
LB2V2 pulmonary artery	2.06	2.01	2.04	2.06	2.04	0.02
LB2V2 pulmonary vein	1.42	1.67	1.69	1.39	1.54	0.16
LB2V3	2.07	2.24	2.22	1.9	2.11	0.16
LB2V3 pulmonary artery	3.49	3.24	3.25	3.49	3.37	0.14
LB2V3 pulmonary vein	1.68	1.83	1.7	1.82	1.76	0.08

Table 1.17 Measurements of Cat No12 with mean values and standard deviation

CAT No 13

	DIAMETER 1	DIAMETER 2	DIAMETER 3	DIAMETER 4	Mean	SD
TRACHEA	7.71	7.47	7.73	7.34	7.56	0.19
RPB	7.5	6.09	6.01	7.52	6.78	0.84
RB1	3.99	3.64	3.82	4.02	3.87	0.18
RB1 pulmonary artery	5.03	3.82	3.79	5.03	4.42	0.71
RB1 pulmonary vein	3.82	2.08	3.89	2.12	2.98	1.01
RB1D1	1.72	1.64	1.68	1.7	1.69	0.03
RB1D1 pulmonary artery	1.58	1.76	1.61	1.8	1.69	0.11
RB1D1 pulmonary vein	1.08	1.01	1.06	0.92	1.02	0.07
RB1V1	3.13	3.04	3.03	3.22	3.11	0.09
RB1V1 pulmonary artery	3.39	3.02	3.36	3.04	3.20	0.20
RB1V1 pulmonary vein	1.36	1.63	1.36	1.59	1.49	0.15
RB2	2.2	1.9	2.24	2.06	2.10	0.15
RB2 pulmonary artery	2.56	2.57	2.57	2.65	2.59	0.04
RB2 pulmonary vein	2.04	1.76	2.03	1.62	1.86	0.21
RB2R1	0.8	0.7	1.03	0.67	0.80	0.16
RB2R1 pulmonary artery	1.01	0.98	1.07	0.99	1.01	0.04
RB2R1 pulmonary vein	0.98	0.93	1.02	0.95	0.97	0.04
RB2C1	1.52	1.06	1.66	1.41	1.41	0.26
RB2C1 pulmonary artery	2.16	2.16	2.19	2.16	2.17	0.02
RB2C1 pulmonary vein	1.92	1.96	1.92	1.96	1.94	0.02
RB3	2.2	1.88	1.92	1.98	2.00	0.14
RB3 pulmonary artery	2.28	2.2	2.31	2.29	2.27	0.05
RB3 pulmonary vein	1.97	1.96	1.95	1.98	1.97	0.01
RB3V1	1.94	1.24	1.19	1.62	1.50	0.35
RB3V1 pulmonary artery	1.53	1.56	1.52	1.59	1.55	0.03
RB3V1 pulmonary vein	1.77	1.83	1.87	1.76	1.81	0.05
RB3D1	0.89	0.69	0.72	0.98	0.82	0.14
RB3D1 pulmonary artery	1.75	1.64	1.63	1.81	1.71	0.09
RB3D1 pulmonary vein	1.13	0.93	0.91	1.18	1.04	0.14
RB4	3.62	3.37	3.39	3.55	3.48	0.12
RB4 pulmonary artery	5.29	4.94	5.27	4.91	5.10	0.21
RB4 pulmonary vein	4.1	3.63	3.6	4.2	3.88	0.31
RB4V1	2.04	1.88	1.74	1.83	1.87	0.13

	DIAMETER 1	DIAMETER 2	DIAMETER 3	DIAMETER 4	Mean	SD
RB4V1 pulmonary artery	2.51	2.7	2.57	2.67	2.61	0.09
RB4V1 pulmonary vein	2.24	2.01	1.99	2.17	2.10	0.12
RB4V2	1.95	1.88	1.8	1.94	1.89	0.07
RB4V2 pulmonary artery	2.36	2.52	2.56	2.35	2.45	0.11
RB4V2 pulmonary vein	de				#####	######
RB4V3	3.3	3.3	3.3	3.23	3.28	0.03
RB4V3 pulmonary artery	3.99	4.03	3.93	4.01	3.99	0.04
RB4V3 pulmonary vein	2.4	2.44	2.42	2.46	2.43	0.03
LPB	4.71	5.37	5.38	4.59	5.01	0.42
LB1	3.49	1.92	1.94	3.56	2.73	0.92
LB1 pulmonary artery	6.15	6.16	6.12	6.23	6.17	0.05
LB1 pulmonary vein	4.8	1.75	4.82	1.17	3.14	1.95
LB1D1	2.04	1.85	1.78	1.96	1.91	0.12
LB1D1 pulmonary artery	4.82	4.74	4.66	4.72	4.74	0.07
LB1D1 pulmonary vein	3.09	3.03	3.04	3.02	3.05	0.03
LB1V1	1.73	1.31	1.53	1.23	1.45	0.23
LB1V1 pulmonary artery	3.02	2.87	3.03	2.9	2.96	0.08
LB1V1 pulmonary vein	2.22	2.38	2.19	2.38	2.29	0.10
LB2	3.81	3.97	4.03	3.91	3.93	0.09
LB2 pulmonary artery	4.43	4.55	4.5	4.46	4.49	0.05
LB2 pulmonary vein	4.02	3.98	4.05	4.11	4.04	0.05
LB2V1	1.68	1.85	1.62	1.42	1.64	0.18
LB2V1 pulmonary artery	2.06	1.93	1.91	2.08	2.00	0.09
LB2V1pulmonary vein	1.89	2.08	1.86	2.11	1.99	0.13
LB2V2	1.68	1.71	1.6	1.83	1.71	0.10
LB2V2 pulmonary artery	2.23	2.02	1.97	2.21	2.11	0.13
LB2V2 pulmonary vein	1.63	1.8	1.62	1.79	1.71	0.10
LB2V3	3.06	3.39	3.23	2.99	3.17	0.18
LB2V3 pulmonary artery	3.44	3.23	3.56	3.18	3.35	0.18
LB2V3 pulmonary vein	2.85	2.91	2.85	2.92	2.88	0.04

Table 1.18 Measurements of Cat No13 with mean values and standard deviation

CAT No 14

	DIAMETER1	DIAMETER 2	DIAMETER 3	DIAMETER 4	Mean	SD
TRACHEA	8.06	8.11	8.07	8.09	8.08	0.02
RPB	6.88	7.58	7.62	6.87	7.24	0.42
RB1	5.25	3.46	3.57	5.19	4.37	0.99
RB1 pulmonary artery	6.31	5.97	6.28	6.02	6.15	0.17
RB1 pulmonary vein	5.46	3.66	3.7	5.39	4.55	1.01
RB1D1	1.71	1.53	1.87	1.64	1.69	0.14
RB1D1 pulmonary artery	2.11	2.24	2.25	2.12	2.18	0.08
RB1D1 pulmonary vein	1.81	1.83	1.87	1.88	1.85	0.03
RB1V1	3.88	2.73	3.98	2.79	3.35	0.68
RB1V1 pulmonary artery	3.29	3.58	3.52	3.33	3.43	0.14
RB1V1 pulmonary vein	2.43	2.72	2.74	2.47	2.59	0.16
RB2	1.44	1.85	1.49	1.86	1.66	0.23
RB2 pulmonary artery	2.03	2.16	2.16	2.03	2.10	0.08
RB2 pulmonary vein	2.81	2.6	2.84	2.65	2.73	0.12
RB2R1	1.05	1.2	1.01	1.26	1.13	0.12
RB2R1 pulmonary artery	1.59	1.31	1.62	1.38	1.48	0.15
RB2R1 pulmonary vein	1.09	0.96	0.96	1.11	1.03	0.08
RB2C1	2.01	1.77	1.64	1.96	1.85	0.17
RB2C1 pulmonary artery	2.19	2.2	2.2	2.23	2.21	0.02
RB2C1 pulmonary vein	1.72	1.74	1.69	1.72	1.72	0.02
RB3	1.98	1.92	1.96	1.83	1.92	0.07
RB3 pulmonary artery	2.7	1.96	2.71	1.99	2.34	0.42
RB3 pulmonary vein	2.62	2.79	2.7	2.58	2.67	0.09
RB3V1	1.4	1.32	1.5	1.36	1.40	0.08
RB3V1 pulmonary artery	1.8	2.06	1.82	2.07	1.94	0.15
RB3V1 pulmonary vein	1.63	1.73	1.61	1.69	1.67	0.06
RB3D1	1.01	1.18	0.95	1.12	1.07	0.10
RB3D1 pulmonary artery	1.12	1.17	1.1	1.21	1.15	0.05
RB3D1 pulmonary vein	1.4	1.55	1.43	1.54	1.48	0.08
RB4	3.02	3.21	3.02	3.34	3.15	0.16
RB4 pulmonary artery	4.8	4.87	4.84	4.78	4.82	0.04
RB4 pulmonary vein	4.76	4.07	4.19	4.81	4.46	0.38
RB4V1	2.37	1.99	2.36	2.14	2.22	0.18

	DIAMETER 1	DIAMETER 2	DIAMETER 3	DIAMETER 4	Mean	SD
RB4V1 pulmonary artery	2.11	2.25	2.24	2.11	2.18	0.08
RB4V1 pulmonary vein	3.41	3.04	3.43	3.07	3.24	0.21
RB4V2	1.96	1.88	1.96	1.73	1.88	0.11
RB4V2 pulmonary artery	1.55	1.67	1.72	1.53	1.62	0.09
RB4V2 pulmonary vein	de	0	0	0	0.00	0.00
RB4V3	3.27	3.06	3.04	3.41	3.20	0.18
RB4V3 pulmonary artery	2.94	2.9	2.97	2.88	2.92	0.04
RB4V3 pulmonary vein	3.37	3.46	3.42	3.37	3.41	0.04
LPB	4.09	6	4.09	6.02	5.05	1.11
LB1	2.78	2.48	2.5	2.75	2.63	0.16
LB1 pulmonary artery	5.47	4.96	5.5	4.97	5.23	0.30
LB1 pulmonary vein	4.98	2.8	2.74	4.95	3.87	1.27
LB1D1	1.48	2.64	2.65	1.54	2.08	0.66
LB1D1 pulmonary artery	2.68	2.93	2.68	2.97	2.82	0.16
LB1D1 pulmonary vein	4.47	2.33	4.35	2.27	3.36	1.22
LB1V1	1.83	1.84	1.87	1.85	1.85	0.02
LB1V1 pulmonary artery	3.48	3.1	3.13	3.45	3.29	0.20
LB1V1 pulmonary vein	2.89	2.97	2.84	3	2.93	0.07
LB2	3.01	3.24	3	3.26	3.13	0.14
LB2 pulmonary artery	4.55	4.98	4.47	4.93	4.73	0.26
LB2 pulmonary vein	3.33	3.86	3.4	3.85	3.61	0.28
LB2V1	2.05	2.33	2.3	2.01	2.17	0.17
LB2V1 pulmonary artery	1.99	1.91	1.97	1.9	1.94	0.04
LB2V1 pulmonary vein	2.27	2.33	2.32	2.29	2.30	0.03
LB2V2	2.01	1.88	1.95	2.22	2.02	0.15
LB2V2 pulmonary artery	2.28	1.97	1.95	2.28	2.12	0.18
LB2V2 pulmonary vein	2.23	2.27	2.24	2.28	2.26	0.02
LB2V3	2.44	2.96	3.09	2.48	2.74	0.33
LB2V3 pulmonary artery	3.16	3.18	3.17	3.2	3.18	0.02
LB2V3 pulmonary vein	3	3.13	3.03	3.13	3.07	0.07

Table 1.19 Measurements of Cat No14 with mean values and standard deviation

Tables were performed separating the left from the right lung and the trachea using the mean values. This division was made every time for the bronchial lumen, arteries and veins. The seven categories that we produced are trachea (table 2.1), right lung (table 2.2a, 2.2b, 2.2c), left lung (table 2.3), pulmonary arteries of the right lung (table 2.4a, 2.4b, 2.4c), pulmonary arteries of the left lung (table 2.5), pulmonary veins of the right lung (table 2.6a, 2.6b, 2.6c) and pulmonary veins of the left lung (table 2.7) are reported in the following tables. Statistical analysis demonstrates a linear correlation only for tracheal diameter to the felines weight (fig.1).

	Trachea
Cat No1	7.78
Cat No 2	6.37
Cat No 3	5.94
Cat No 4	6.68
Cat No 5	6.78
Cat No 6	6.30
Cat No 7	7.68
Cat No 8	7.63
Cat No 9	8.03
Cat No 10	7.00
Cat No 11	7.57
Cat No 12	6.66
Cat No 13	7.56
Cat No 14	8.08
Mean	7.15
SD	0.70

Table 2.1 Mean values and standard deviation of the mean values of the tracheal diameter

RIGHT LUNG BRONCHIAL LUMEN

	RPB	RB1	RB1D1	RB1V1	RB2
Cat No 1	6.60	4.23	1.81	3.24	2.85
Cat No 2	5.73	3.36	0.88	2.78	2.22
Cat No 3	4.83	3.48	1.16	2.75	1.91
Cat No 4	5.60	4.03	1.97	3.4	1.9
Cat No 5	5.44	3.72	1.43	3.28	2.45
Cat No 6	4.87	3.63	1.69	2.88	1.91
Cat No 7	6.40	4.09	2.51	4.33	3.64
Cat No 8	6.69	3.96	2.39	3.09	2.17
Cat No 9	6.52	3.57	1.66	3.21	2.44
Cat No 10	5.82	3.22	0.64	2.83	1.98
Cat No 11	5.90	3.86	1.8	3.07	1.96
Cat No 12	6.26	3.36	1.5	2.75	1.76
Cat No 13	6.78	3.87	1.69	3.11	2.1
Cat No 14	7.24	4.37	1.69	3.35	1.66
Mean	6.05	3.77	1.63	3.15	2.21
SD	0.72	0.35	0.51	0.41	0.52

Table 2.2a Mean values and standard deviation of the diameter of the bronchial lumen of the right lung

	RB2R1	RB2C1	RB3	RB3V1	RB3D1
Cat No 1	1.38	1.97	2.77	2.15	1.6
Cat No 2	1.20	1.21	1.73	0.86	1.05
Cat No 3	0.84	0.81	1.88	1.24	1.37
Cat No 4	0.66	1.45	1.87	1.55	0.81
Cat No 5	0	1.45	1.76	1.14	1.63
Cat No 6	1.3	1.36	1.95	1.76	1.68
Cat No 7	2.98	3	3.3	3.41	3.3
Cat No 8	1.24	2.02	2.56	1.21	1.34
Cat No 9	0.9	1.22	2.69	1.6	1.06
Cat No 10	0.6	1.3	1.8	0.98	0.81
Cat No 11	0.89	1.4	1.71	1.71	1.3
Cat No 12	0.8	1.12	1.72	0.84	0.73
Cat No 13	0.8	1.41	2	1.5	0.82
Cat No 14	1.13	1.85	1.92	1.4	1.07
Mean	1.05	1.54	2.12	1.53	1.33
SD	0.66	0.53	0.50	0.66	0.65

Table 2.2b Mean values and standard deviation of the diameter of the bronchial lumen of the right lung

	RB4	RB4V1	RB4V2	RB4V3
Cat No 1	4.93	2.6	2.05	3.48
Cat No 2	3.74	1.20	1.34	1.88
Cat No 3	3.87	0	0	0
Cat No 4	3.07	1.83	1.59	2.6
Cat No 5	3.74	1.53	1.75	2.49
Cat No 6	3.37	2.02	1.59	2.9
Cat No 7	5.03	3.16	3.42	4.61
Cat No 8	4.41	1.91	1.56	4.17
Cat No 9	4.72	1.91	1.66	2.86
Cat No 10	3.79	0.69	0.85	2.49
Cat No 11	4.12	1.93	2.54	3.32
Cat No 12	3.24	1.69	1.83	2.22
Cat No 13	3.48	1.87	1.89	3.28
Cat No 14	3.15	2.22	1.88	3.2
Mean	3.90	1.75	1.71	2.82
SD	0.65	0.77	0.77	1.09

Table 2.2c Mean values and standard deviation of the diameter of the bronchial lumen of the right lung

LEFT LUNG BRONCHIAL LUMEN

	LPB	LB1	LB1D1	LB1V1	LB2	LB2V1	LB2V2	LB2V3
Cat No 1	6.11	4.16	2.12	2.17	4.22	1.95	2.38	3.87
Cat No 2	4.87	3.39	2.5	1.17	3.74	1.86	0	1.27
Cat No 3	3.92	2.24	1.5	1.33	4.2	nv	nv	nv
Cat No 4	4.57	3.28	2.78	3.05	4.03	1.6	1.53	2.58
Cat No 5	4.62	3.91	2.93	2.43	3.84	1.33	1.75	2.54
Cat No 6	4.86	3.26	2.22	1.86	3.67	2.02	2.09	3.95
Cat No 7	5.31	3.69	2.92	2.41	4.88	3.23	3.11	4.51
Cat No 8	5.95	4.35	2.93	2.55	4.16	1.73	2.34	3.92
Cat No 9	5.36	2.97	1.93	2.04	3.67	1.8	1.95	3.41
Cat No 10	4.56	2.51	1.87	1.19	3.37	1.09	1.05	1.92
Cat No 11	4.95	2.7	1.72	2.12	3.55	1.93	1.68	3.23
Cat No 12	5.03	3.05	1.95	1.51	3.25	1.24	1.33	2.11
Cat No 13	5.01	2.73	1.91	1.45	3.93	1.64	1.71	3.17
Cat No 14	5.05	2.63	2.08	1.85	3.13	2.17	2.02	2.74
Mean	5.012	3.21	2.24	1.94	3.83	1.81	1.76	3.02
SD	0.561	0.64	0.49	0.56	0.46	0.53	0.74	0.93

Table 2.3 Mean values and standard deviation of the diameter of the bronchial lumen of the left lung

RIGHT LUNG PULMONARY ARTERIES

	RB1	RB1D1	RB1V1	RB2	RB2R1
Cat No 1	4.54	1.46	3.21	2.3	1.09
Cat No 2	4.35	1.98	3.35	3.2	1.52
Cat No 3	4.11	1.99	2.85	2.52	1.71
Cat No 4	5.59	1.73	3.36	3.17	0.99
Cat No 5	4.68	1.93	3.53	3.66	1.36
Cat No 6	5.01	2.21	3.69	3.02	1.41
Cat No 7	4.46	2.19	3.39	2.96	1.98
Cat No 8	4.36	2.44	3.46	2.28	1.03
Cat No 9	5.47	2.32	3.8	1.71	1.2
Cat No 10	4.5	2.13	2.81	3.7	1.61
Cat No 11	5.72	2.69	3.85	3.35	0.95
Cat No 12	2.91	1.51	2.91	2.3	1.02
Cat No 13	4.42	1.69	3.2	2.59	1.01
Cat No 14	6.15	2.18	3.43	2.1	1.48
Mean	4.73	2.03	3.35	2.78	1.31
SD	0.81	0.35	0.33	0.61	0.32

Table 2.4a Mean values and standard deviation of the diameter of the pulmonary arteries of the right lung

	RB2C1	RB3	RB3V1	RB3D1	RB4
Cat No 1	1.47	2.58	2.09	1.6	5.03
Cat No 2	2.47	2.62	2.12	2.18	4.31
Cat No 3	2.61	3.07	2.29	2.44	5.33
Cat No 4	2.19	2.92	1.78	1.34	4.64
Cat No 5	2.77	3.39	2.28	2.79	5.16
Cat No 6	2.32	2.74	2.09	1.83	4.32
Cat No 7	2.04	3.61	2.15	2.09	5.51
Cat No 8	2	2.12	1.49	1.7	3.8
Cat No 9	2.45	2.52	1.38	1.16	4.79
Cat No 10	2.06	3.02	1.71	2.33	4.25
Cat No 11	2.37	2.98	2.1	1.79	5.48
Cat No 12	1.98	3.05	2.07	2.07	4.43
Cat No 13	2.17	2.27	1.55	1.71	5.1
Cat No 14	2.21	2.34	1.94	1.15	4.82
Mean	2.22	2.80	1.93	1.87	4.78
SD	0.32	0.43	0.30	0.48	0.52

Table 2.4b Mean values and standard deviation of the diameter of the pulmonary arteries of the right lung

	RB4V1	RB4V2	RB4V3
Cat No 1	2.57	2.15	3.26
Cat No 2	1.58	2.11	3.05
Cat No 3	3.12	2.76	3.73
Cat No 4	2.71	2.24	3.1
Cat No 5	3.11	2.53	3.53
Cat No 6	2.8	1.8	3.12
Cat No 7	2.87	2.67	3.83
Cat No 8	1.7	1.64	3.1
Cat No 9	2.49	2.1	2.95
Cat No 10	2.54	2.13	3.02
Cat No 11	2.64	2.33	3.4
Cat No 12	2.19	2.15	2.83
Cat No 13	2.61	2.45	3.99
Cat No 14	2.18	1.62	3.92
Mean	2.51	2.19	3.35
SD	0.46	0.35	0.39

Table 2.4c Mean values and standard deviation of the diameter of the pulmonary arteries of the right lung

LEFT LUNG PULMONARY ARTERIES

	LB1	LB1D1	LB1V1	LB2	LB2V1	LB2V2	LB2V3
Cat No 1	5.36	2.88	2.37	5.78	1.92	1.95	3.7
Cat No 2	6.06	3.85	3.04	4.8	2.32	1.71	2.77
Cat No 3	5.02	3.03	2.81	5.58	2.86	2.39	3.76
Cat No 4	5.59	2.64	3.03	5.56	2.86	2.62	3.25
Cat No 5	5.14	3.52	3.06	5.72	2.56	2.73	3.53
Cat No 6	5.3	3.05	3.05	4.55	2.36	2.04	3.35
Cat No 7	6.64	3.13	2.85	5.26	2.64	2.3	4.02
Cat No 8	4.86	3.43	2.99	4.01	2.02	1.23	3.22
Cat No 9	6.11	2.76	2.41	4.5	2.05	2.45	3.32
Cat No 10	5.38	3.45	3.13	5.35	2.6	2.31	3.08
Cat No 11	5.17	3.06	2.95	5.39	2.24	2.48	3.2
Cat No 12	4.8	2.54	2.03	4.49	2.15	2.04	3.37
Cat No 13	6.17	4.74	2.96	4.49	2	2.11	3.35
Cat No 14	5.23	2.82	3.29	4.73	1.94	2.12	3.18
Mean	5.49	3.21	2.86	5.02	2.32	2.18	3.36
SD	0.55	0.57	0.35	0.57	0.33	0.39	0.31

Table 2.5 Mean values and standard deviation of the diameter of the pulmonary arteries of the left lung

RIGHT LUNG PULMONARY VEINS

	RB1	RB1D1	RB1V1	RB2	RB2R1
Cat No 1	3.77	1.41	2.45	1.41	0.82
Cat No 2	3.49	1.11	1.87	2.63	1.43
Cat No 3	3.51	2.14	1.96	2.44	0.91
Cat No 4	3.3	2.3	2.52	2.09	1.31
Cat No 5	3.1	1.64	3.54	1.75	0
Cat No 6	3.75	2.5	3.15	2.87	0.86
Cat No 7	5.72	3	3.92	3.59	1.76
Cat No 8	4.91	2.2	2.59	2.25	1.04
Cat No 9	4.51	2.62	3.29	2.05	1.24
Cat No 10	3.58	1.68	2.36	2.24	0.96
Cat No 11	4.7	2.47	3.76	2.78	1.35
Cat No 12	3.08	1.43	2.31	1.64	0.73
Cat No 13	2.98	1.02	1.49	1.86	0.97
Cat No 14	4.55	1.85	2.59	2.73	1.03
Mean	3.93	1.96	2.70	2.31	1.03
SD	0.82	0.60	0.73	0.58	0.41

Table 2.6a Mean values and standard deviation of the diameter of the pulmonary veins of the right lung

	RB2C1	RB3	RB3V1	RB3D1	RB4
Cat No 1	1.14	2.15	1.95	1.47	3.93
Cat No 2	2.73	1.35	0.68	0.94	2.4
Cat No 3	1.37	2.63	2.16	1.75	4.69
Cat No 4	0.95	2.66	1.88	1.59	3.4
Cat No 5	1.74	2.78	83	1.33	3.66
Cat No 6	1.73	2.5	1.59	1.54	3.98
Cat No 7	1.97	2.56	1.51	1.59	5.07
Cat No 8	1.52	2.24	1.63	0.9	3.82
Cat No 9	1.66	3.06	2.39	1.72	5.34
Cat No 10	1.82	1.73	1.2	0.83	3.06
Cat No 11	2.15	2.98	1.99	1.77	4.57
Cat No 12	1.28	2.47	1.77	1.17	3.66
Cat No 13	1.94	1.97	1.81	1.04	3.88
Cat No 14	1.72	2.67	1.67	1.48	4.46
Mean	1.69	2.41	7.52	1.37	3.99
SD	0.45	0.48	21.73	0.33	0.79

Table 2.6b Mean values and standard deviation of the diameter of the pulmonary veins of the right lung

	RB4V1	RB4V2	RB4V3
Cat No 1	2.22	1.61	2.39
Cat No 2	1.24	1.3	1.11
Cat No 3	3.14	de	2.79
Cat No 4	2.45	de	2.58
Cat No 5	2.29	de	2.62
Cat No 6	2.59	1.82	2.23
Cat No 7	3.45	de	2.34
Cat No 8	2.02	de	3.07
Cat No 9	2.94	de	3.49
Cat No 10	1.89	1.3	1.37
Cat No 11	2.52	1.65	2.47
Cat No 12	2.02	1.23	2
Cat No 13	2.1	de	2.43
Cat No 14	3.24	de	3.41
Mean	2.44	1.49	2.45
SD	0.60	0.24	0.67

Table 2.6c Mean values and standard deviation of the diameter of the pulmonary veins of the right lung

LEFT LUNG PULMONARY VEINS

	LB1	LB1D1	LB1V1	LB2	LB2V1	LB2V2	LB2V3
Cat No 1	3.29	2.3	1.8	3.77	1.7	1.61	2.79
Cat No 2	3.62	2.01	1.92	4.34	2.11	0.94	1.28
Cat No 3	2.81	2.76	2.62	4.73	2.89	2.24	2.43
Cat No 4	2.93	1.77	2.45	5.2	2.39	1.81	2.19
Cat No 5	4.51	2.02	2.59	4.11	2.11	1.59	1.48
Cat No 6	3.04	2.53	2.95	4.74	2.71	1.13	2.8
Cat No 7	3.05	3.09	2.53	4.11	2.51	2.37	2.12
Cat No 8	3.48	3.48	2.71	4.35	1.84	1.05	2.55
Cat No 9	3.07	3.17	2.79	4.96	2.63	2.59	3.62
Cat No 10	2.47	1.57	2.44	3.88	1.92	1.26	1.75
Cat No 11	nv	2.03	2.14	5.54	2.53	1.95	2.61
Cat No 12	2.42	1.76	1.13	4.03	1.82	1.54	1.76
Cat No 13	3.14	3.05	2.29	4.04	1.99	1.71	2.88
Cat No 14	3.87	3.36	2.93	3.61	2.3	2.26	3.07
Mean	3.21	2.49	2.38	4.39	2.25	1.72	2.38
SD	0.57	0.65	0.50	0.57	0.37	0.52	0.66

Table 2.7 Mean values and standard deviation of the diameter of the pulmonary veins of the left lung

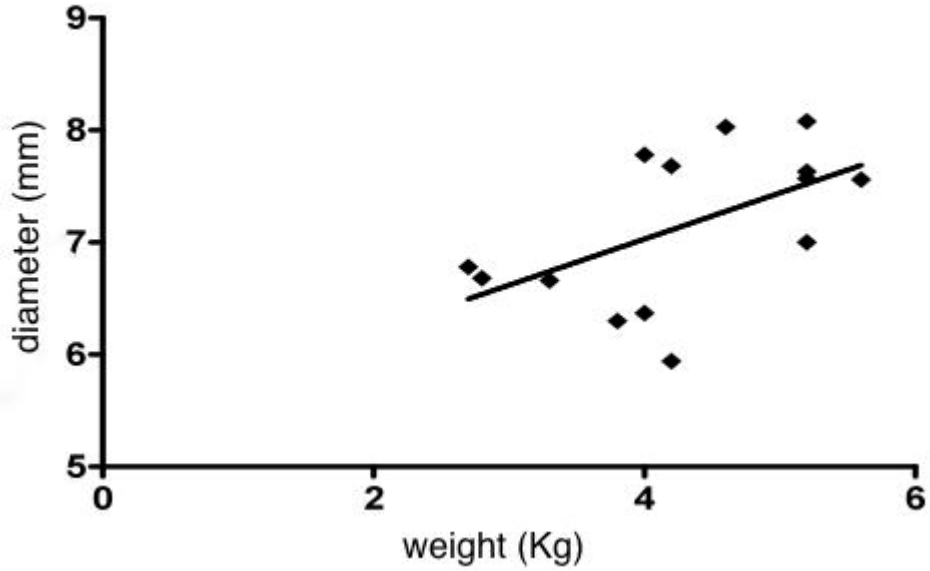

Fig.1. Axis x demonstrates the felines weight in Kg and the axis Y the tracheal diameter measured in millimeters.p=0.042

Segmental arterial branches were clearly identified in computed tomographic angiographic study and their number was calculated for each cat as it is reported (table 2.8a, 2.8b, 2.8c). The mean number of all the thoracic segmental arterial branches is seen in fig.2.

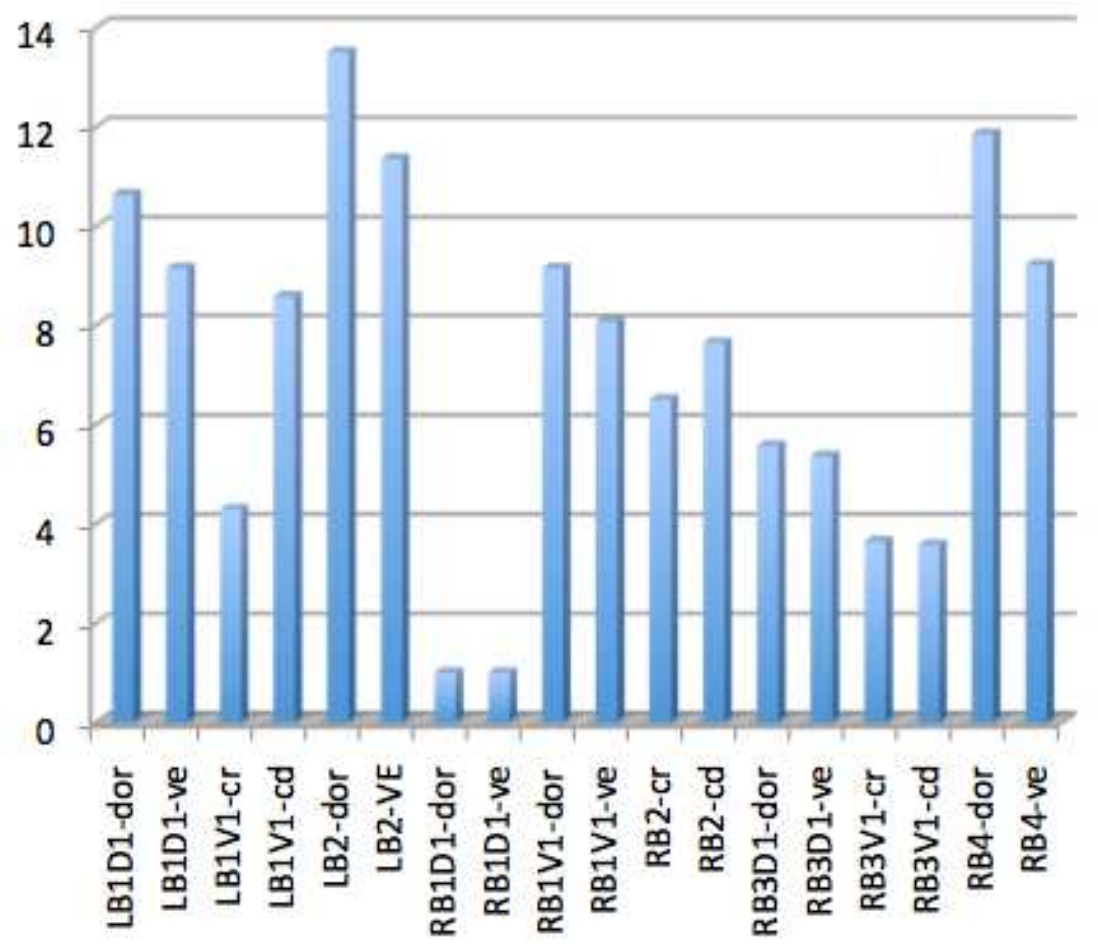

Fig. 2 Mean values of the number of segmental arterial branches

SEGMENTAL ARTERIAL BRANCHES

Segmental	LB1D1-dor	LB1D1-ve	LB1V1-cr	LB1V1-cd	LB2-dor	LB2-ve	RB1D1-dor
Cat No 1	12.00	11	5	10	14	12	1
Cat No 2	12.00	8	4	8	15	12	1
Cat No 3	11.00	8	4	8	15	12	1
Cat No 4	11.00	10	4	8	13	12	1
Cat No 5	10.00	10	4	8	13	12	1
Cat No 6	11.00	8	4	8	14	12	1
Cat No 7	10.00	10	4	8	13	12	1
Cat No 8	11.00	11	4	8	12	10	1
Cat No 9	12.00	11	4	8	15	10	1
Cat No 10	11.00	9	5	10	14	11	1
Cat No 11	10.00	8	5	10	13	10	1
Cat No 12	6.00	6	4	8	13	12	1
Cat No 13	10.00	10	4	8	12	10	1
Cat No 14	12.00	8	5	10	13	12	1
Mean	10.64	9.14	4.29	8.57	13.50	11.36	1.00
SD	1.55	1.51	0.47	0.94	1.02	0.93	0.00

Table 2.8a Mean values and standard deviation of the number of segmental arterial branches

Segmental	RB1D1-ve	RB1V1-dor	RB1V1-ve	RB2-cr	RB2-cd	RB3D1-dor	RB3D1-ve	RB3V1-cr
Cat No 1	1	11	9	7	7	8	8	4
Cat No 2	1	11	12	9	12	9	7	4
Cat No 3	1	5	5	6	7	0	0	0
Cat No 4	1	8	6	6	7	6	6	4
Cat No 5	1	10	9	8	8	5	6	4
Cat No 6	1	11	6	6	6	6	6	4
Cat No 7	1	10	8	6	7	6	5	4
Cat No 8	1	9	10	6	7	1	1	2
Cat No 9	1	5	5	6	9	6	5	4
Cat No 10	1	10	12	7	6	8	6	4
Cat No 11	1	8	7	6	7	4	7	4
Cat No 12	1	9	6	6	8	7	8	5
Cat No 13	1	9	9	6	8	6	5	4
Cat No 14	1	12	9	6	8	6	5	4
Mean	1.00	9.14	8.07	6.50	7.64	5.57	5.36	3.64
SD	0.00	2.11	2.34	0.94	1.50	2.50	2.31	1.22

Table 2.8b Mean values and standard deviation of the number of segmental arterial branches

Segmental	RB3V1-cd	RB4-dor	RB4-ve
Cat No 1	4	11	9
Cat No 2	4	10	8
Cat No 3	0	0	0
Cat No 4	4	13	11
Cat No 5	4	14	9
Cat No 6	4	14	9
Cat No 7	4	12	8
Cat No 8	1	14	13
Cat No 9	4	12	10
Cat No 10	4	17	12
Cat No 11	4	10	8
Cat No 12	5	13	11
Cat No 13	4	12	9
Cat No 14	4	14	12
Mean	3.57	11.86	9.21
SD	1.34	3.88	3.12

Table 2.8c Mean values and standard deviation of the number of segmental arterial branches

DISCUSSION

The following discussion reports and compares the results of a CTPA examination of the feline thorax in 14 normal cats using a 64-multidetector row scanner with the till now data that are published in anatomic and in diagnostic imaging. CTPA is the gold standard diagnostic imaging technique for the evaluation of the pulmonary arteries and the detection of pulmonary embolism which is a life threatening pathology. This advanced method could explain better the anatomy of the pulmonary vasculature till the level of minor segmental branches. In our study all the examined cats had a successful CTPA protocol which allowed the visualization of the normal pulmonary vascular and bronchial anatomy using a 64 MDCT. Vascular variants were noticed. Incidental findings of sudden cut-off vessels has to be further studied in the future. Peripheral embolism was an incidental finding in one case and was clearly noticed in 2D images and in 3D models. Limitations of the study due to minor dimensions of these structures are correlated with blooming artifact and possible influence of the anesthetic protocol. During CTPA protocol the venous hepatic vasculature is well enhanced without having yet portal flow.

Many reports describe radiographic or tomographic findings in feline patients with pulmonary disease but there is not yet well described the normal aspect and anatomy of the feline thorax. The past decade correlation of the gross cross anatomy and computed tomographic anatomy of the cat was reported (Sammi, 1998). The purpose of this study is to evaluate and demonstrate the normal aspects of the feline thorax using an advanced technique and 3D models. Our study provided an in vivo study of the feline thoracic structures concentrating on the pulmonary arteries. In comparison with the studies of the anatomist we could evaluate and measure all the structures without changing the normal anatomy, although we have to

consider the influence of the anesthetic ventilatory protocol and that the scanning time in the pulmonary arterial phase could possibly influence the measurements of the bronchial lumen and pulmonary veins. Limitations of the scanning technique are present due to the minor dimensions of the examined structures and the blooming artifact that was most possibly decreased and could still influence the dimensions of these structures. The ventilatory protocol that we performed has published cardiovascular depression effects and this could effect the injection protocol and the vascular dimensions considering possible that venous system could be overestimated due to the reduced venous return of blood to the heart (Heano-Guerrero, 2012).

Pulmonary disease is a common pathology of the feline patient, although is challenging the evaluation due to owner's difficulty in recognizing during early stages and to limitations of the clinical examination of the thorax. These reasons are the common explanation of controlling usually clinically severe diseases. Computed tomography is more sensitive than radiography for determination of the location and extent of pulmonary disease. A normal radiographic examination of the feline thorax does not exclude the detection of pathology with a computed tomographic examination (Miller, 2007).

In human medicine 64-row CT scanners are used to perform fast acquisition studies. Cardiac and vascular computed tomography imaging is a standard method of obtaining accurate diagnosis in human medicine. In veterinary medicine few reports about this technology and the specifications of the scanner are reported. A 64 MDCT scanner was used in a CTA study of normal dogs in order to evaluate the pulmonary arteries (Drees, 2011a) in which anatomical details and scanning technique procedure are described. Another study using the same technology in order to evaluate the coronary

arteries in normal dogs was reported the same year (Drees, 2011b). In our study in order to decide the technology of the scanner that we needed and could provide high quality images of the feline CTPA study, we studied many parameters such as image quality, dose management and workflow integration. Image quality is influenced by scanner's technical specifications such as slice thickness, noise characteristics, uniformity, temporal resolution and artifacts. There are not yet well studied limits about the dose management in animals but we thought to achieve a scanning protocol that could have a dose modulation in order to keep the radiation dose at lower limits with high quality imaging. Workflow integration was based on clinical experience of radiologists and technicians, image acquisition performance and post processing software. Features such as bone removal, vessel analysis, lung analysis, virtual bronchoscopy were the basic software that were needed for our study. Therefore, we had to select the appropriate 3-D processing, based on specific technical and clinical needs. The Aquilion 64 exceeds many of our criteria.

An anesthetic protocol with a manual compression of the reservoir bag in a standard pressure was performed in order to provide an inspiration apnea during the CTPA scanning time. Comparison of four anesthetic protocols has been evaluated in order to study and minimize the effects of confounding factors in healthy cats (Heano-Guerrero, 2012). None of the studied ventilatory protocols in the above report did not eliminated atelectasis in cats. Based on the above study our ventilatory protocol belongs to the deep breath by manual compression of the reservoir bag with an increased PIP of 20cm H_2O. This protocol is reported for providing highest mean lung volume and more severe cardiovascular depression than was detected in other ventilatory protocols that were studied under the same examination

conditions. Caution should be used when this protocol is used for hemodynamically unstable cats or for cats suspected to have restrictive lung disease. We have to notice that in our protocol dexmedetomidine was not suspended with atipamezole after intubation but always at the end of the examination. The time of CTPA scanning was always at least twenty minutes after the administration of dexmedetomidine. Dexmedetomidine is reported of producing cardiovascular effects decreasing the heart rate and cardiac output and increasing the blood pressure and systemic and pulmonary vascular resistances (Pyperdop, 2011). The effect of the anesthetic drugs must be considered when evaluating bronchial and vascular structures. In our study we did not documentated any negative influence on our CTPA protocol from the anesthetic protocol.

In a report of evaluation bronchial to arterial ratio in order to evaluate bronchiectasis the anesthetic protocol was considered of affecting the BA ratio and needed to be further studied in the future (Reid, 2012). The purpose of the study is to achieve an adequate protocol in which we could have clear and reliable images of the vascular and bronchial structures of the feline thorax. Considering their minimal dimensions, we had to think and try the most adequate scanning parameters and the correct contrast medium administration protocol respectively to the technology and the type of scanner that we used for this study. We thought that a human protocol of a CTPA would be the base for our protocol. Scanning techniques in human medicine helped us to decide and achieve our final CTPA protocol for feline patients. In human medicine CTPA is performed in patients with atypical chest pain, D-dimer elevation, unclear dyspnea, follow-up patients with known pulmonary embolism and screening for high risk patients with known deep-vein thrombosis. Pulmonary embolism is a life threatening condition

also in animals. Pulmonary angiography is the gold standard for the evaluation of pulmonary embolism in human medicine. The latest generation of MDCT devices can obtain thin sections up to 0,5mm with a high spatial and temporal resolution. This may improve the diagnosis of pulmonary embolism and is especially important for determining the location and extent of the thrombus. The high spatial resolution of sub millimeter collimation data sets now allows evaluation of pulmonary vessels down to sixth-order branches and substantially increases the detection rate of segmental and sub segmental pulmonary emboli. Latest studies describe the confidence in the evaluation of sub segmental arteries with thin-section MDCT that far exceeds the reproducibility of selective pulmonary angiography.

The clinical importance of small peripheral emboli in sub segmental pulmonary arteries in the absence of a central embolus is uncertain. In human medicine is considered the fact that the presence of peripheral emboli may be indicator of concurrent deep venous thrombosis, thus potentially heralding more severe embolic events. The presence of some peripheral emboli may be a clinical importance in patients with cardiopulmonary restriction and in evaluating the development of chronic pulmonary hypertension in patients suffering from thromboembolism disease. However no study has yet proven its clinical superiority over conventional scanning techniques especially when taking the considerably higher radiation dose into consideration (Kuettner, 2006).

Artifacts in MDCT that we usually have to consider are the beam-hardening, blooming, partial volume, motion, spiral and cone beam artifact. The most prominent beam-hardening artifact is known as the Hounsfield bar. Beam hardening artifacts typically appear in the vicinity of dense bones, in vessels with high concentrated iodine contrast media or implanted metals (Raupach,

2006). As a result reconstructs images show dark areas of streaks between, for example, thick bones. Its strength depends significantly on the atomic composite, the size of the object and the voltage used. High-attenuating objects generally appear larger than they are. Any negative effects of beam hardening or structure-related artifacts on the accuracy of image interpretation can be avoided with a review of the axial source images (Choi, 2004). In our study we avoided the streak artifacts by using saline chase injection after contrast medium administration. The dilution of the contrast medium to a concentration of 150 mg iobitridol/ml decreased the blooming artifact but it could still influence our measurements due to the minor dimensions of the examined structures. Contrast agent dilution could reduce streak and blooming artifact (Pollard, 2011). In one case a motion artifact due to minor breathing movement was present due to incomplete holding of the reservoir bag with standard pressure in apnea.

Iobitridol is an iodinated contrast agent, nonionic water soluble tri-iodinated product that may include mild/severe intolerance reaction, that is not yet studied in feline patients. Our primary goal was to achieve adequate opacification of the thoracic vascular structures synchronized with the CT acquisition. Lack of an already published CTPA protocol for feline patients using a 64-slice CT scanner was the base of studying better the parameters of a contrast medium administration strategy in human and canine CTPA. Reports for the evaluation of canine pulmonary vasculature have published different CTPA protocols using 16 and 64 multidetector row computed tomography scanners. Various protocols of contrast medium administration in canine CTPA protocols have been studied with successful angiographic examinations (Habing, 2010; Brewer, 2012; Drees, 2011). An angiographic study of canine pulmonary arteries using a 40-multidetector row CT studied

the effect of contrast medium injection and concluded that an injection protocol with an injection duration adjusted to the scan duration is suitable for CTPA scanning of the canine thorax (Makara, 2011). For an angiographic study it was suitable to use a non-ionic and low-osmolar contrast agent. Viscosity that has been considered less important factor than osmolarity in the past has regained importance in newest studies (Fleischmann, 2009). Important role had the standard temperature of the contrast medium in a baby warmer at 36 Celsius grade and followed by the heating cuff of the injector. Generally a non-ionic CM is safer than ionic CM and extravasation is well tolerated respectively to ionic CM (Fleischmann, 2009). Safety issues such as anaphylactic reaction, contrast medium extravasation, cardiovascular effects, nephrotoxicity and drug interactions were considered based on human bibliography due to lack of veterinary studies. Vascular enhancement and parenchymal organ enhancement are affected by different kinetics. Early vascular enhancement is determined by the relationship between iodine administration per unit of time versus blood flow per unit of time. Parenchymal enhancement is governed by the relationship of total iodine dose versus volume of distribution. Arterial enhancement can be controlled by the injection flow rate and the iodine concentration. Longer injection durations increases arterial enhancement and improves vascular opacification (Fleischmann, 2009). Peak enhancement also is influenced by the central blood volume and cardiac output. Increased arterial peak enhancement due to decreased cardiac output produce decreased mixing and dilution of the contrast medium (Makara, 2011). Central blood volume is affected from the weight of the patient and affects recirculation and tissue enhancement than first pass dynamics. A dose of 2 ml/Kg of body weight is an adequate quantity for a CTPA in feline patients. There are also user's selectable parameters that affect arterial enhancement.

In human medicine maximum iodine flux can be achieved when high iodine concentration and high injection flow rate are combined. This is a problem in a feline patients and we had to modify these parameters to a flow rate of 2 ml/sec, maximum pressure of 300 lb/in^2 and a CM concentration of 150 mg iobitridol /ml. Important note is the temperature of the CM and the secure and well checked intravenous access. A 20G intravenous catheter of the cephalic vein had an adequate diameter for the free pass of the CM with 150 mg I/ml concentration and 2ml/sec flow rate. To control all these parameters a double-barrel system with heating cuff (keeping the CM in the syringe of the injector warm), extravasation detection device (interrupts the mechanical injection when a skin-impedance change is detected) and communication interface between scanner and injector was used in our study. A first saline flush of 20 ml before the CM administration was always in the CM administration protocol and checked the function of the injector and the free intravenous pass. A second saline flush after the CM administration with the same volume improves the arterial opacification, prolongs the arterial enhancement phase and reduces the perivenous streak artifact. In human medicine many reports describe different injection strategies in MDCT. Acquilion 64 scanner belongs to the fast acquisitions injection strategies and has a bolus triggering software to perform the CTA scans. Four basic parameters were considered before choosing the CTPA protocol the monitoring delay, monitoring interval, trigger threshold and trigger delay. Bolus triggering could produce scanning delays compared with the test bolus but our injection protocol was perfectly imbalanced with the scanning duration (Habing, 2010). Our strategy allowed breath holding in inspiration and produced a reliable strong arterial enhancement. Image quality was constant within and across individuals by using automated tube-current modulation.

A critical consideration in the visualization process lies in the setting of the grayscale window and level for image review. When performing cardiovascular imaging, the vessel lumen should never be rendered with the highest gray values. If the lumen is rendered with the highest gray values, then the grayscale is truncated, which can misrepresent vessel dimensions. Based on our isotropic study with 0,5 millimeter (mm) of slice thickness, measurements till o,5 mm were made and considered accurate.

Canine pulmonary embolism has been documented with computed tomography in cases of experimentally infected with Dirofilaria immitis (Seiller, 2010; Jung, 2010) and in cases following canine total hip replacement (Tidwell, 2007). Our study reports an incidental detection of pulmonary embolism with multidetector computed tomography in feline patient. This could be a result of an older pulmonary parasitic infection, a blood parasitic infection or a coagulation disorder, examinations that were not included in our standard enrolment protocol. A CTPA protocol is reported of identifying also pathologies of the thorax that are not correlated to the pulmonary arteries (Lee, 2009). In our study during a CTPA protocol cats we could identify other pulmonary pathology (pulmonary nodules, mild spontaneous pneumothorax) and exclude these cats from our study.

From this study is reported that the trachea bifurcates in right principal bronchus and left principal bronchus. Trachea has a linear correlation with the weight of the cat. The right principal bronchus detaches firstly the right cranial and in a different distance for every cat the right medial lobe. The right cranial lobe is detaching from the right principal bronchus and not directly from the trachea, so we cannot talk about trifurcation of the trachea in the feline thorax as is reported in canine's. Many authors (Ishaq, 1980; Getty, 1982) report that in carnivores the accessory lobe origins directly

from the right principal bronchus , while is observed in other cases detaching from the right caudal lobe, which is the direct continuation of the right principal after the right medial lobe. The left principal bronchus is reported that detaches the left cranial lobe and continues as left caudal lobe(Ishaq, 1980; Getty,1982; Barone,2003). The pulmonary arteries tend to have a close relation with the bronchial lumen till the smallest segmental branches, while the pulmonary veins show this relation only in the principal diramation and have a wider relation to the bronchial lumen at the level of the segmentals.

The right cranial lobe origins from the right principal bronchus and detaches immediately a dorsal-lateral branch, which bifurcates in a dorsal and in a lateral segmental one. The right cranial lobe detaches a lateral branch which is named “bronchus P” (Ishaq, 1980). Bronchus P in our study was considered as a segmental of the ventral branch of the right cranial lobe while in another study was considered as the dorsal-lateral one (Coccolini, 2012). Another opinion is reported (Barone, 2003) considering the right cranial lobe as one branch that detaches dorsal and ventral segmental branches. A single case is reported (Coccolini, 2012) in which the right cranial lobe bifurcates in a dorsal and in a ventral branch. The right pulmonary artery detaches the pulmonary artery of the right cranial lobe. In all the cats of the study the pulmonary artery of the dorsal-lateral branch detaches directly from the right pulmonary artery. The pulmonary veins of the right cranial lobe anastomose with the pulmonary vein of the middle lobe and attach the left atrium consisting the right ostia. Three cats of the study show a sudden cut-off of the left and right cranial pulmonary arteries and veins, fact that is not yet explained and need to be further studied in the future.

The right middle lobe origins from the right principal bronchus and runs ventral detaching cranial and caudal segmental branches. An endoscopic study reports that only the origin of the first cranial segmental branch (RB2C1) is visible (Caccamo, 2006). The right pulmonary artery detaches the middle lobar pulmonary artery (Barone, 2003). Medial to the middle lobar branch runs the pulmonary vein that anastomose with the right cranial lobar pulmonary vein and consist the right ostia.

The right caudal lobe detaches the accessory lobe as is reported (Barone, 2003) while in canine thorax and in carnivores in general origin directly from the right principal bronchus (Ishaq,1980; Getty, 1982). The accessory lobar pulmonary artery origins from the right caudal lobar pulmonary artery and the accessory lobar pulmonary vein attach the right caudal lobar pulmonary vein (Schaller, 1999). The accessory lobe is devised in a ventral-medial and in a caudal branch. An endoscopic study divides the accessory lobe in a dorsal (RB3D1) and in a ventral branch (RB3V1) (Caccamo, 2006). Considering the above study the ventral-medial is correlated with the RB3V1 and the caudal with the RB3D1. The accessory lobar pulmonary artery origins from the right caudal lobar artery, runs ventral/ventral-lateral and has an attached relation to the bronchus. Accessory lobar pulmonary vein drains the accessory lobe and attaches the right caudal lobar pulmonary vein.

The direct continuation of the right principal bronchus consist the right caudal lobe. The right caudal lobe detaches a ventral, a ventral-caudal and a caudal branch. Dorsal segmental branches are detaching. Right pulmonary artery after detaching the right cranial lobar pulmonary artery continues as caudal lobar pulmonary artery and detaches multiple dorsal segmental branches. The right pulmonary lobar vein drains the right caudal lobe. The

caudal, ventral-caudal and ventral pulmonary vein anastomose in the right caudal pulmonary vein. Eight of the fourteen cats do not have the ventral-caudal pulmonary vein and show a wider ramification of the ventral pulmonary vein which drains a wider pulmonary parenchyma. Eight of the fourteen cats do not have the right caudal-ventral pulmonary vein and it seems to be a common variant in DSH cats from our study, even though we have to consider that the studied population is small.

Left lung is devised in two lobes, one cranial and one caudal (Schaller, 1999). The left cranial lobe bifurcates in a cranial and a caudal branch. The left cranial lobe in our study has minor dimensions respectively to the left caudal lobe, fact that is reported also in other studies (Barone, 2003; Coccolini, 2012). Two branches origin from the left cranial lobe , the cranial-ventral and the caudal-ventral branch which correspond to the till nowadays references (Getty, 1982; Barone, 2003; Caccamo, 2006; Coccolini, 2012). Dorsal and ventral segmental branches arise from the left cranial lobe. Major dimensions of the left caudal lobe are prominent in all the cats of the study (Coccolini, 2012). The left cranial lobar pulmonary artery divides in two branches that run attached to the respectively bronchus and detaches multiple dorsal and ventral segmental branches. The LB1D1 pulmonary vein runs dorsal-lateral to the bronchus while the LB1V1 runs lateral to its bronchus, fact that is seen also in another study (Coccolini, 2012). The left ventral-cranial and the left ventral-caudal pulmonary vein anastomose before attaching the left atrium and consist the left ostia. In one case these two pulmonary veins attach separately the left atrium providing a different aspect of the left ostia. These findings are reported recently in an anatomic study of the feline thorax (Coccolini, 2012). More pulmonary venous variations can be found increasing the number of examined animals

as is reported in human medicine (Tekbas, 2011) and could contribute at the understanding of the different aspects of pulmonary edema. Direct continuation of the left principal bronchus, after detaching the left cranial lobe, performs the left caudal lobe (Caccamo, 2006). The left caudal lobe detaches the ventral, ventral-caudal and caudal branch while multiple dorsal segments are detaching dorsally. These findings correspond to the anatomic studies and in an endoscopic correlation (Caccamo, 2006; Coccolini, 2012). The left caudal lobar pulmonary artery has a similar path with the right caudal lobar pulmonary artery. A single caudal lobar pulmonary vein drains the left caudal lobe. Respectively to the contralateral pulmonary vein the left caudal do not show any anatomic differences. The left caudal lobar pulmonary vein anastomose with the right caudal lobar pulmonary vein and attach as one the left atrium consisting the caudal ostia.

Pulmonary variations of the venous system is well studied in human medicine with computed tomography and influence the implications for radiofrequency ablation (Marom, 2004). In human medicine four ostia are ussually present in the pulmonary venous drainage system to the left atrium. Right sided venous drainage system is more variable than the left(Wannasopha, 2012). Canine anatomical variations of the pulmonary and cardiac venous system are poorly reported (Abraham, 2003). In our study the only variation of the drainage venous system was noticed in the left ostia.

From the morphometric study of the feline's thoracic bronchial and vascular components an individual variability is seen. The statistical analysis demonstrates a linear correlation of the tracheal diameter to the feline's weight. The number of the identified segmental arterial branches is major in the right and left caudal lobe, fact that is logical due to their major thoracic

space occupying volume. The number of the arterial segments in the left cranial lobe is major to the number of the right cranial lobe segments.

Correlating the dimensions of the bronchial to the vascular we can conclude that the bronchial have major dimensions to the pulmonary arteries and the pulmonary veins have minor to the arteries, findings that are similar reported (Coccolini, 2012) while another study reports that pulmonary arteries have minor dimensions that pulmonary veins (Horsfield, 1986). Although we have to consider that in our study the peak enhancement of contrast medium is at the level of pulmonary arteries fact that can overestimate the arterial to the venous dimensions.

A recent anatomic study of the feline thorax (Coccolini, 2012) did not conclude if the architecture of the feline bronchial lumen is monopedial or dichotomic as is clearly reported in other species (Schlesinger, 1981). These authors demonstrate that animal species have a monopedial form of the bronchial lumen in which the principal bronchus has major dimension than the branches. There is the major branch and a minor one. In our study the accessory lobe demonstrates a dichotomic architecture, finding that is similar to recent anatomic study of the feline lung (Coccolini, 2012). In one case the accessory lobe show a monopedial architecture finding that is not till now reported in other anatomic studies. The model of the human bronchial tree is not suitable to the canines and felines because in human they have a dichotomic diramation while in canines and felines they have monopedial (Schlesinger, 1981; Caccamo, 2006). The monopedial model helps due to the major dimensions of the main branches that provides ultimate visualization via endoscopy. While in human the dichotomic model provides branches of similar dimensions and provides difficulty for the orientation during an endoscopic procedure (Coccolini, 2012).

Three types of relation between bronchial and vascular thoracic structures are reported (McLaughlin, 1959). The feline thorax belongs to type II in which the pulmonary arteries have an attached relation with the bronchial lumen and the pulmonary veins tend to have a wider relation to the bronchus.

A common finding in our study was the well enhanced hepatic veins during our CTPA protocol. At the beginning we thought that this could happen due to small amount of contrast medium passes throught the celiac and hepatic artery because we did not had yet a portal flow. But the most probable scenario is that the pressure of the power injector and the flow rate is too high producing an increased right atrium volume and an amount of contrast medium passes in opposite direction of the caudal vena cava blood flow into the hepatic veins and in some cases arrives till the renal veins.

CONCLUSION

CTPA imaging of the feline thorax could explore the pulmonary arteries, pulmonary veins and bronchial lumen till dimension of 0,5 millimeter. The scanning protocol during contrast medium peak enhancement at the pulmonary arterial phase could evaluate the pulmonary arterial lumen and detect pulmonary embolism, which is a life threatening condition. Beyond pulmonary arteries a CTPA protocol could evaluate all the thoracic. Pulmonary arteries tend to have a closer attached relation to the bronchial lumen, while pumonary veins have a wider one. Pulmonary arteries run dorsal/lateral to the bronchus while pulmonary veins drain ventral/ medial to the bronchial lumen. Exception of the venous ventral aspect is the accessory lobe that drains dorsal to the bronchus. This computed tomography anatomic study of the feline thorax achieved an ultimate visualization not only of the pulmonary arteries by also of the venous pulmonary system and bronchial lumen till minor segmental branches. Pulmonary venous anatomic variants were noticed among the cats of the study. A computed tomography nomenclature till to date is not reported and is introduced in our study. Bronchial diameter is major than arterial and venous dimensions are minor to the arterial. The feline bronchial lumen has an architecture of a mixed type, monopedial model of the feline lung with exception the dichotomic assessment of the accessory lobe. Sudden cut-off of the right and left cranial pulmonary vessels need to be further studied in the future. The enhancement of the hepatic veins could be explained from the high injection rate and pressure and needs to be further studied.

REFERENCES

Abraham LA, Slocombe RF. (2003): “Asymptomatic anomalous pulmonary veins in a siberian husky”. Aust Vet J, **81**(7): 406-408.

Barone R. (2003): “Anatomia Comparata dei Mammiferi Domestici”. Vol III: Splancnologia – Apparecchio Digerente e Respiratorio; Edizione italiana a cura di R. Bortolami. Ed agricole - Bologna.

Barone R. (2003): “Anatomia Comparata dei Mammiferi Domestici”. Vol V: Angiologia- parte I: Cuore e Arterie, parte II: Vene e Sistema Linfatico; Edizione Italiana a cura di R. Bortolami. Ed agricole – Bologna.

Beaulieu CF, Jeffrey RB Jr, Karadi C, et al. (1999): “Display modes for CT colonography. II. Blinded comparison of axial CT and virtual endoscopic and panoramic endoscopic volume- rendered studies”. Radiology, **212**: 203-212.

Bertolini G, Rolla EC, Zotti A et al. (2006a): “Three-dimensional multislice helical computed tomography techniques for canine extra-hepatic portosystemic shunt assessment”. Veterinary Radiology & Ultrasound, **47**(5): 439-443.

Bertolini G, Furlanello T, De Lorenzi D et al. (2006b): “Computed tomographic quantification of canine adrenal gland volume and attenuation”. Veterinary Radiology & Ultrasound, **47**(5): 444-448.

Bertolini G, De Lorenzi D, Ledda G, et al. (2007): “Esophageal varices due to a probable arteriovenous communication in a dog”. Journal of Veterinary Internal Medicine, **21**: 1392- 1395.

Bertolini G, Furlanello T, Drigo M et al. (2008): “Computed tomographic adrenal gland quantification in canine ACTH-dependent hyperadrenocorticism”. Veterinary Radiology & Ultrasound, **49**(5): 449-453.

Bertolini G. (2009a): “3D-Multidetector-row CT: the new era in the diagnosis of liver diseases”. In: Proceedings of the 19th Congress of the European College of Veterinary Internal Medicine, Porto, 105-107.

Bertolini G. (2009b): “Multidetector-Row Computed Tomography for Abdominal Vascular Assessment in Dog”. <http://paduaresearch.cab.unipd.it/1560/>.

Bertolini G, Stefanello C, Caldin M. (2009c): “Imaging diagnosis-pulmonary interstitial emphysema in a dog”. Veterinary Radiology & Ultrasound, **50**(1): 80-82.

Bertolini G. (2010a): “Acquired portal collateral circulation in the dog and cat”. Veterinary Radiology & Ultrasound, **51**(1): 25-33.

Bertolini G, Prokop M. (2010b): “Multidetector-row computed tomography: technical basics and preliminary clinical applications in small animals”. Veterinary Journal, **189**: 15-26.

Borsetto A. (2011). “Multidetector-row computed tomography” in doctoral thesis “Hepatobiliary diseases in small animals: a comparison of ultrasonography and multidetector-row computed tomography”.

Brewer F, Moise S, Kornreich B, Bezuidenhout A. (2012): “Use of computed tomography and silicon endocasts to identify pulmonary veins with echocardiography”. Journal of Veterinary Cardiology, **14**: 293-300.

Caccamo R, Twedt D, Buracco P, McKiernan B**.** (2006): “Endoscopic Bronchial Anatomy in the Cat”. Journal of Feline Medicine and Surgery, 140-149.

Cademartiri F, Luccichenti G, Van Der Lugt A, et al. (2004): “Sixteen-row multislice computed tomography: basic concepts, protocols, and enhanced clinical applications”. Seminars of Ultrasound, CT, MR, **25**: 2-16.

Choi H, Choi B, Choe K, Choi D, Yoo K, Kim M, Kim J. (2004): “Pitfalls, artifacts and remedies in multi-detector row ct coronary angiography”. Radiographics, **24**: 787-800.

Coccolini R (2012): Graduation thesis in veterinary medicine-Univeristy of Bologna, “Studio anatomo-topografico ed indagine morfometrica dei bronchi principali, lobari e segmentari nel gatto”.

Desser TS, Sommer FG, Jeffrey RB Jr. (2004): “Value of curved planar reformations in MDCT of abdominal pathology”. Am J Roentgenol, **182**: 1477-1484.

Drees R, Frydrychowicz A, Reeder S, Pinkerton M, Johnson R. (2011a): “64-multidetector computed tomographic angiography of the canine coronary arteries”. Veterinary Radiology & Ultrasound, **52**(5): 507-515.

Drees R, Frydrychowicz A, Keuler N, Reeder S, Johnson R. (2011b): “Pulmonary angiography with 64-multidetector-row computed tomography in normal dogs”. Veterinary Radiology & Ultrasound, **52**(4): 362-367.

Echandi RL, Morandi F, Daniel WT et al. (2007): “Comparison of transplenic multidetector CT portography to multidetector CT-angiography in normal dogs”. Veterinary Radiology & Ultrasound, **48**(1): 38– 44.

Eom K, Kwak H, Kang H, Park S, Lee H, Kang H, Kwon J, Kim I, Kim N, Lee K. (2008): “Virtual CT otoscopy of the middle ear and ossicles in dogs”. Veterinary Radiology & Ultrasound, **49**(6): 545-550.

Fleischmann D. (2009): “Contrast medium administration in computed tomographic angiography”. In: Rubin G., Rofsky N. CT and MR Angiography(Comprehensive Vascular Assessment). First Edition. China: Lippincott Williams& Wilkins.

FlohrT, Stierstorfer K, Bruder H. (2002a): “New technical developments in multislice Ct, part 1: approaching isotropic resolution with sub-mm 16-slice scanning”. Rofo Fortschr Geb Rontgenstr Neuen Bildgeb Verfahr, **174**: 839-845.

Flohr T, Bruder H, Stierstorfer K. (2002b): “New technical developments in multislice Ct, part 2: sub-millimeter 16-slice scanning and increased gantry rotation speed for cardiac imaging”. Rofo Fortschr Geb Rontgenstr Neuen Bildgeb Verfahr, **174**: 1022-1027.

Flohr T, Stierstorfer K, Bruder H, et al. (2003). “Image reconstruction and image quality evaluation for a 16 slice CT scanner”. Med Phys, **30**: 832-845.

Flohr T, Shaller S, Stierstorfer K, et al. (2005): “Multidetector-row CT systems and image reconstruction techniques”. Radiology, **235**: 756-773.

FuchsT, Krause J, Schaller S, et al. (2000): “Spiral interpolation algorithms for multislice spiral CT—part II: measurement and evaluation of slice sensitivity profiles and noise at a clinical multislice system”. IEEE Trans Med Imaging, **19**(9): 835-847.

Getty R. (1982): Anatomia degli animali domestici. Volume II. Edizione italiana a cura di A. Fasolo, M.F. Franzoni, G.Garinei, C. Vellano. Piccin Editore - Padova.

Habing A, Coelho J, Nelson N, Brown A, Beal M, Kinns J. (2011): "Pulmonary angiography using 16 slice multidetector computed tomography in normal dogs". Veterinary Radiology & Ultrasound, **52**(2): 173-178.

Horsfield K, Kemp W, Phillips **S.** (1986): "Diameters of Arteries, Veins, and Airways in Isolated Dog Lung". The Anatomical Record, **216**: 392-395.

Henao-Guerrero N, Ricco C, Jones J, Buechner-Maxwell V, Daniel G. (2012): "Comparison of four ventilatory protocols for computed tomography of the thorax in healthy cats". Am J Vet Res, **73**: 646-653.

Henninger W. (2003): "Use of computed tomography in the diseased feline thorax". J Small Anim Pract., **44**(2): 56-64.

Horger M. (2006): "Multidetector CT-Diagnosis of infectious Pulmonary Disease". In: Bruening R., Kuettner A., Flohr Th. Protocols for Multislice CT. Second edition. Germany: Springer-Verlag Berlin Heidelberg.

Horton KM, Sheth S, Corl F, et al. (2002): "Multidetector row CT: principles and clinical applications". Crit Rev Comput Tomogr, **43**: 143–181.

Hurst DR, Kazerroni EA, Stafford-Johnson D, Williams DM, Platt JF, Cascade PN, Prince MR. (1999): “Diagnosis of pulmonary embolism: comparison of CT angiography and MR angiography in canines”. Journal of vascular internal radiology, **10**(3):309-318.

Ishaq M. (1980): “A morphological study of the lungs and bronchial tree of the dog: with a suggested system of nomenclature for bronchi”. Journal of Anatomy, **131**(4): 589-610.

Jung J, Chang J, Oh S, Yoon J, Choi M. (2010): “Computed tomography angiography for evaluation of pulmonary embolism in an experimental model and heartworm infested dogs”. Veterinary Radiology & Ultrasound, **51**(3): 288-293.

Kalender W. (1995): “Thin section three dimensional spiral CT: is isotropic imaging possible?”. Radiology, **176**: 181-183.

Kalra MK, Maher MM, D’Souza R et al. (2004): “Multidetector computed tomography technology: current status and emerging developments”. J Comput Assist Tomogr, **28**(suppl 1): S2 – S6.

Kim HC, Park SJ, Park SI et al. (2005): “Multislice CT cholangiography using thin-slab minimum intensity projection and multiplanar reformation in the evaluation of patients with suspected biliary obstruction: preliminary experience”. Clinical Imaging, **29**: 46-54.

Kohler T, Proska R, Grass M. (2001): “A fast and efficient method for sequential cone-beam tomography”. Med Phys, **28**: 2318-2327.

Kohler T, Proska R, Bontus C, et al. (2002): “Artifact analysis of approximate helical cone-beam CT reconstruction algorithms”. Med Phys, **29**: 51-64.

Kuettner A, Kopp A.F. (2006): “MSCT imaging of pulmonary embolism”. In: Bruening R., Kuettner A., Flohr Th. Protocols for Multislice CT. Second edition. Germany: Springer-Verlag Berlin Heidelberg.

Lee CH, Goo JM, Bae KT, Lee HJ, Kim KG, Chun EJ, Park CM, Im JG. (2007): “CTA contrast enhancement of the aorta and pulmonary artery: the effect of saline chase injected at two different rates in a canine experimental model”. European journal of radiology, **64**(2): 296-301.

Lee E, Kritsaneepaiboon S, Zyrakowski D, Martinez C, Strauss K, Boiselle P. (2009): “Beyond the pulmonary arteries: alternative diagnoses in children with MDCT pulmonary angiography negative for pulmonary embolism”. AJR: 888-894.

Liang Y, Kruger RA. (1996): “Dual-slice spiral versus single-slice spiral scanning: comparison of two computed tomography scanners”. Med Phys, **23**: 205-220.

Mahesh M. (2002): “Search for isotropic resolution in CT from conventional through multiple-row detector”. Radiographics, **22**: 949-962.

Makara M, Dennler M, Kuhn K, Kalchofner K, Kircher P. (2011): “Effect of contrast medium injection duration on peak enhancement and time to peak enhancement of canine pulmonary arteries”. Veterinary Radiology & Ultrasound, **52**(6): 605-610.

Marom E, Herndon J, Kim Y, Mc Adams A. (2004): “Variations in pulmonary venous drainage to the left atrium: implications for radiofrequency ablation”. Radiology, **230**: 824-829.

McLaughlin R.F, Tyler W.S, Canada R.O. (1959): “A study of the Sub-gross Pulmonary Anatomy in Various Mammals”. American Journal of Anatomy, **108**: 149-165.

Miller C. (2007): “Approach to the respiratory patient”. Vet Clin Small Anim, **37**: 861-878.

Napel S, Marks MP, Rubin GD, et al. (1992): “CT angiography with spiral CT and maximum intensity projection”. Radiology, **185**: 607-610.

Napoli A, Fleischmann D, Chan FP, et al. (2004): “Computed tomography angiography: state-of- the-art imaging using multidetector-row technology”. J Comput Assist Tomogr, **2**: S32– S45.

Nino-Murcia M, Jeffrey RB Jr, Beaulieu CF, et al. (2001): “Multidetector CT of the pancreas and bile duct system: value of curved planar reformations”. Am J Roentgenol, **200**(176): 689-693.

Oechtering GU, Kiefer I, Ludewig E. (2005): “Virtual endoscopy of the upper and central airways of small animals with multi-row detector CT - preliminary results”. In: Proceedings of the Annual Conference of the European Association of Veterinary Radiology, Naples.

Oliveira CR, Ranallo FN, Pijanowski GJ, Mitchell MA, O’Brien MA, McMichael M, Hartman Sk, Matheson JS, O’Brien RT. (2011): “The VetMousetrap: a device for computed tomographic imaging of the thorax of awake cats”. Veterinary Radiology & Ultrasound, **52**(1): 41-52.

Prather A, Berry C, Thrall D. (2005): “Use of radiography in combination with computed tomography for the assessment of noncardiac thoracic disease in the dog and cat”. Veterinary Radiology & Ultrasound, **46**(2): 114-121.

Prokop M, Shin HO, Schanza, et al. (1997): “Use of maximum intensity projections in CT angiography: a basic review”. Radiographics, **17**: 433-451.

Prokop M. (2009): “Principles of computed tomographic angiography”. In: Rubin G., Rofsky N. CT and MR Angiography(Comprehensive Vascular Assessment). First Edition. China: Lippincott Williams& Wilkins.

Pypendop B, Barter L, Stanley S. (2011): “Hemodynamic effects of dexmedetomidine in isoflurane –anesthetized cats”. Veterinary anaesthesia and analgesia, **38**: 555-567.

Raman R, Napel S, Beaulieu CF, et al. (2002): “Automated generation of curved planar reformations from volume data: method and evaluation”. Radiology, **223**: 275-280.

Raman R, Napel S, Rubin GD. (2003): “Curved maximum intensity projection: method and evaluation”. Radiology, **229**: 255-260.

Ravenel JG, Mc Adams HP. (2003): “Multiplanar and three dimensional imaging of the thorax”. Radiologic Clinics of North America, **41**: 475-489.

Raupach R. (2006): “Artifacts inMSCT”. In: Bruening R., Kuettner A., Flohr Th. Protocols for Multislice CT. Second edition. Germany: Springer-Verlag Berlin Heidelberg.

Reid L, Dillon R, Hathcock J, Brown L, Tillson M, Wooldridge A. (2012): “High-resolution computed tomography bronchial lumen to pulmonary artery diameter ratio in anesthetized ventilated cats with normal lungs”. Veterinary Radiology & Ultrasound, **53**(1): 34-37.

Rubin G, Sedati P, Wei J. (2009): “Postprocessing and data analysis”. In: Rubin G., Rofsky N. CT and MR Angiography(Comprehensive Vascular Assessment). First Edition. China: Lippincott Williams& Wilkins.

Samii V, Biller D, Koblik P. (1998): “Normal cross-sectional anatomy of the feline thorax and abdomen: comparison of computed tomography and cadaver anatomy”. Veterinary Radiology & Ultrasound, **39**(6): 504-511.

Schaller O. (1999): Nomenclatura Anatomica Veterinaria illustrata. Edizione italiana a cura di F. Mascarello e B. Cozzi; Antonio Delfino editore - Roma.

Schermerhorn T, Pembleton-Corbett J, Kornreich B. (2004): “Pulmonary Thromboembolism in cats”. J Vet Intern Med, **18**: 533-535.

Schlesinger R.B, McFadden L.A**.** (1981): “Comparative morphometry of the upper bronchial tree in six mammalian species”. The Anatomical Record, **199**(1): 99-108.

Schoepf U, Meaney J. (2009): “Pulmonary vasculature”. In: Rubin G., Rofsky N. CT and MR Angiography(Comprehensive Vascular Assessment). First Edition. China: Lippincott Williams& Wilkins.

Schreiner S, Paschal CB, Galloway RL. (1996): “Comparison of projection algorithms used for the construction of maximum intensity projection images”. J Comput Assist Tomogr, **20**: 56-67.

Schlueter C, Budras K, Ludewig E, Mayrhofer E, Koenig H, Walter A, Oechtering G. (2009): “Brachycephalic feline noses. CT and anatomical study of the relationship between head conformation and the nasolacrimal drainage system”. Journal of feline medicine and surgery, **11**: 819-900.

Schwarz T, Johnson V. (2011a): “Lungs and bronchi”. In: Schwarz T. and Saunders J. Veterinary Computed Tomography. First edition. UK: John Wiley and Sons Ltd.

Schwarz T. (2011b): “Artifacts in CT”. In: Schwarz T. and Saunders J. Veterinary Computed Tomography. First edition. UK: John Wiley and Sons Ltd.

Scrivani P, Thompson M, Dykes N, Holmes N, Southard T, Gerdin J, Bezuidenhout A. (2012): “Relationships among subgross anatomy, computed tomography, and histopathologic findings in dogs with disease localized to the pulmonary acini”. Veterinary Radiology & Ultrasound,

53(1): 1-10.

Seiller GS, Nolan TJ, Withnall E, Reynolds C, Lok JB, Sleeper MM. (2010): “Computed tomograhic changes associated with the prepatent and early patent phase of dirofilariasis in an experimentally infected dog”. Veterinary Radiology & Ultrasound, **51**(3): 288-293.

Stadler K, Hartman S, Matheson J, O'Brein R. (2011): "Computed tomographic imaging of dogs with primary laryngeal or trachea airway obstruction". Veterinary Radiology & Ultrasound, **52**(4): 377-384.

Staffieri F, De Monte V, De Marzo C, Grasso S, Crovace A. (2010): "Effects of two fractions of inspired oxygen on lung aeration and gas exchange in cats under inhalant anaesthesia". Vet Anaesth Analg, **37**(6): 483-490.

Szuba A, Gosk-Bierska I, Hallett R. (2009): "Thromboembolism". In: Rubin G., Rofsky N. CT and MR Angiography(Comprehensive Vascular Assessment). First Edition. China: Lippincott Williams& Wilkins.

Tekbas G, Gumus H, Onder H, Ekici F, Hamidi C, Tekbas E, Gulicetincakmak M, Yanuz C, Bilici A. (2011): "Evaluation of pulmonary vein variations and anomalies with 64 slice multi detector computed tomography". AJR, **197**(6): 1460-1465.

Tidwell S, Graham J, Peck J, Berry C. (2007): "Incidence of pulmonary embolism after non-cemented total hip arthroplasty in eleven dogs: computed tomographic pulmonary angiography and pulmonary perfusion scintigraphy". Veterinary surgery, **36**: 37-42.

Udupa JK. (1999): "Three-dimensional visualization and analysis methodologies: a current perspective". Radiographics, **19**: 783-806.

Van Bemmel CM, Viergever MA, Niessen WJ. (2004): “Semiautomatic segmentation and stenosis quantification of 3D contrast-enhanced MR angiograms of the internal carotid artery”. Magn Reson Med, **51**: 753-760.

Vos FM, Van Gelder RE, Serlie Iwo, et al. (2003): “Three-dimensional display modes for CT colonography: conventional 3D virtual colonoscopy versus unfolded cube projection”. Radiology, **228**, 878-885.

Wannasopha Y, Oilmungmool N, Euathongchit J. (2012): “Anatomical variations of pulmonary venous drainage in Thai people: multidetector CT study”. Biomedical imaging and intervention journal, **8**(1): e4.

Wintersperger B, Helmberger T, Herzog P, et al. (2002a): “New abdominal CT angiography protocol on a 16 detector row CT system”. Radiologe, **42**: 722-727.

Wintersperger B, Herzog P, Jakobs T, et al. (2002b): “Initial experience with the clinical use of a 16 detector row CT system”. Crit Rev Comput Tomogr, **43**: 283-316.

Yamada K, Morimoto M, Kishimoto M et al. (2007a): “Virtual endoscopy of dogs using multi- detector row CT.” Veterinary Radiology & Ultrasound, **48**(4): 318-22.

Yamada K, Taniura T, Tanabe S, et al. (2007b): “The use of multi-detector row computed tomography (MDCT) as an alternative to specimen preparation for anatomical instruction”. Journal of Veterinary medical Education, **34**: 143-150.

http://www.medvet.umontreal.ca/etudes/FormationContinue.html

Acknowledgements

I would like to dedicate my doctoral thesis to my father MD. Theofanis Panopoulos and my uncle MD. Nicolaos Chalatsis, who inspired me and encouraged me to provide my knowledge in diagnostic imaging.

I am grateful of having my thesis with Prof. Mario Cipone and Prof. Alessia Diana, who are great mentors and they enlighted me with the Bologna's University Alma Mater Studiorum.

I would like also to mention the important help of Michael Tsikalakis, expert in computed tomography protocols, who inspired me in advanced imaging modalities. The perfect imaging, during these quiet times of inspiration apnea, was possible due to the important help of the anesthetist Dr. Anastasia Papastefanou.